OCTOBER 2023

IN COMPLIANCE™

THE COMPLIANCE INFORMATION RESOURCE FOR ELECTRICAL ENGINEERS

GaN/SiC Transistors for Your Next Design

Fight or Flight?

PLUS

Local PCB Layout Tweaks for Improved Signal Integrity When Using ESD Protection Devices

Is Wireless Measurement of Human Body Voltage Possible?

(Re)Discovering the Lost Science of Near-Field Measurements, Part 4

2024 PRODUCT RESOURCE GUIDE

In Compliance Magazine
ISSN 1948-8254 (print)
ISSN 1948-8262 (online)
is published by

IN COMPLIANCE

Same Page Publishing Inc.
451 King Street, #458
Littleton, MA 01460
tel: (978) 486-4684
fax: (978) 486-4691

publisher/editor-in-chief
Lorie Nichols
lorie.nichols@incompliancemag.com
(978) 873-7777

business development director
Sharon Smith
sharon.smith@incompliancemag.com
(978) 873-7722

production director
Erin C. Feeney
erin.feeney@incompliancemag.com
(978) 873-7756

marketing director
Ashleigh O'Connor
ashleigh.oconnor@incompliancemag.com
(978) 873-7788

circulation director
Alexis Evangelous
alexis.evangelous@incompliancemag.com
(978) 486-4684

features editor
William von Achen
bill.vonachen@incompliancemag.com
(978) 486-4684

senior contributors
Bruce Archambeault
bruce@brucearch.com

Keith Armstrong
keith.armstrong@cherryclough.com

Leonard Eisner
Leo@EisnerSafety.com

Daryl Gerke
dgerke@emiguru.com

Ken Javor
ken.javor@emcompliance.com

Ken Ross
kenrossesq@gmail.com

Werner Schaefer
wernerschaefer@comcast.net

columns contributors
EMC Concepts Explained
Bogdan Adamczyk
adamczyb@gvsu.edu

Hot Topics in ESD
EOS/ESD Association, Inc
info@esda.org

On Your Mark
Erin Earley
eearley@clarionsafety.com

advertising
For information about advertising contact Sharon Smith at sharon.smith@incompliancemag.com.

subscriptions
In Compliance Magazine subscriptions are free to qualified subscribers in North America. Subscriptions outside North America are $129 for 12 issues. The digital edition is free. Please contact our circulation department at circulation@incompliancemag.com

PRINTED WITH SOY INK

OCTOBER 2023 CONTENTS

Volume 15 | Number 10

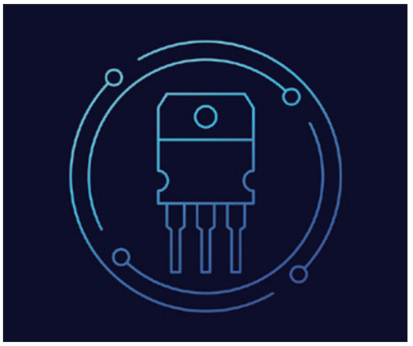

FCC Grants Waiver for Connected Vehicle Spectrum Access

In a potentially groundbreaking move to facilitate the expanded use of smart automotive capabilities, the U.S. Federal Communications Commission (FCC) has recently issued a number of individual waivers permitting limited deployment of cellular vehicle-to-everything (C-V2X) technologies.

The FCC decision was issued in response to petitions from 17 separate state, local, and municipal transportation authorities across the country and two equipment manufacturers. Each individual petitioner sought a waiver of certain Part 90 and Part 95 rules that regulate the operation of dedicated short-range communication (DSRC) based roadside units and onboard units in the upper 30 megahertz of the 5.9 GHz band.

According to the petitioners, the waiver would allow for the deployment of C-V2X technologies within the 5.895-5.925 GHz band in support of intelligent transportation systems (ITS) operations.

In issuing its decision granting the individual waivers, the FCC stated that "the underlying purpose of the rules governing ITS operations would not be served by denying these requests and thereby delaying or precluding C-V2X operations." Further, "a waiver in this case will facilitate early C-V2X deployment… and serves the public interest by encouraging the widespread deployment of ITS operations using C-V2X technology."

ARRL Battles Stock Traders for Spectrum

Spectrum directly adjacent to amateur HF bands could be used for high-frequncy stock trading

Amateur radio users and enthusiasts are stepping up against what they see as a direct threat to the security of amateur radio frequencies.

According to a press release published on its website, the National Association for Amateur Radio (ARRL) has filed comments against a proposal that would allow the introduction of high-power digital communications in spectrum directly adjacent to amateur HF bands. The proposal for the change was filed as a petition to the U.S. Federal Communications Commission (FCC) by the Shortwave Modernization Coalition (SMC), a group that reportedly represents organizations involved in high-frequency stock trading.

Specifically, the proposal would allow data communications on multiple bands within the HF 2-25 MHz range with up to 20 KW, including those immediately adjacent to spectrum allocated to the Amateur Radio Service. The ARRL says that its own evaluation and testing has concluded that, if the proposed rules were to be adopted, it would lead to "significant harmful interference to many users of adjacent and nearby spectrum, including Amateur Radio licensees."

EU Commission Updates Energy Labeling Requirements for Smartphones/Tablets

The Commission of the European Union (EU) has supplemented its energy labeling requirements to include smartphones and tablets.

Published in the *Official Journal of the European Union*, the stated goal of Commission Delegated Regulation (EU) 2023/1669 is to "limit the energy consumption of smartphones and slated tablets in 2030 to 23.3 TWh, meaning 35% of primary energy consumption is saved compared to what would happen if no measures were taken."

Toward that end, the Delegated Regulation sets forth in Annex III specific requirements for the labeling of smartphones and tablets. Details to be shown on the label include the supplier's model identifier, battery endurance data, and a QR code allowing users to access additional information. Further, Annex II details "energy efficiency classes," which are assigned based on the energy efficiency index rating of a given device, from "most efficient" to "least efficient." Information regarding a device's energy efficiency class must also be included on the product energy label.

The requirements under the Delegated Regulation are applicable to smartphones and tablets from June 20, 2025.

Apple Experimenting with 3D Printing for Production

Technology giant Apple is reportedly testing the use of additive manufacturing (AM) technology (also known as 3D printing) in the production of its newest smartwatch models.

According to reports listed on multiple media platforms, Apple is testing 3D printing in the production of its upcoming Apple Watch 9. Currently, the casing of Apple watches is created by cutting pieces of metal into exactly the correct shape. So, the use of 3D printing would likely reduce the amount of material required for production as well as production time.

If Apple's 3D testing experiments meet its expectations and requirements, the company is expected to integrate 3D printing technologies into the production processes of additional product lines. This includes the next generation of the Apple Watch Ultra, a titanium-encased watch scheduled for sometime next year.

FDA Issues Warning About Ultraviolet Wands

UV wands expose users to unsafe levels of UV-C radiation

The U.S. Food and Drug Administration (FDA) has issued a warning to consumers about potential risks associated with the use of certain brands of ultraviolet (UV) wands promoted to disinfect surfaces.

UV wands are consumer products designed to give off UV-C radiation as a method of disinfecting surfaces outside of healthcare settings. However, testing by the FDA shows that some UV wands currently being marketed to consumers expose users to unsafe levels of UV-C radiation. In some cases, FDA testing showed that certain UV wands generate as much as 3000 times more UV-C radiation than the exposure limit recommended by the International Commission on Non-Ionizing Radiation Protection (ICNIRP).

The FCC has posted an updated list on its website of 13 specific UV wands that give off unsafe levels of UV-C radiation. The FDA warns against the use of any UV wand product that fails to provide safety instructions or information about potential risks associated with emissions radiated from UV wands.

FCC Releases Data on U.S. Internet Access

After a nearly four-year hiatus, the U.S. Federal Communications Commission (FCC) has released its most recent report on access in the United States to Internet connections, including information on the gap between current service levels and the benchmark Internet connection speeds recommended under the Commission's National Broadband Plan.

According to the Commission's report, entitled Internet Access Services: Status as of December 31, 2021, over 95% of fixed Internet connections to households meet or exceed the speed tier that most closely approximates the target set in the National Broadband Plan of 3 megabits per second (Mbps) downstream and 768 kilobits per second (kbps) upstream. This penetration rate for fixed high-speed service compares with approximately 81% at the end of 2013, 70% at the end of 2012, and just 49% in 2009.

Without accounting for speed, Internet connections overall are growing. By the end of December 2021, at least 510 million Internet connections were operating

at speeds over 200 kbps, a 4% year-over-year increase. Overall growth continues to be driven by dramatic increases in mobile connections. At the end of December 2021, there were approximately 384 million mobile Internet connections, compared with only about 126 million fixed Internet connections.

FCC Releases NPRM on Cybersecurity Labeling Program

The U.S. Federal Communications Commission (FCC) is proceeding with plans to develop and implement a voluntary labeling program for connected smart devices that meet rigorous cybersecurity requirements.

According to a Notice of Proposed Rulemaking (NPRM) issued in mid-August, the FCC's "U.S. Cyber Trust Mark" Program would enable manufacturers of internet-enabled devices to qualify their products in accordance with rigorous cybersecurity requirements based on criteria developed by the National Institute of Standards and Technology (NIST). Devices that meet those requirements would then be permitted to apply the Cyber Trust Mark to their products, similar to the Energy Star logo currently applied to energy-efficient appliances.

As we previously reported, the FCC's proposed Cyber Trust Program is intended to help consumers make informed decisions regarding their purchases of internet-enabled devices, while also providing an incentive for manufacturers to meet higher cybersecurity standards.

The FCC's NPRM seeks public comments on several questions regarding the implementation of the Cyber Trust Program, including:

- The scope of devices or products that should be considered for inclusion in the labeling program;
- Who should be responsible for managing the program and program oversight;
- How to develop the security standards that could apply to different types of devices;
- How to demonstrate compliance with those standards;
- How to safeguard the cybersecurity label against unauthorized use; and
- How to educate consumers about the program.

NIST Releases Cybersecurity Framework 2.0 Draft

Feedback on the public draft may be submitted to NIST until November 4.

The National Institute of Standards and Technology (NIST) has recently published for public comment the first draft of its Cybersecurity Framework 2.0 (CSF 2.0).

First published in 2014, the NIST Cybersecurity Framework is a voluntary framework that includes standards, guidelines, and best practices to help organizations more effectively manage cybersecurity risks. The Framework also fosters increased communications between both internal and external stakeholders about risk and cybersecurity issues.

The release of the public draft of CSF 2.0 follows the April release of a "Discussion Draft" of CSF 2.0 that detailed proposed changes to the core elements of the framework.

The complete draft of NIST's CSF 2.0 is available at https://csrc.nist.gov. Feedback on the draft may be submitted to NIST at cyberframework@nist.gov until November 4, 2023.

NIST has also released a reference tool to foster greater access and use of its draft Cybersecurity Framework 2.0 (CSF 2.0). According to NIST, the new "Cybersecurity Framework (CSF) 2.0 Reference Tool" will allow users to explore the core elements of the framework (Functions, Categories, Subcategories, and Implementation Examples) more easily. The Reference Tool also provides both human and machine-readable versions of the draft, enabling users to create their own customized versions of the framework with personally selected information and references.

FCC Calls Out More Pirate Radio Operators

The FCC is continuing its active efforts to curb pirate radio operations across the country.

The Enforcement Bureau of the U.S. Federal Communications Commission (FCC) is continuing its active efforts to curb pirate radio operations across the country.

Notices of Apparent Liability for Forfeiture were issued to two pirate radio operators, one in Burney, CA and the other in Rockford, IL. In the first instance, the operator was found to have willfully and repeatedly interfered with radio communications of the Western Amateur Radio Friendship Association (WARFA) during the Association's regularly scheduled on-air meetings.

In the second case, the operator made multiple one-way radio transmissions for an extended period of time, including recorded comedy routines, air raid siren sounds, and digital noises. One transmission observed by an Enforcement Bureau field agent continued for over 30 minutes, during which time other users were blocked from accessing the channel. The FCC proposed financial penalties of $24,000 and $25,000 respectively in these cases.

In a separate action, the FCC issued a Notice of Unlicensed Operation to a Utica, NY operator who reportedly made unauthorized transmissions on frequencies used for police dispatch communications in Herkimer County, NY. The operator was given 10 days to cease the illegal interference and to notify the FCC of the specific steps they have taken to avoid operating on unlicensed frequencies in the future.

In the Miami area, nine separate warnings were issued to landowners and property managers in the Miami area.

The Notices of Illegal Pirate Radio Broadcasting were issued by the Atlanta Regional Office of the Enforcement Bureau. In each case, violators were identified by Bureau enforcement officers from the Miami Office using direction-finding techniques to identify the location and source of the illegal radio signals. And in each case, a search of FCC records showed no license issued for radio operation at the identified location.

The federal PIRATE Act allows the FCC to propose penalties of up to $115,802 per day with a maximum of $2,316,034 for violations of its illegal radio broadcasting rules. In addition, FCC is empowered to conduct periodic enforcement sweeps as well as the authority to take enforcement action against landlords and property owners that willfully and knowingly permit illegal radio broadcasting on their properties.

FCC's STIR/SHAKEN Standards Now In Effect for Small Providers

All IP-based voice service providers are now required to adopt the caller ID authentication framework adopted by the U.S. Federal Communications Commission (FCC) in 2021 to reduce the incidence of spoofed robocalls.

In a press release, the U.S. Federal Communications Commission (FCC) reminded gateway and facilities-based small service providers of the June 30, 2023 deadline to implement the requirements of the Commission's STIR/SHAKEN standards (the acronyms stand for Secure Telephone Identity Revisited (STIR) and Signature-based Handling of Assorted information using toKENS (SHAKEN)).

The STIR/SHAKEN standards provide a common digital language that can be used by phone networks to pass valid information from provider to provider, thereby helping individual service providers strengthen their own blocking tools to reduce the incidence of unwanted calls. The largest U.S.-based voice service providers were required to adopt the STIR SHAKEN standards as of June 30, 2021.

"While there is no single cure-all when it comes to robocalls, having this technology in our networks is real progress," noted FCC Chair Jessica Rosenworcel in the press release. "We will continue to push forward with this and every other tool we have to fight these junk calls."

FDA Issues Guidance on Qualification of Medical Device Development Tools

The U.S. Food and Drug Administration (FDA) has published its final Guidance on the qualification of tools for evaluating medical devices.

The Guidance, "Qualification of Medical Device Development Tools," describes a voluntary program for the qualification of medical device development tools (MDDTs) used in the evaluation of devices regulated by the Administration's Center for Devices and Radiological Health (CDRH).

According to the Guidance, MDDTs are "a method, material, or measurement used to assess the safety, effectiveness, or performance of a medical device." Some examples of MDDTs include non-clinical assessment models (NAMs), biomarker tests (BTs), and clinical outcome assessments (COAs).

The CDRH says that the use of MDDTs will help to "facilitate the development and timely evaluation of medical devices by providing a more efficient and predictable means for collecting information to support regulatory submissions."

Guidance documents issued by the FDA are intended only to represent the current thinking of the agency and are not binding on either the FDA or the public.

FCC Proposes Record $300 Million Fine for Illegal Robocalls

The U.S. Federal Communications Commission (FCC) has issued a record $300 million fine against a network of companies for making illegal robocalls in support of an automotive warranty scam.

According to a Forfeiture Order issued by the Commission, the multi-unit enterprise headed by Roy M. Cox and Aaron Michael Jones made over five billion robocalls to more than 500 million phone numbers during a three-month span in 2021. The calls prompted recipients to "Press 1" to speak with a "warranty specialist" about either extending a current auto warranty or reinstating an expired one. Call recipients who complied were ultimately connected with a "client sales agent," who would push the consumer to purchase a new vehicle service contract.

The robocall campaign violated several robocall prohibitions, including making pre-recorded voice calls to mobile phones without consent, placing telemarketing calls without written consent, and dialing numbers listed on the National Do Not Call Registry. The robocalls also violated current spoofing laws by using a misleading call ID to get consumers to answer the call.

The FCC says that the Forfeiture Order follows the issuance of a Notice of Apparent Liability for Forfeiture in December 2022, to which the enterprise never responded. Should the enterprise now fail to pay the $299,997,000 fine, the case will be turned over to the U.S. Department of Justice for collection and further action as necessary.

GAN/SIC TRANSISTORS FOR YOUR NEXT DESIGN – FIGHT OR FLIGHT?

Getting EMC ready for the next generation of power electronics devices

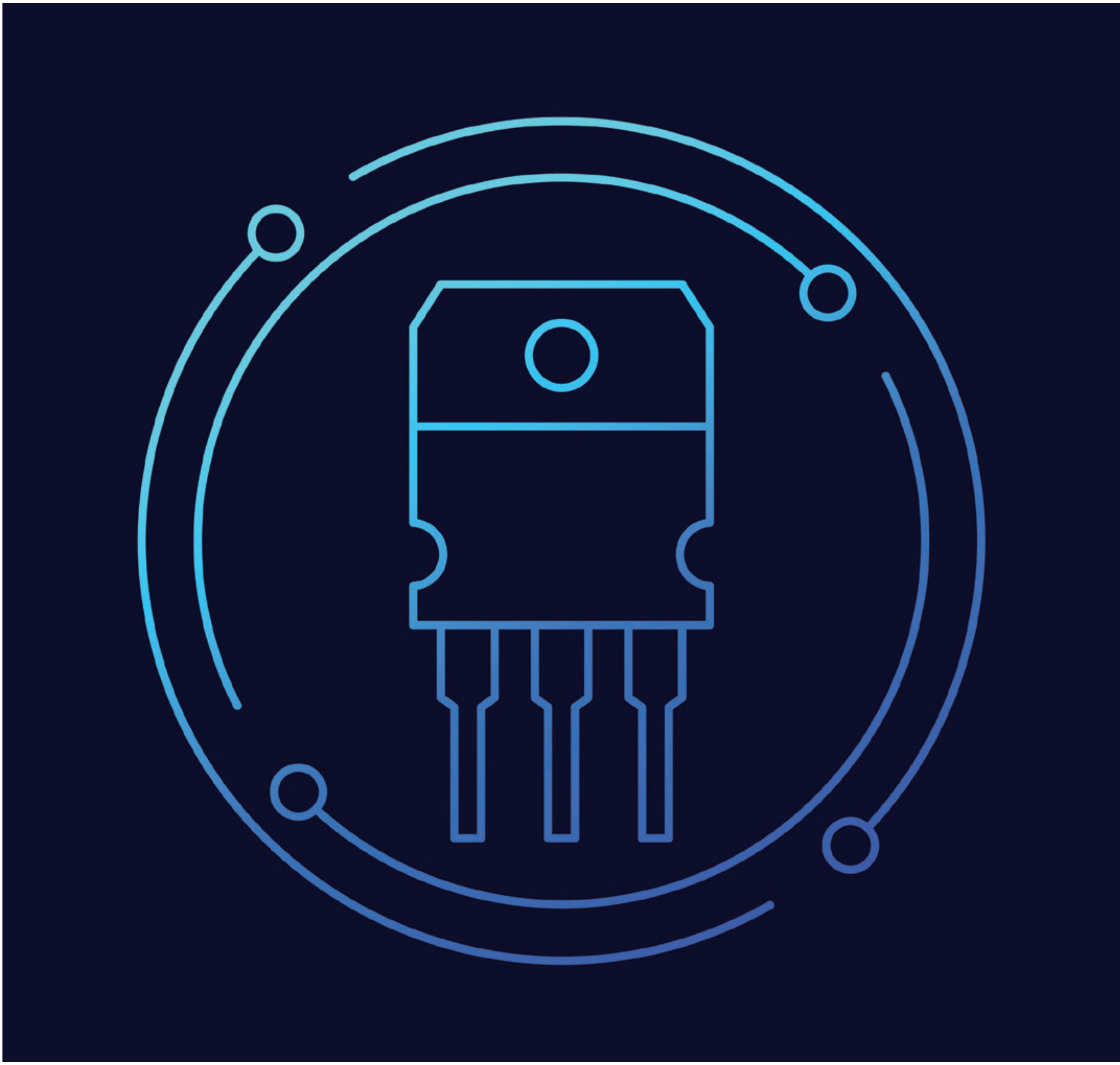

Dr. Min Zhang is the founder and principal EMC consultant of Mach One Design Ltd, a UK-based engineering firm that specializes in EMC consulting, troubleshooting, and training. His in-depth knowledge of power electronics, digital electronics, electric machines, and product design has benefitted companies worldwide. Zhang can be reached at info@mach1design.co.uk.

By Dr. Min Zhang

As a technical consultant, I have seen various new technologies implemented in both new and old applications. In the semiconductor industry, WBG devices such as SiC and GaN transistors have been gaining attention due to their small size, fast speed, and better thermal performance. The introduction of these new semiconductors into the consumer market came after a series of military and other commercial applications of the technology in everything from electric vehicles to radar systems.

GaN devices have enabled a much better form factor for product design than their silicon counterparts. As they become cheaper and more available, it is expected that we will see them widely adopted in power-switching modules worldwide.

Technically speaking, GaN semiconductors are high-electron-mobility transistors (HEMTs), meaning they do not have the doped region in a PN junction like MOSFETs. This enables faster electron flow, hence higher switching speed. Because HEMTs do not have the PN structure, they also do not have a body diode. This can have a great impact in applications such as motor drives, where we can now switch on the HEMT for freewheeling rather than relying on the body diode.

From the EMC perspective, this feature can be useful as, traditionally, EMI issues associated with the reverse recovery charge of a body diode during deadtime can be a problem [1]. To fix the issues, engineers often place a Schottky diode in parallel with the MOSFET as Schottky diodes switch faster and do not have a reverse recovery charge effect [1]. Now that the switching speed of a GaN is faster than a Schottky diode, it does not have a reverse recovery charge effect either. The HEMT has a "quasi diode" mode in the deadtime region, and we need to control the deadtime well.

But new technology often presents a double-edged sword. The most significant advantage of a GaN device (superfast switching, say 100V/ns) also brings a challenge for controlling EMI. As we all know, the faster the switching action (i.e., defined by the rise time), the harder it is to contain EMI, especially above the frequency of 1/πt, where *t* is the rise/fall time of a switching event. This can be seen in Figure 1.

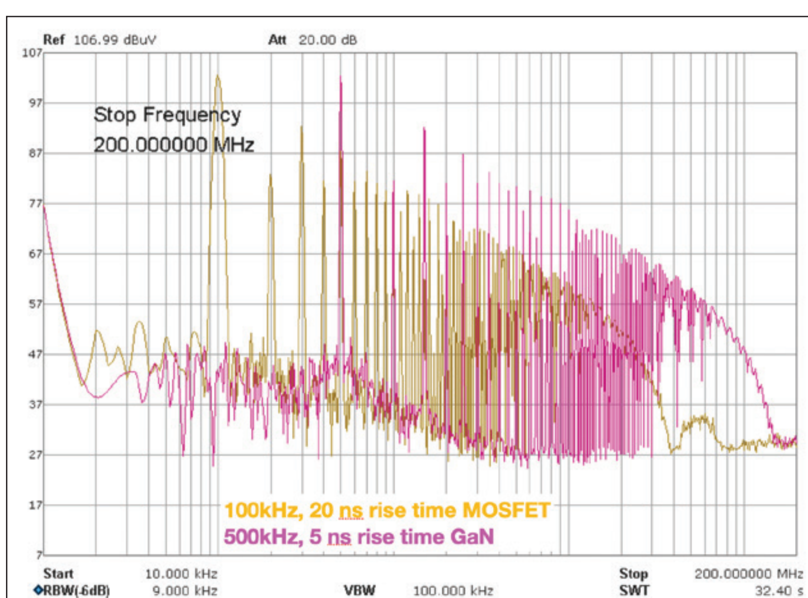

Figure 1: Near-field probe measurement of two switching devices, the device under test is a forward converter, with a duty ratio close to 50%.

Facing an EMC test failure, many engineers have chosen to swap the WBG device with a silicon MOSFET to pass EMC tests, considering time-to-market is often critical for companies to profit. But this defeats the spirit of making a higher-efficiency product. Facing greater EMI challenges, many engineers choose to "flight" rather than "fight" under time and cost pressure.

In other cases, engineers have chosen to use silicon MOSFETs based on trade-off calculations in the design. For instance, if using a WBG device results in requiring an additional filter to pass EMC, it is not a good idea as the filter would add cost and weight. But, given a good product design with EMC consideration in the design stage, it is believed that a WBG device should be the device of choice, supporting efforts to achieve the best possible product form factor and resulting in higher performance and lower cost. This can already be seen in the laptop/mobile phone charger market, where GaN chargers have started dominating the market.

THE MAIN CHALLENGES

The main EMI challenges in WBG-based power converters can be summarized as shown in Figure 2. These challenges can be categorized into different frequency ranges:

1. *150 kHz to 5 MHz range*: This constitutes the low-frequency conducted emission test range. Here, strong electromagnetic noise is generated due to the hard switching event, typically associated with the switching frequency. While most of the noise in this range is differential mode, in high-power applications with WBG devices it can also be common mode dominant, as demonstrated in [2].
2. *5 MHz to 30 MHz range:* In this range, common mode noise becomes prevalent. It's important to note the presence of a "hump" in this region, caused by structural resonance introduced by the test setup. When the device under test experiences a hard switching event, it exhibits a resonance peak in the test results [3]. The energy level is determined by the rise time of the switching event in the 10s of MHz frequency range.
3. *30 MHz to 300 MHz range:* This is the far-field radiated emission test range. In this frequency range, it is most likely that the failure mode is caused by the cable acting as an efficient antenna, leading to radiated emission issues. Beyond 300 MHz, radiated emission failures caused by power electronic devices become less common.

In addition to the EMI challenges mentioned earlier, there are other EMC-related concerns in such applications. These include low-frequency harmonics and immunity to surge and electric fast transients (EFTs). To improve harmonics and power quality performance, incorporating a power factor correction (PFC) circuit in the front end can be beneficial and has become a general practice in mains-powered products. A front-end filter can enhance immunity to surge and electric fast transients. This will be explored in more detail later.

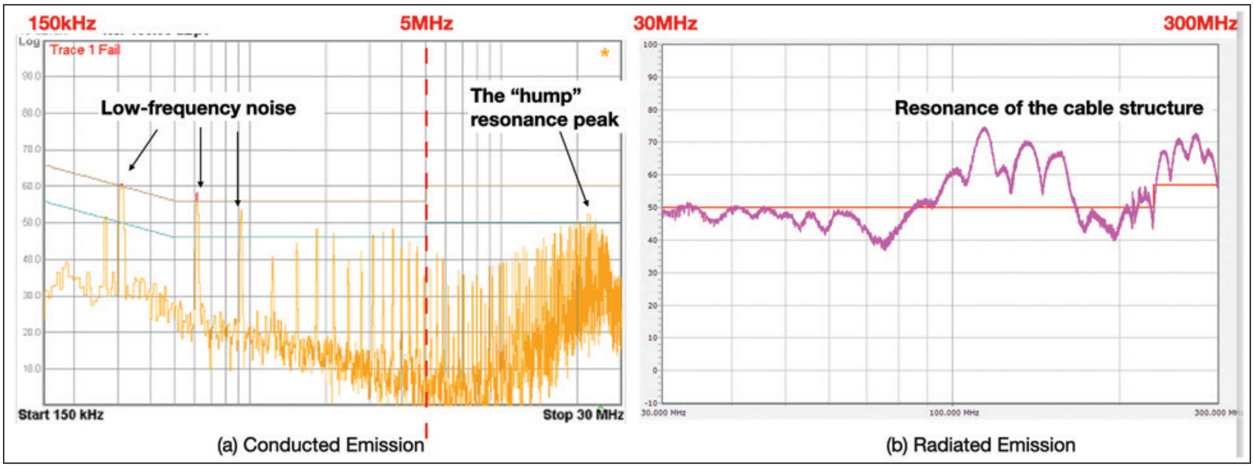

Figure 2: Common EMC test failures seen in applications with wide band gap devices

Tests	Option 1 – with a spectrum analyzer	Option 2 – with an oscilloscope
Conducted Emissions	Test the unit with a LISN (with a transient limiter preferred).	Use an oscilloscope and then perform FFT analysis.
Radiated Emissions	Measure the common-mode noise on the cables with an RF current probe and predict far-field radiation.	Measure the voltage difference between primary and secondary ground or measure the common-mode noise on the cables with an RF current probe.
Troubleshooting	Combine both options using a near-field probe and an RF current probe.	

Table 1: Proposed benchtop EMC tests for WBG applications

BENCHTOP TESTS AND TROUBLESHOOTING

Before delving into the design techniques for WBG device applications, it is essential to touch on the subject of benchtop tests and troubleshooting, which become more expensive and critical due to the unique characteristics of WBG devices:

1. *Expensive test equipment:* With faster switching frequencies and shorter rise times, an oscilloscope with a bandwidth of at least 500 MHz is necessary to accurately measure the rise time. This means investing in higher-end and more expensive testing instruments. It's worth mentioning that a 500 MHz bandwidth oscilloscope proves more advantageous for electronics development tasks than for EMC purposes (although a higher bandwidth always helps). This is particularly beneficial as engineers frequently require accurate rise time measurements to calculate switching losses and ensure overall system efficiency.
2. *Challenges with measuring:* Using a standard 500 MHz passive probe might not yield the most accurate results when measuring the switching events of WBG devices. Probe resonance and ground lead issues can introduce common impedance-induced errors, leading to inaccuracies in the measurements [4]. For precise measurements, a high-end optical isolated differential probe is preferred, but the cost of such a probe alone can easily exceed $10,000.

Moreover, the cost and lead time associated with taking the unit to an anechoic chamber for EMC tests adds further challenges to the development process. For companies with limited budgets, the high cost associated with developing new technology should not become a stumbling block. Therefore, we present here some effective and low-cost benchtop test methods that can often achieve reasonably accurate results. These methods are summarized in Table 1.

The test set-up for Option 1 is illustrated in Figure 3, where the device under test is a GaN

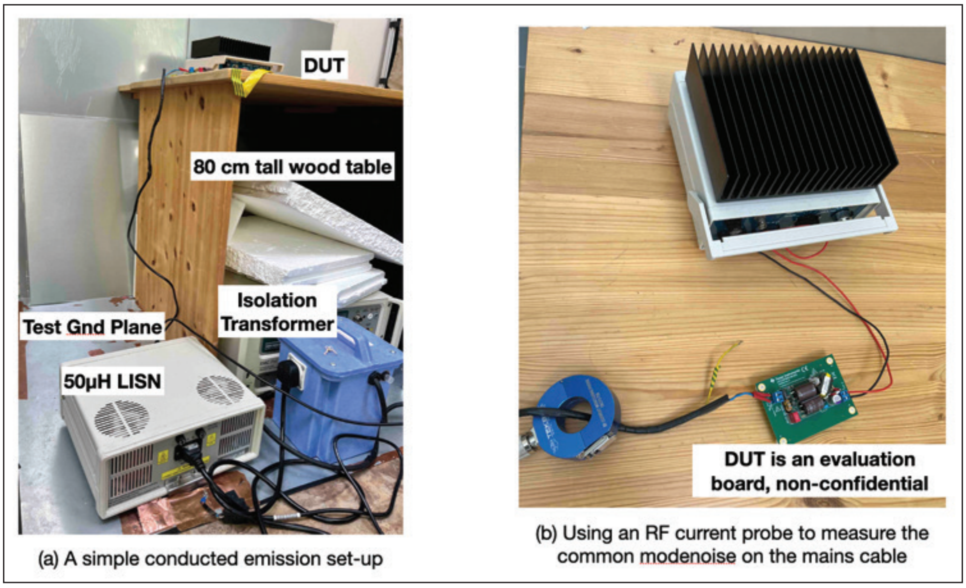

Figure 3: Proposed benchtop EMC tests, (a) measuring conducted emissions, and (b) measuring common mode current on cables to predict far-field emissions

transistor-controlled, mains-powered power supply. Conducted emission testing using a LISN is relatively straightforward, and the method of using an RF current monitoring probe to predict far-field emissions is detailed in [5].

For the Option 2 test setup, it's worth noting that one can accurately measure the rise time without the need for an expensive probe. Instead, a near-field magnetic field probe (even a simple homemade one like the 2 cm field loop in Figure 4) can be employed [6].

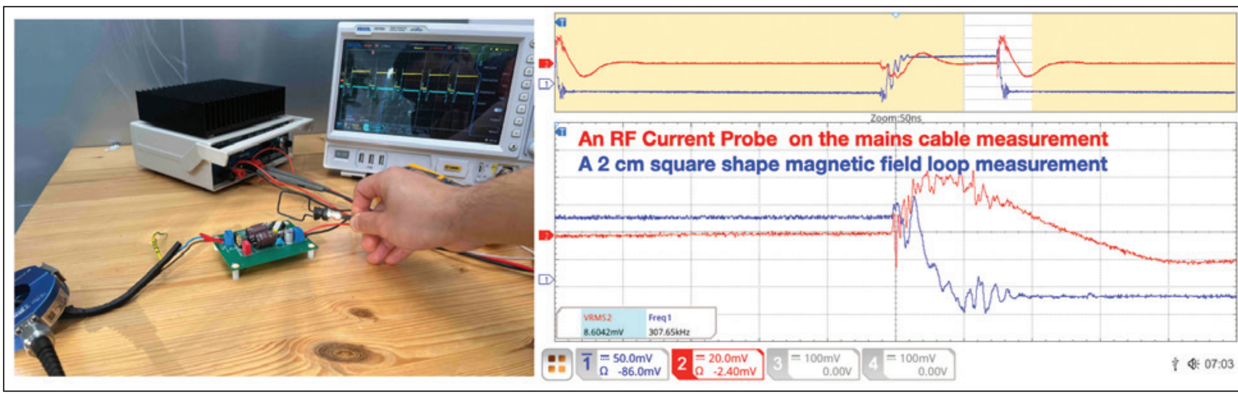

Figure 4: Using a near-field magnetic field loop to determine the switching characteristics

The significant advantage of this non-contact method is that it avoids direct electrical connections to the circuit under test, thereby eliminating common measurement errors.

Common-mode noise currents have the ability to flow between an isolated output ground (often referred to as 0V_gnd or secondary ground) and the power supply input ground (commonly known as HV- or primary ground). These currents can attain considerable amplitudes, leading to Ldi/dt voltage drops between the grounds. Additionally, when both input and outputs are wire-connected to the source and the load, these wires function as efficient dipole antennas.

A near-field probe can also serve to estimate the emissions level, although not with pinpoint accuracy; however, we can rely on some useful rules of thumb. For instance, as illustrated in Figure 5, using a square-shaped, near-field probe (with a measuring side conductor length of 1 cm in this case) to measure the potential difference between the primary and secondary "ground," any voltage exceeding 50 mV (I normally use 50 mV/cm rule) would be cause for concern in passing CE/FCC emission tests.

USEFUL DESIGN TECHNIQUES

In this section, we will delve into the converter design, front-end filter, and shielding techniques, taking a GaN transistor-based charger as an example.

For chargers below 100 watts, the most popular topology is an active-clamped flyback converter. On the other hand, for chargers above 100W, the design of choice often involves an LLC with a PFC converter. Despite the topology specifics, we can generalize this type of isolated power supply as depicted in Figure 6.

The Converter Design

In converter design, WBG devices find their primary application in the switching circuit on the primary side, including the PFC circuit (if present). However, on the secondary side, due to the lower voltage requirements,

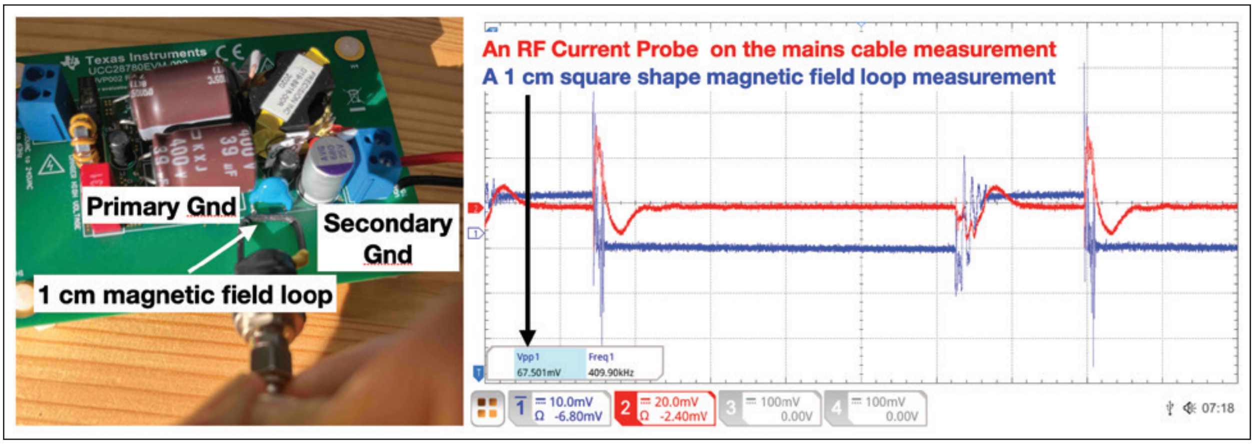

Figure 5: A 1 cm magnetic field loop can be used to predict far-field emissions

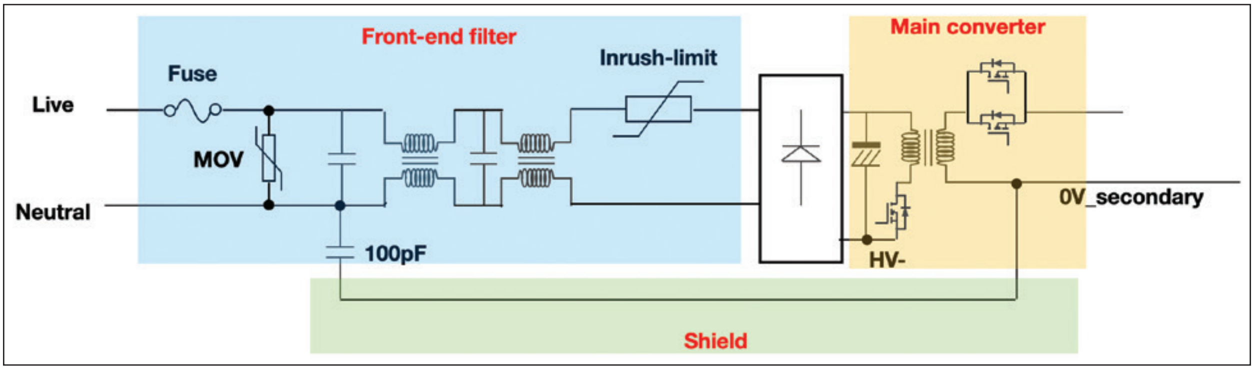

Figure 6: A simplified isolated power supply circuit

engineers tend to favor the use of MOSFETs for synchronous switching. As the power level increases, achieving this is often accomplished by either putting MOSFETs in parallel or employing interleave methods. To ensure the best EMC performance given design constraints, engineers should focus on three areas:

- *Transformer:* Whether designed in-house or bought off-the-shelf, the key consideration for EMC is the parasitic capacitance introduced by the windings. Minimizing the parasitic capacitance is essential, preferably aiming for it to be at least ten times smaller than the capacitance value of the Y-class capacitors used in such systems. Detailed design techniques for various converters are beyond the scope of this article. Another useful technique is to use a copper sheet (nicknamed "belly band") around the transformer (see Figure 7(a) on page 20). This sheet acts as a "flux cancellation" plane (as the induced eddy current forms a magnetic flux which is opposite to the transformer flux), and there is no need to "ground" the sheet, easing the manufacturing process.
- *Grounds:* Both the primary and secondary grounds should have substantial copper areas on the PCB, preferably placed on the same side, with minimal distance between them (HV safety permitted). A Y-class capacitor is essential to join the two grounds, providing a low-impedance path for common mode currents. However, the capacitance value is limited by the maximum leakage current requirements.
- *DC link capacitors:* Achieving a low-impedance DC link is crucial, and this is typically accomplished through a combination of electrolytic capacitors and ceramic caps. Film caps are not suitable for the DC link in this application due to cost and size requirements. There have been discussions within some R&D projects regarding the replacement of electrolytic capacitors with high-capacitance ceramic capacitors to achieve a higher form factor. However, this proposition faces challenges currently:

    1. Too many ceramic capacitors in parallel can lead to excessive and uncontrollable system resonance; and

2. Datasheets suggest that ceramic capacitors can exhibit very high equivalent series resistance (ESR) in the very low-frequency range, which adversely affects the performance of low-order harmonics if they replace electrolytic caps (see Figure 7 (b)).

As of now, these obstacles prevent the practical replacement of electrolytic capacitors with high-capacitance ceramic capacitors.

If not designed properly, significant ringing can be observed on the primary side switching with a GaN/SiC device. The ringing frequency depends on the stray inductance in the design (often the transformer leakage inductance) and the parasitic capacitance of the switching device. To reduce this ringing, considerable effort should be focused on the following approaches:

1. Implementing an RC snubber circuit;
2. Placing DC link decoupling capacitors close to the switch; and
3. Optimizing transformer design and implementing a shield over the transformer.

Since the primary switching event contributes significantly to high differential mode noise in the low-frequency range, minimizing the DC link impedance is crucial. This can often be achieved by optimizing the layout between the DC link and the switch. Additionally, utilizing spread spectrum techniques can help reduce low-frequency conducted emissions. From a control perspective, incorporating zero voltage switching (ZVS) as a feature in the control chip can lead to reduced switching loss and EMI.

It is worth noting that a control feature such as ZVS can sometimes introduce noise in light load conditions. It is the design engineer's job to check the EMI performance in all operation modes (light and heavy loads).

The Front-End Filter

Considering the EMC challenges posed by WBG devices, the front-end filter plays a crucial role in ensuring the product passes EMC tests. While the MOV and in-rush current limiter designs follow standard processes, special attention must be given to the RF filter design.

Employing a two-stage filter is critical. The low-frequency conducted emission failures seen in the evaluation board (in Figure 2) occur due to the sole use of a one-stage filter. The capacitors used in the front-end filter should be film-type. For a more effective solution, a typical two-stage filter should incorporate two types of common mode chokes as key magnetic components:

- A sectional wound high inductance common mode choke to suppress noise between 150 kHz and 5 MHz; and
- A bi-filar wound, low inductance common mode choke for higher frequency noise suppression.

The sectional wound common mode choke, with its numerous turns and flat wire winding, unavoidably

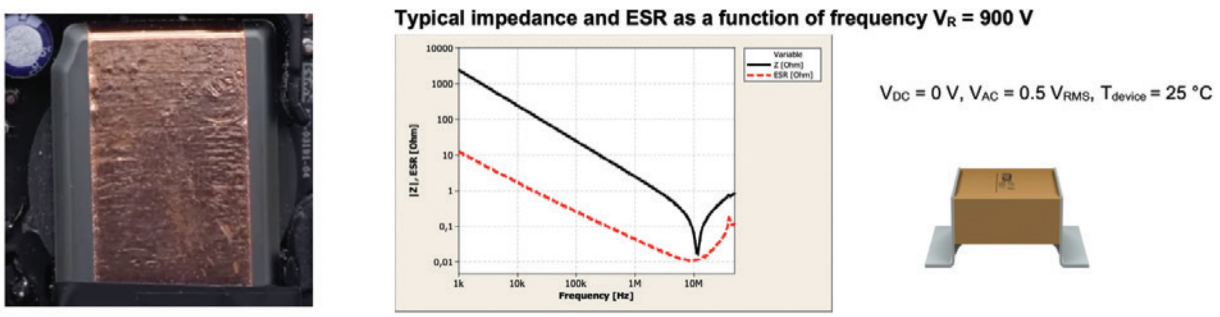

(a) "belly band" around a transformer

(b) ESR curve of an HV ceramic capacitor

Figure 7: (a) a magnetic flux band around a transformer (b) High-voltage ceramic capacitors enjoy lower ESR & ESL at high frequencies, making them perfect for WBG applications. However, it's worth noting that at low frequencies, the ESR is high, courtesy of TD

possesses high turn-to-turn capacitance, rendering it unsuitable for high-frequency suppression. However, it boasts a high leakage inductance, allowing for add-on differential mode filtering.

On the other hand, the bifilar wound common mode choke, designed for high-frequency filtering, cannot have too many turns. Its bifilar winding configuration wound on a toroidal core offers minimum leakage inductance (close to zero), making it ideal for high common mode noise suppression. Figure 8 illustrates both types of common mode chokes used in a charger.

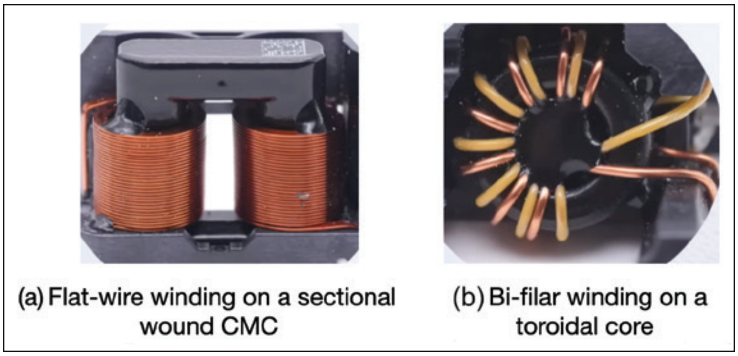

Figure 8: Two types of common-mode choke used in a front-end filter; photo taken from a 140 W Apple charger

By strategically combining these two-stage filters with different choke designs, a comprehensive and effective front-end filter can be achieved, ensuring successful EMC performance for WBG-based devices.

The Shielding

In a GaN charger, a thin aluminum or copper sheet is often employed to further enhance EMC performance. While the metal's thickness means it may not be as effective for low-frequency magnetic fields, the shield serves its purpose due to the following reasons:

1. When wrapped around a transformer, it cancels some of the magnetic field by inducing eddy currents on the metal sheet; and
2. It provides electrical field shielding when properly "grounded." For manufacturing convenience, the ideal "grounding" point should be 0V_ground on the secondary side of the transformer. The other grounding point should be the earth point (if present). In the case of safety Class II products, where user protection from electric shock is achieved through two levels of insulation (double or reinforced) without the need for earthing, the shield is often connected to the neutral line via a small Y-class capacitor, as depicted in Figure 6.

SUMMARY

This article aims to educate design engineers who are tasked with creating a product using wide-band-gap devices like GaN or SiC transistors. We've introduced the EMC challenges associated with WBG devices and propose cost-effective benchtop tests and troubleshooting methods. Additionally, we've presented useful design techniques that design engineers can follow to ensure their product's compliance when conducting EMC tests for the first time.

REFERENCES

1. M. Zhang, "Demystifying EMC in an Electric Vehicle's Drive Unit," *Interference Technology.* https://interferencetechnology.com/demystifying-emc-in-an-electric-vehicles-drive-unit
2. M. Zhang, "Troubleshooting Low-Frequency Common Mode Emissions," *Signal Integrity Journal.* https://www.signalintegrityjournal.com/articles/2965-troubleshooting-low-frequency-common-mode-emissions
3. T. Williams, *EMC for Product Designers,* Fifth Edition, Newnes, 2017.
4. D. Smith, *High Frequency Measurements and Noise in Electronic Circuits,* Springer, 1993.
5. M. Zhang, "In-Situ Radiated Emission Testing of Large Systems Installations," *In Compliance Magazine,* July 2023. https://incompliancemag.com/article/in-situ-radiated-emission-testing-of-large-systems-installations
6. S. Sandler, "How Fast is the Switching Speed of a GaN Switch?" *Signal Integrity Journal.* https://www.signalintegrityjournal.com/blogs/15-extreme-measurements/post/2309-how-fast-is-the-switching-speed-of-a-gan-switch

LOCAL PCB LAYOUT TWEAKS FOR IMPROVED SIGNAL INTEGRITY WHEN USING ESD PROTECTION DEVICES

Slight increases in line impedance can significantly improve the SI behavior of high-speed links

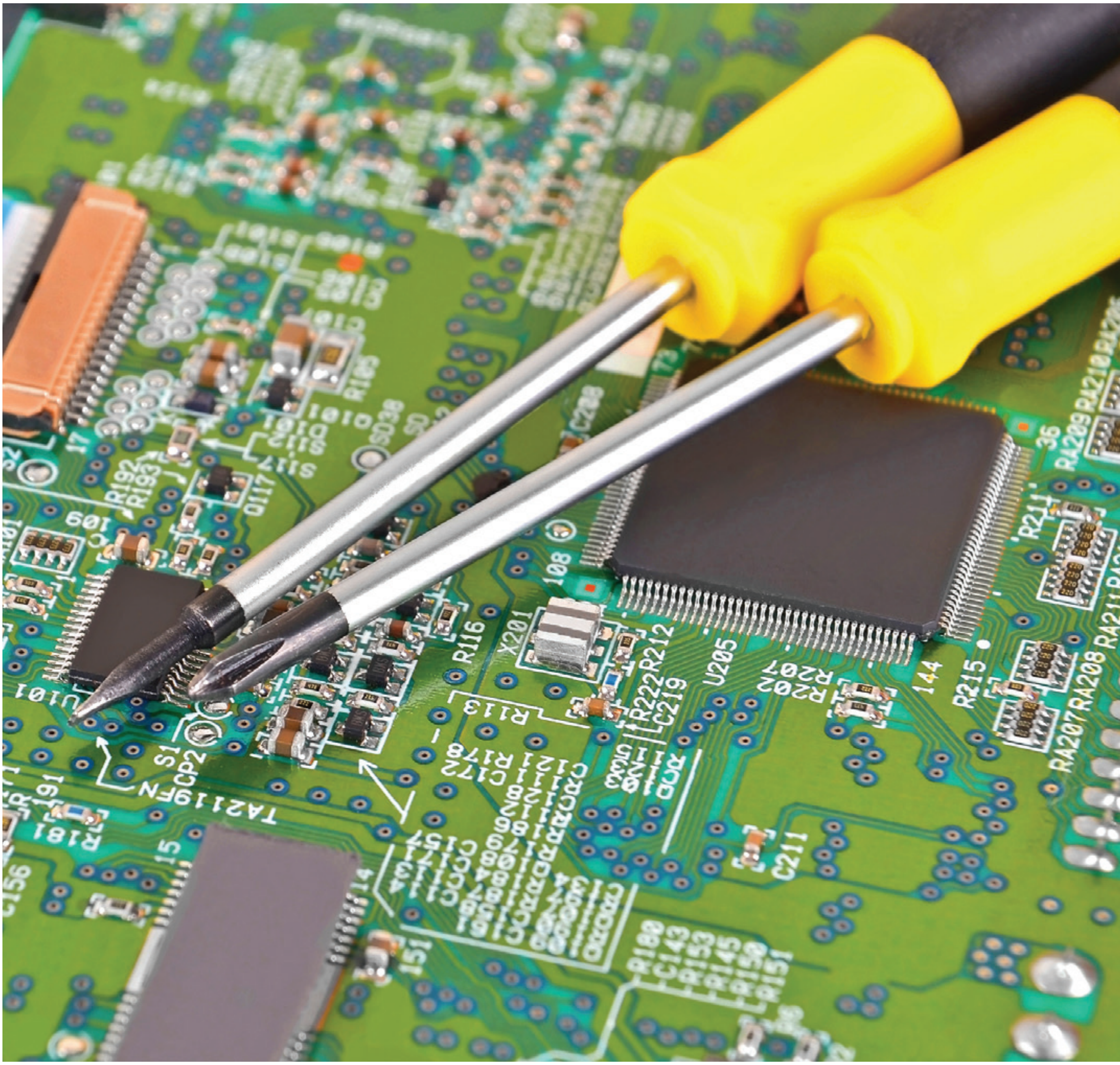

Andreas Hardock is a Principal Product Application Engineer at Nexperia, with a focus on ESD and EMC issues impacting the automotive domain. He can be reached at andreas.hardock@nexperia.com.

Martin Pilaski is responsible for worldwide product application support of Nexperia's bipolar discretes portfolio, with a focus on ESD and EMC for mobile, portable, consumer, and computing applications. He can be reached at martin.pilaski@nexperia.com.

By Andreas Hardock and Martin Pilaski

High-speed interfaces are essential to satisfy the need for processing massive amounts of data. In all market segments, from consumer and computing to industrial and automotive, the trend is to introduce innovative technologies or to increase the data rate of existing interfaces to reach gigabit speeds. The computing segment usually leads the race for higher data rates. Just recently, the USB standard was extended to support 80Gbps with its latest revision USB 4.2. In automotive ethernet applications, the data rate will increase up to 25Gbps over a single differential pair.

The extremely high functional density of physical layer (PHY) circuits for all these high-speed interfaces usually does not allow robust on-chip protection against electrostatic discharge (ESD). That is why external ESD protection devices are used to fulfill the system's ESD requirements. Besides the ESD requirements, all high-speed interfaces need to fulfill the requirements on signal integrity (SI). The ESD device itself introduces a discontinuity into the interface and might violate the limits of SI.

In this article, we will show how the SI of high-speed interfaces including an ESD protection device can be improved by modifying the layout of printed circuit boards (PCB).

CONCEPT

In detail, the ESD device can be seen as a small capacitance. In a single-ended configuration, this ESD device is placed on a transmission line, e.g., a microstrip line (MS) as shown in Figure 1a.

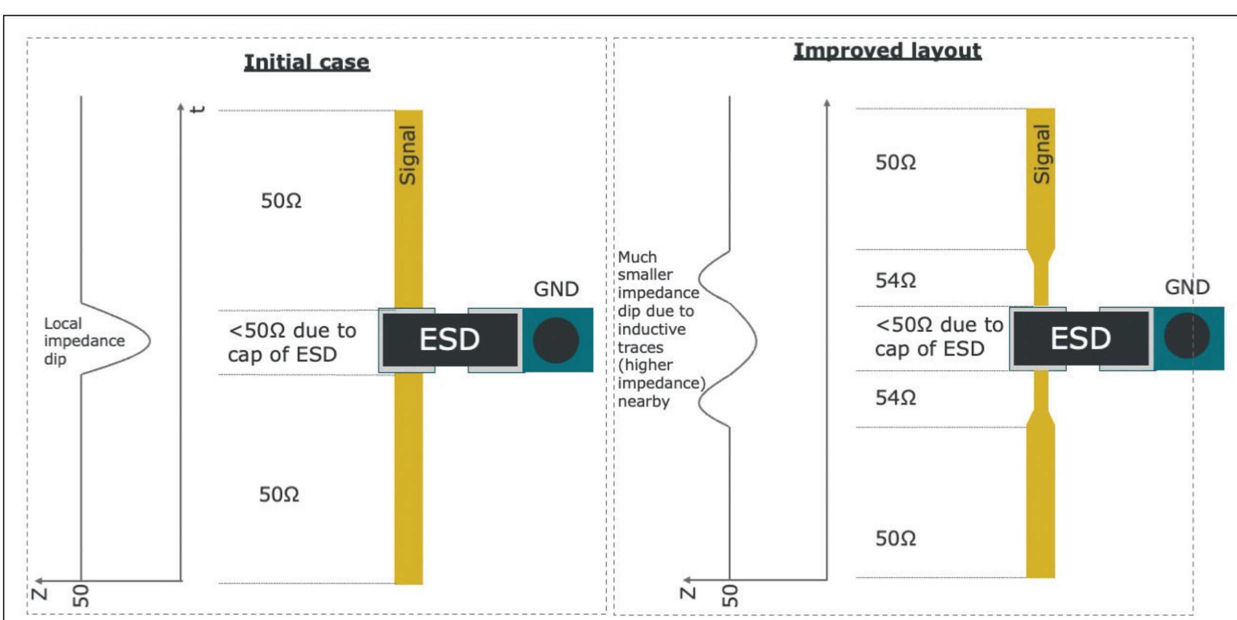

Figure 1: ESD protection in an interface placed on a 50Ohm transmission line. 1a (left) with 50 Ohm impedance, 1b (right) with local 54 Ohm impedance

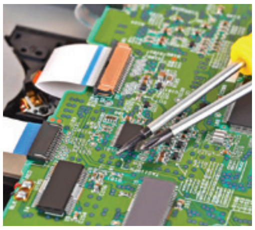

From the microwave theory's point of view, the increase of the impedance means that trace becomes more "inductive," which in our case can compensate for the capacitance of the ESD protection device.

In microwave theory, the impedance (Z) of a transmission line is mainly defined as the square root of the ratio of the intrinsic inductance and capacitance (C) per length (L), as follows:

$$Z = \sqrt{\frac{L}{C}} \tag{1}$$

This means that the ESD device locally introduces an additional capacitance to the MS's impedance. This can be clearly seen as an impedance drop in the impedance profile which can be determined by means of time domain reflectometry (TDR, see Figure 1a). Such an impedance drop can potentially violate the SI limits (usually ± 10% of the system impedance which is typically 50Ω and 100Ω for single-ended and differential, respectively).

One highly effective method to overcome this is to modify the impedance of the trace around the ESD protection device. Since the ESD device lowers the impedance due to its capacitance one can locally increase the value of the MS impedance (typically within the limits of 10%) as shown in Figure 1a.

From the microwave theory's point of view, the increase of the impedance means that trace becomes more "inductive," which in our case can compensate for the capacitance of the ESD protection device. In the impedance profile, it can be observed that the microstrip line pushes the impedance at the ESD device back to the targeted system impedance, e.g., 50 Ω, as shown in Figure 1b.

To verify the theoretical considerations which were presented before, two simulations were performed in

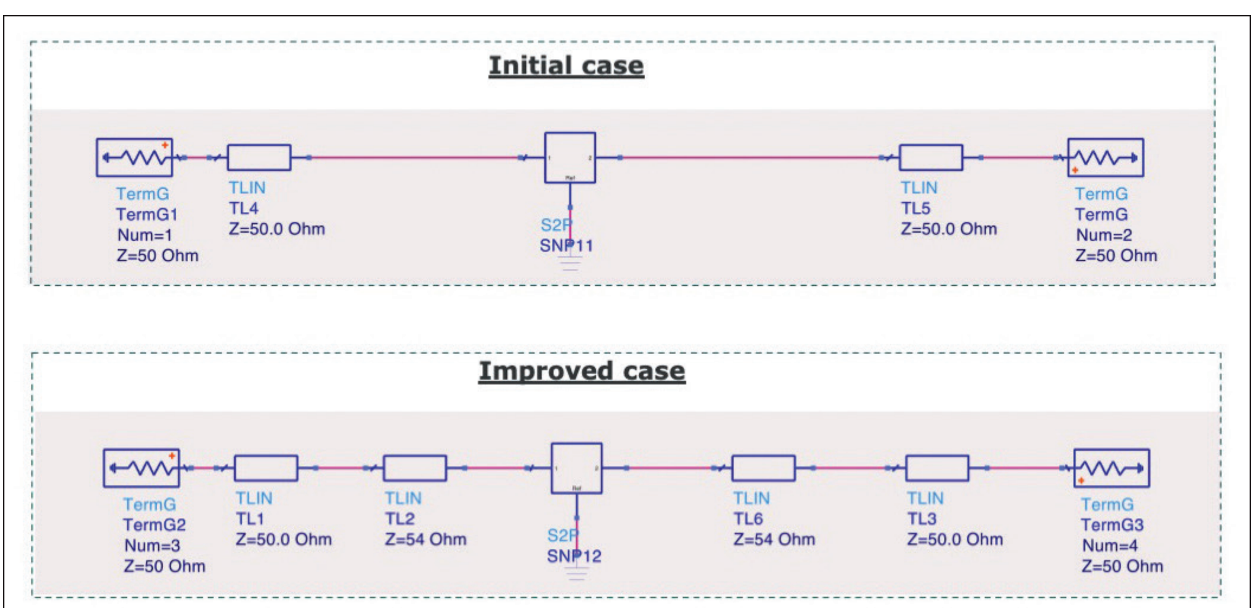

Figure 2: Simulation set-up for the initial and the improved case. For transmission lines build-in models from ADS are used. For ESD protection, device-measured S-parameters are used.

Keysight ADS using built-in transmission line models and measured scattering parameters (S-parameters) of a real ESD device. The setups for both cases are shown in Figure 2.

SIMULATION RESULTS AND IMPLEMENTATION ON A REAL PCB DESIGN

The S-parameters used in this example originate from an ESD protection device with a device capacitance of 0.3 pF that comes in a two-terminal, leadless DFN1006 package, with a pitch of 0.65 mm and body dimensions of 1 mm x 0.6 mm x 0.47 mm. This package is frequently used in gigabit applications with frequencies up to several GHz. The S-parameters are measured via VNA.

Example designs of 50 Ω microstrip lines that can accommodate the aforementioned package are shown in Figures 3a and 3b on page 26. Simulating the impedance profile using TDR with a rise time of 100 ps for these components results in the graphs in Figure 3a. It shows an impedance drop down to 43.5 Ω, which is caused by the ESD protection device. This can be a violation of the SI limits for some sophisticated applications such as HDMI.

Based on the concept introduced before, a short section of the transmission lines on both sides of the ESD device is tuned to an impedance of 54 Ω. The resulting microstrip line dimensions are shown in Figure 3b. A simulation of this design yields an improvement of the overall impedance profile as can be seen in Figure 3b. The impedance drop can be successfully reduced from roughly 43.5 to 47 Ω which is typically within the SI requirements.

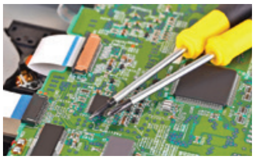

Unfortunately, what sounds like the perfect trick to mitigate the impact of the ESD protection impedance does not come without consequences.

Unfortunately, what sounds like the perfect trick to mitigate the impact of the ESD protection impedance does not come without consequences. The downside is that shifting the PCB trace impedance up for a short section may cause SI problems when the impedance of the PCB deviates from its target due to production spread. Local impedance tuning plus an upward production shift may violate an upper impedance boundary. Thus the length of the modified microstrip line section needs to be made just as long as needed to compensate for the drop that is caused by the ESD protection capacitance.

To find the optimum length, we refer to the impedance equation for a typical transmission line, as shown in *Microwave Engineering* by Pozar, Fourth Edition, p 148:

$$Z_0 = \begin{cases} \dfrac{60}{\sqrt{\varepsilon_{eff}}} \ln\left(\dfrac{8d}{W} + \dfrac{W}{4d}\right) & (\Omega) \;\; for \dfrac{W}{d} < 1 \\ \dfrac{120\pi}{\sqrt{\varepsilon_{eff}}\left[\dfrac{W}{d} + 1.393 + 0.667 \ln\left(\dfrac{W}{d} + 1.444\right)\right]} & (\Omega) \;\; for \dfrac{W}{d} > 1 \end{cases} \tag{2}$$

Here, $\varepsilon_{eff} \approx (\varepsilon + 1)/2$, d is the thickness of the prepreg and W is the width of the transmission line. From this formula, we can further calculate the value for capacitance per length by

$$C' = \frac{\sqrt{\varepsilon_r}}{Z_0 C_0}$$

where c_0 the is the speed of light.

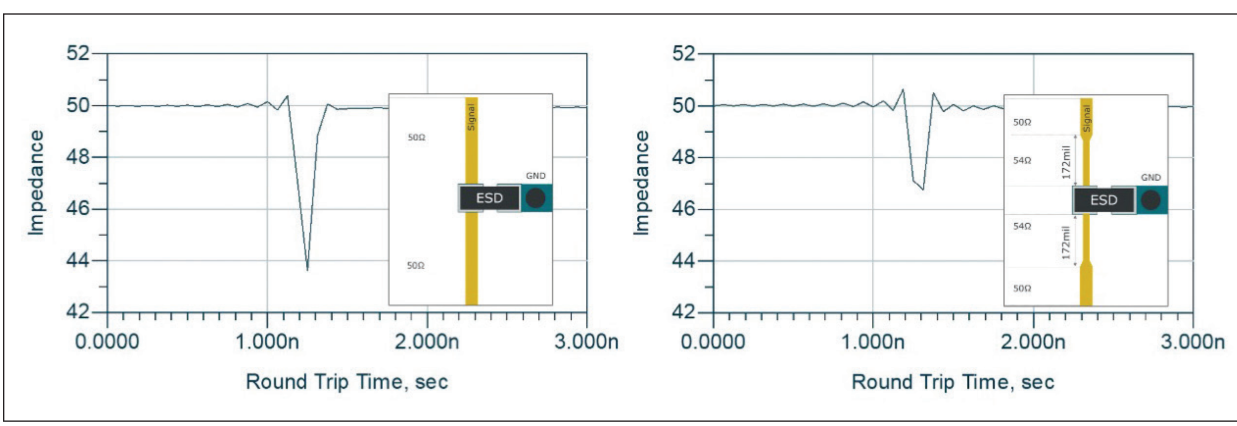

Figure 3: Results for the initial case (3a, left) and the improved case (3b, right) with adding a 54 microstrip line with the length of 172mil (4.1mm). An improvement of roughly 3.5 Ohms can be observed.

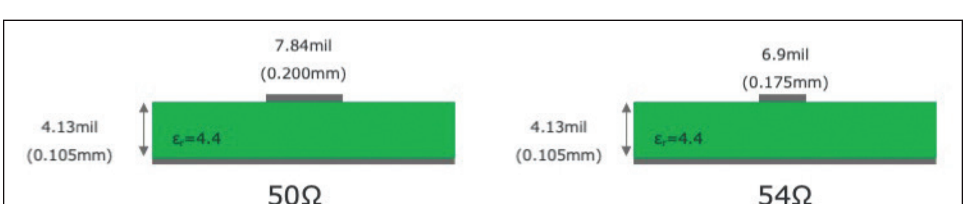

Figure 4: Example of a 50Ohm (4a, left) and 54 Ohm (4b, right) configuration of a microstrip line just by reducing the width of the trace

In our specific example, we see that our impedance in the TDR drops down to 43 Ω. The capacitance per length for a 43 Ω microstrip line is 0.14 pF/mm. With 0.3 pF of added ESD device capacitance, this leads to an equivalent microstrip line length of 2.1 mm (86mil).

We can now take this value to estimate the length of the higher impedance trace which we want to add to compensate for the capacitance. Based on our experience, it is most efficient to take roughly double the length, which is then 4.2 mm (172 mil). As outlined in Figure 3b, the resulting microstrip line has one impedance-adjusted section of the calculated length before the ESD protection footprint and one behind it.

It should be mentioned that the length of the microstrip line section tuned to 54 Ω should not be too short to be efficient but also not too long due to reflections when the added piece of microstrip is in the range of the wavelength. In our case, the wavelength at 7 GHz for a microstrip is roughly 79 4mil (20 mm). We estimated 172 mil, so we are in an acceptable range without expecting any reflections in this frequency range.

In addition, the presented concept works to compensate for capacitive discontinuities which are electrically not too long. It means the dimension of the discontinuity should be $<\lambda/4$. This is usually valid for most of the high-speed links just because the dimensions of the ESD devices used for those applications are very small (0603, 0402, or smaller). So, in most cases, we can consider the ESD device much smaller than the frequency range of interest.

Without a doubt, the main advantage of this method is its simple way of implementation. To achieve an increased transmission line impedance, just a slight reduction of trace width is needed. An example is shown in Figure 4 based on a microstrip configuration in FR4 (ε_r=4.4). In order to realize the intended tuning, the trace width needs to be reduced by roughly 1 mil (0.025 mm). All other parameters can be left untouched. This easy-use fact makes this method very easy to implement and, hence, very effective. There are many tools for calculating the trace impedance which are available to all users for a broad range of uses.

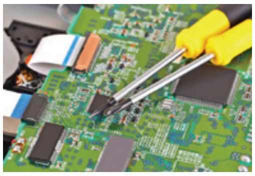

In this article, we have shown that slightly increasing the line impedance adjacent to a discontinuity can significantly improve the SI behavior of high-speed links.

In addition to the time domain simulation results previously presented, a performance improvement can also be observed in the frequency domain. Looking at the simulated S-parameters, shown in Figure 5, the bandwidth shows an increase up to 7.5 GHz for the IL and RL.

To focus once again on the length of the additional trace. Figure 6 compares the S-parameters between the initial case and a modified case where the additional trace is too long, which means that it is 800 mil (ca 20 mm) which corresponds roughly to 1λ. The IL is dropping at some frequencies (@4 GHz and 8 GHz) and the RL is increased correspondingly. From the microwave theory point of view, when we increase the length of the high impedance trace, we observe that more reflections stepping into the frequency range of interest decrease the SI performance of the link.

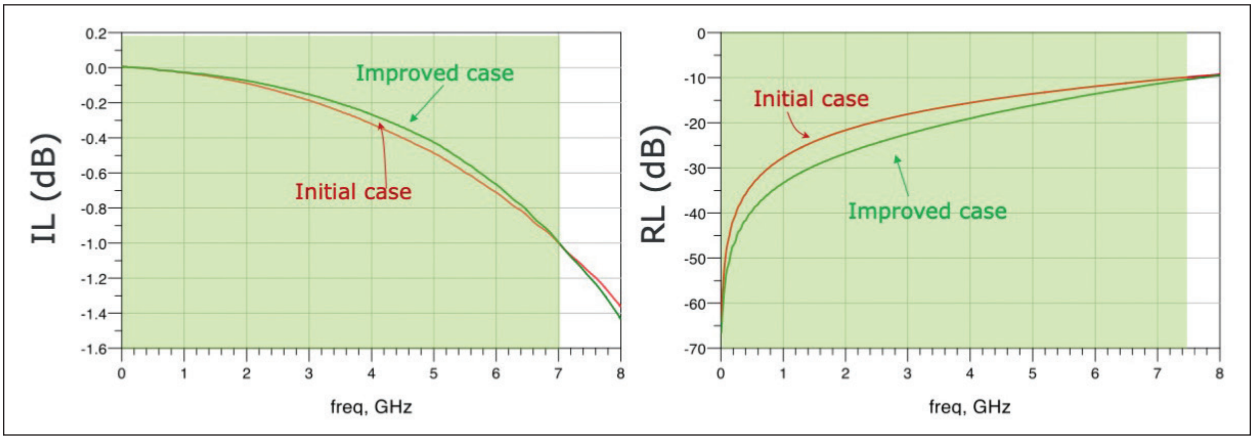

Figure 5: Results for the initial and the improved case in the frequency domain using S-parameters. In 5a (left), the IL is significantly improved up to 7 GHz. In 5b (right), the RL is improved up to 5dB in the range of up to 7.5 GHz.

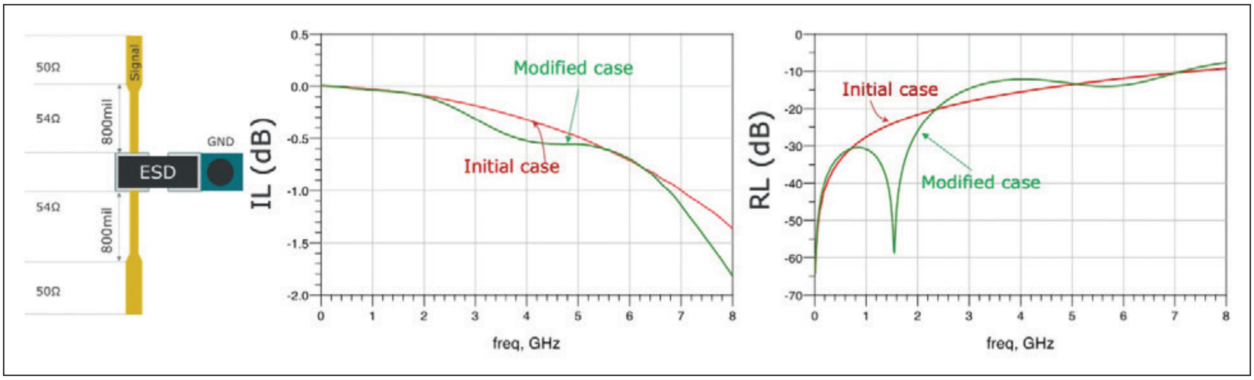

Figure 6: S-parameter for a modified case with a much too long compensation trace. The trace is in the range of the wavelength (800 mil) and the reflections due to the mismatch are now in the frequency range of interest.

CONCLUSION

In this article, we have shown that slightly increasing the line impedance adjacent to a discontinuity can significantly improve the SI behavior of high-speed links. In a real PCB design, this impedance increase can be achieved by simply narrowing down the trace width which is in most cases quick and easy to implement. The length of the changed line segment can be calculated from the capacitance per length and should be below the quarter wavelength of high frequency of interest. This makes this method very easy to use.

However, it should be mentioned that for some PCB technologies with higher manufacturing tolerances, the impedance range can be violated by introducing this method. In addition, this method works only when the rise time of the TDR signal is not too short. In this case, a rise time of 100 ps was used. For much shorter rise times with greater resolution, this method might deliver expected results. The length of the trace should be not too long which would lead to additional reflections and limiting the link performance.

IS WIRELESS MEASUREMENT OF HUMAN BODY VOLTAGE POSSIBLE?

Why human body voltage is important in managing ESD and how to measure it

Jonathan Tapson is the
Chief Technology Officer at Iona Tech,
and can be reached at jon@ionatech.com.

Daan Stevenson is the
Chief Executive Officer of Iona Tech,
and can be reached at daan@ionatech.com.

By Jonathan Tapson and Daan Stevenson

Our ability to measure the charge accumulated by a human being is a critical part of managing electrostatic discharge (ESD) in industrial environments. Unfortunately, these measurements require that the person involved is connected by wire to a high-impedance or electrostatic voltmeter. This is fine in the laboratory but severely limits our possibilities on the factory floor. In this article, we describe how wireless measurements of human body voltage can be made, and why they are important for ESD managers.

INTRODUCTION

It's been a long time since any of us had to untwist a telephone cord to put a handset back in the cradle. But we still seem to have an awful lot of cables and wires to contend with on the factory floor. Wi-Fi networks and IoT sensors are reducing the clutter, but it seems as though there are some domains, particularly in managing ESD, where we still have to have a physical wire connection to remove charge or make a measurement. So we're going to question one of the sacred cows of electronics by asking: do we really need wired connections to measure the voltage on a person's body?

Controlling human body potential and static charge is a key part of any ESD control program, and actually measuring body voltage is how we validate these programs. For example, the ANSI/ESD STM 97.2, *Floor Materials And Footwear – Voltage Measurement in Combination With A Person*, requires a "walking test" in which an operator walks on the floor while holding an electrode connected to a charge plate monitor (effectively, a very high impedance voltmeter). The operator's voltage is recorded while they walk, and the limits of body voltage determine whether the floor is compliant or not.

The ANSI/ESD standard itself illustrates why wired measurement is a problem here. The operator can't actually walk because they're wired to a fixed instrument. Instead, they perform a statutory set of steps in place (colloquially known as the "ESD Shuffle") which look exactly like a 1950s dance class, right down to the numbered foot movements (Figure 1). To be fair, the test is also designed to qualify small areas of flooring, but many ESD managers would much rather have a method and hardware that would allow them to properly qualify large areas of floor by walking around.

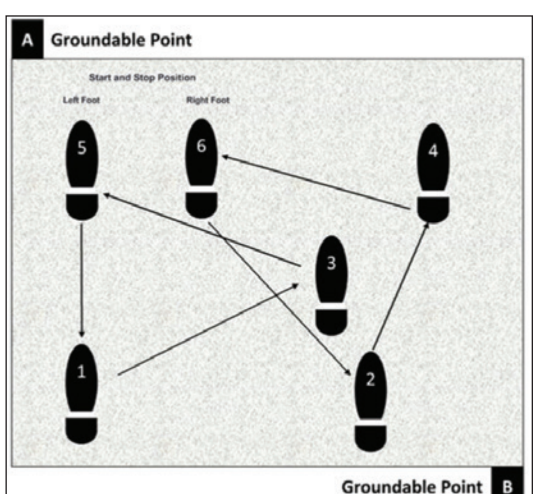

Figure 1: The "ESD Shuffle" as described in the ANSI/ESD STM 97.2 standard – to qualify small areas of flooring with a wired voltmeter, this is how we simulate a "walking" test. The steps are confined because the operator has a wired link to the voltmeter, and the floor area is constrained.

If we can measure body voltage wirelessly, it opens up a wide range of possibilities, where we can continuously monitor the voltage of all our personnel across the entire factory environment. This enables real-time detection of ESD hazards such as non-conducting floors and static-generating equipment. The data gathered on ESD performance becomes a new and useful input into statistical process improvement methods such as Six Sigma and Lean Manufacturing.

WIRELESS VOLTAGE MEASUREMENT

The first point to make about wireless voltage measurement is that we've been using it for years in the form of surface (electrostatic) voltmeters or field meters. These voltmeters measure the electric field generated between the measured object and the voltmeter and convert it to a voltage measurement. However, the voltmeter itself usually requires a ground reference of some kind. But it's possible to simply turn the voltmeter around – we can mount it on the object to be measured and derive the voltage from there.

The key to this type of wireless voltage measurement lies in understanding the relationship between charge, capacitance, electric fields, and voltage. We remember from basic electrostatics that all conductors have an intrinsic self-capacitance. For example, a conducting sphere has $C = 4\pi r\varepsilon$, where r is the sphere radius and ε the permittivity of the surrounding insulator (usually air, for which we approximate ε_0, or the permittivity of free space). Human beings have a self-capacitance. The standards use 100 pF as a generic value, but most people's self-capacitances are significantly larger (we've measured 231 and 205 pF, respectively).

When a conductive object or person acquires charge q (by shuffling feet on a carpet, for example), their voltage changes accordingly: $V = q/C$. This charge distributes itself across the surface of the conductive object, with some dependency of charge density on geometry. The surface charge induces an electric field that is perpendicular to the surface and proportional in strength to the charge density, as follows:

Figure 2: A miniature electric field mill configured as a wireless body voltage monitor (with a quarter for a sense of scale). The unit is 75 x 43 x 18mm in size, weighs 44g, and can run for 18 hours on a single battery charge.

Figure 3: A person wearing a wireless body voltage monitor. The unit is worn over an ESD smock, with the sensor pointing outwards. The upper arm has a good combination of practicality, being close to the body core, while also unlikely to be obstructed by other body parts, and not being obtrusive.

$$E = \frac{q}{A\varepsilon_0}$$

where E is the DC electric field and A is the area over which the charge is distributed.

So, if we can measure the electric field E at the surface, and we can estimate the area A and self-capacitance C, then we can approximate the voltage as follows:

$$V = \frac{EA\varepsilon_0}{C}$$

Note that the area and self-capacitance of a conductor tend to be proportional, so errors in estimation tend to cancel each other out here.

PRACTICAL WIRELESS BODY VOLTAGE MEASUREMENT

We have implemented this method by using a novel wireless miniature electric field mill to measure the DC electric field mill on a person's body. This sensor is about half the size of a pack of cards and weighs less than 50 g (see Figure 2).

We have chosen to wear the sensor on a hook-and-loop strap on the upper arm. The upper arm is chosen because it is close to the bulk of the body, and the sensor is characteristically pointing out. If the sensor were mounted on the wrist, say, there could be two problems. The first is that as a body extremity, the wrist is less likely to reflect a charge density representative of the average body charge density. The second is that if the wrist is tilted so that the electric field sensor points towards the chest, the field measured will be that of the interior of the conductive surface, i.e., close to zero.

Figure 3 shows the sensor unit in use on a wearer's arm. The unit is enclosed in a conductive housing and is connected to the wearer's skin in one of two ways: either it is worn with a short-sleeved shirt so that the base plate is directly contacting the skin, or it is worn over a conductive smock so that the surface of the smock effectively becomes the conductive surface of the body.

Figure 4 shows a comparison of the body voltage measured using the wireless sensor and a simultaneous measurement made with a gold-standard electrostatic voltmeter (a 3M Model 711 Charge

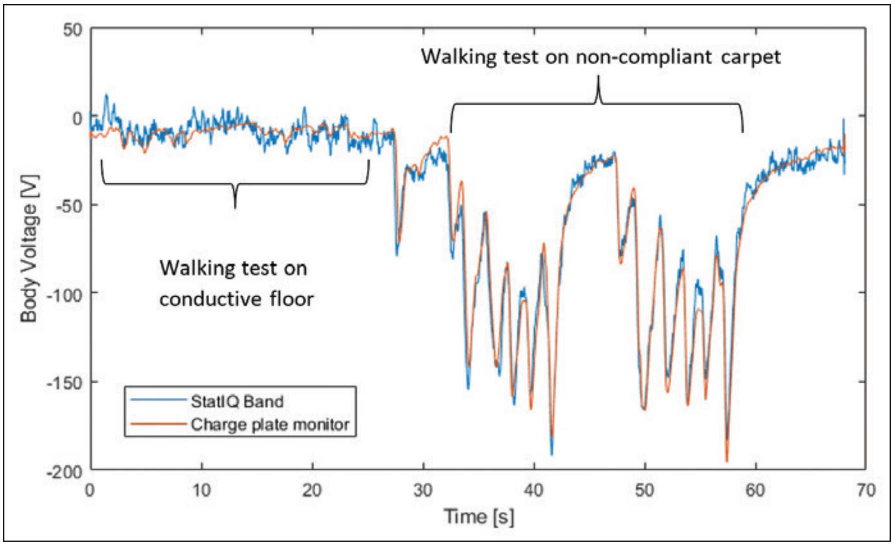

Figure 4: Comparison of a wireless body voltage monitor (the StatIQ Band) with a 3M Model 711 charge plate monitor and handheld electrode. It can be seen that, while the bandwidth of the signals is different, the voltage recorded is essentially identical.

Analyzer). It can be seen that while the dynamics of each signal are somewhat different, owing to different noise filter time constants, the signals are essentially identical.

The differences between the wireless measurement system and any conventional electrostatic voltmeter are typically of the same order as the differences between any two conventional electrostatic voltmeters. This is not surprising given that all of these systems are using the same basic sensors (either rotating electric field mills or vibrating non-contact electric field sensors). In the case of electrostatic voltmeters, the sensor is pointed at a plate that is at approximately the same potential as the user. In the case of our wireless measurement, the sensor is mounted directly on the user and is pointed into free space.

The astute reader will be wondering about the assumptions that are necessary for this method to work. Briefly, they are:

- The field perpendicular to the body at one point should be representative of the average field induced by the average charge density on the body;
- The charge density under the sensor is representative of the charge density of the whole body;
- The field induced at the point of measurement is not significantly affected by external sources of charge; and
- The total capacitance of the body does not increase significantly from the self-capacitance.

All of these assumptions are valid under a wide range of conditions of interest. The most commonplace departure from them is when there is a strongly charged object in close proximity to the user. (This is most often another person, ungrounded, wearing a synthetic fiber garment; or a piece of office furniture, such as a chair, made with insulating plastics.)

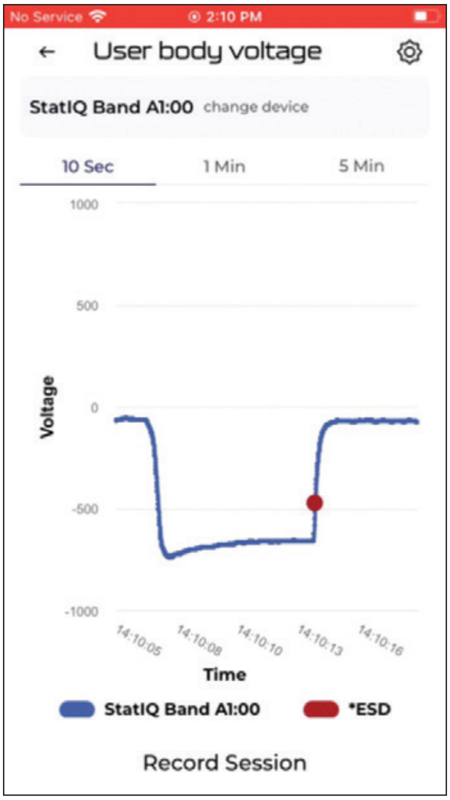

Figure 5: A screenshot from our mobile phone app showing the detection of an ESD discharge event (the red dot) superimposed on the voltage waveform (blue) measured by the wearable device. It can be seen that the discharge is assessed as being approximately 500V, allowing an ESD manager to make an immediate decision as to whether the workpiece that received the discharge was likely to be damaged or not.

In practice, we are finding that wearing appropriate ESD garments is the single biggest factor in achieving accurate measurement. A person clad in an ESD smock and hat can achieve errors of less than 10V when compared to charge plate analyzer voltmeters. Cotton apparel also gives good results, with errors of typically less than 100V. Not surprisingly, if the device is worn over synthetic apparel, the accuracy degrades significantly, with errors up to 1000V being possible.

The second most common source of error is a charged object in the environment. We have used this feature to "sanitize" our workplace for ESD, as it very quickly reveals the location of any charge. Simply hold a ground point in one hand and then rotate until the device shows a non-zero voltage, at which time the device will be pointing at the errant source of charge. However, there are some sources of charge you simply can't control. For example, we have found that if you use the device while standing next to a picture window with a thunderstorm brewing outside, the strong atmospheric electric field can create a small error in measurement!

Given that the measurement is intrinsically wireless, it makes no sense to interface it to a PC or similar display except by wireless network. The device has a Bluetooth network interface, and we are able to view the data on a mobile phone app or via a browser on a Bluetooth-enabled PC. This makes mobile use of the system within the workplace very simple.

A novel application of this system is that, because we have a real-time measurement of the body voltage, we can detect when a static charge has been discharged from the body into an object (such as a PCB). We do this simply by detecting sudden reductions in body voltage, which allows us to establish a rate of voltage change dV/dt, which is unambiguously a discharge to ground. Figure 5 shows such an event displayed on a mobile phone app. We can measure the actual magnitude of the discharge in voltage terms, allowing an ESD manager or production manager to make an educated guess, on the spot and in real time, as to whether the system which received the discharge should be assessed for ESD damage.

WHAT NEXT?

The ability to wirelessly measure and log the voltage of people and objects in the workplace opens a host of possibilities for ESD control. The obvious applications are to monitor the effectiveness of current ESD mitigation strategies and also to enable ESD safety in cases where continuous grounding is difficult or impossible. In addition, the same physics that applies to personal voltage measurement also applies to objects (with some adjustment factor for self-capacitance).

For example, carts and trolleys, which are the bane of many an ESD manager, can be actively monitored, with alarms generated when they exceed a safe voltage level. In the chemical transport industry, the presence of static on vehicles is an ever-present combustion hazard, and the ability to measure vehicle static levels could be a considerable boon to that sector.

We are in the infancy of understanding this measurement technique, but the sky is the limit (literally – airplanes have their static buildup issues too!).

(RE)DISCOVERING THE LOST SCIENCE OF NEAR-FIELD MEASUREMENTS, PART 4

Understanding Radiated Emissions Measurements Made at One-Meter Separation:
It's Not What You've Been Led to Believe

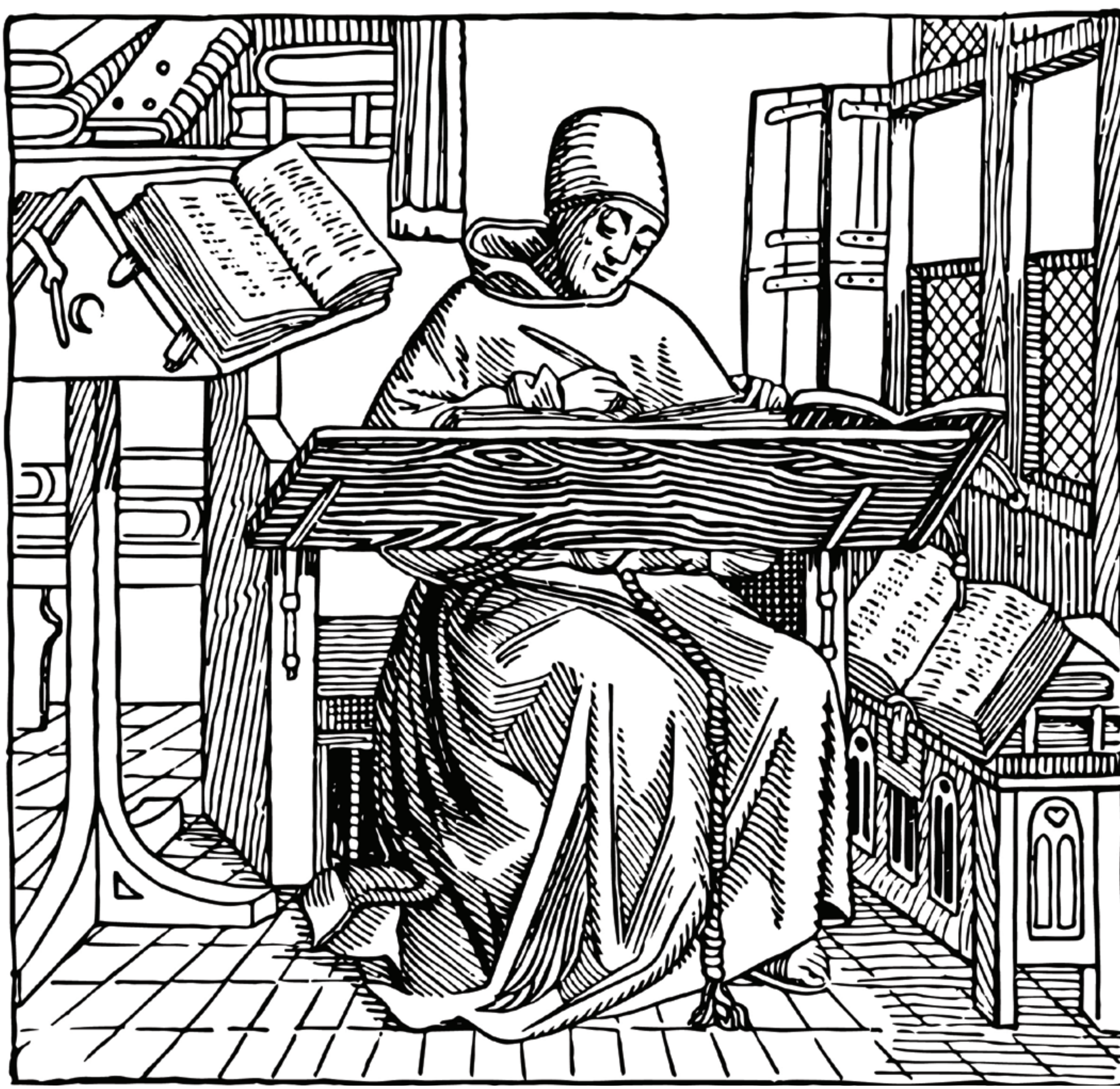

Ken Javor is a Senior Contributor to *In Compliance Magazine* and has worked in the EMC industry for over 40 years. Javor is an industry representative to the Tri-Service Working Groups that maintain MIL-STD-464 and MIL-STD-461. He can be reached at ken.javor@emccompliance.com.

By Ken Javor

This is the final installment of this serialized article. The first installment explained what near and far field measurements entail, and that one-meter measurements are very much near field. The second installment explained the evolution of the earlier 12" and present-day one-meter separation measurements, considerations in antenna selection, the difference between antenna-induced and field strength limits, and the evolution from one to the other. The third installment investigated practical problems arising from the misapplication of field intensity and far-field concepts to near-field phenomena.

This fourth and final installment lists theoretical misunderstandings arising from the erroneous substitution of field intensity for antenna-induced concepts and shows the serious practical outcomes that result from these theoretical mistakes.

THEORETICAL PROBLEMS RESULTING FROM USING FIELD INTENSITY LIMITS WHERE ANTENNA-INDUCED IS MORE APPROPRIATE

Ignorance of the fundamentals of extreme near field measurements and of gain derating and the nature of the Fresnel zone has pronounced and dangerous impacts on both EMI and EMC requirements and verification. The following sections provide some relevant case histories.

Conflating Radiated Emissions and Radiated Susceptibility

With radiated emission and radiated susceptibility requirements both having field intensity limits, the idea that radiated emission (RE) and radiated susceptibility (RS) control were somehow two sides of the same coin became prevalent. People claiming that one controls RE to avoid RS was enough of a problem that in 1993 instructions were included in MIL-STD-461D specifically saying that this belief is not true and that, in fact, RE limits protect antenna-connected receivers and RS limits provide a level of immunity to intentionally generated RF fields from high-power RF transmitters. These instructions have remained in all subsequent revisions of the standard.

Although the RE/RS comparison is extremely damaging, it is still assumed to be true by many engineers, often in the space community.[29] It is easy to see why: the space community doesn't typically use the rf spectrum below several hundred megahertz, so there is no need for RE limits at lower frequencies, and often no or rudimentary RS limits there. Since they have used military limits covering as low as 10 kHz without comprehending the real need for such, they substitute this incorrect duality to justify using incorrect requirements. This leads to two errors. One is complete disrespect for the discipline, since comparing stringent RE limits to even the most rudimentary RS limits shows "margins" on the order of 100 dB.

The second error is to attempt to show the "margins" aren't that high because a culprit (unintentional) emitter source may be placed very close to an (unintentional) victim receiver, requiring "scaling" of the one-meter RE limit to a distance of just a few centimeters. Such "scaling" is done using Hertzian dipole field intensity behavior vs. distance, typically third order (cube of distance ratio).[30] Such comparisons are not accurate in the extreme near field, since the Hertzian dipole derivation assumes the observation distance is large with respect to the radiating structure dimensions – clearly not the case a meter away from a two-meter-long test sample.

While Hertzian dipole equations are often applied to various EMC-related problems and analyses, it is not difficult to see that they are inapplicable or at best only partially applicable to one-meter radiated emission measurements. One need not wade through the several-page derivation in Reference 30. The inapplicability is at the very beginning, where the expression for the magnetic vector potential is derived.[31] The requirement that the distance to the observation point be large with respect to the dimensions of the radiating element is inherent in the Hertzian expression for the magnetic potential vector, from which the entire derivation proceeds. It should not be surprising that the Hertzian dipole field expressions all "blow up" close to the source. The simplifying assumption that the distance to the observation point is large with respect to the dimensions of the radiating element means that the radiating source is a point. If there is current (flow of charge) on a point source, charge separation and potential differences follow.

Reference 24 (presented in the September issue of *In Compliance Magazine* and referenced in Part 3 of this serialization) derives and shows that, in the direction of maximum radiation, the Hertzian expression for the electric field is off by 3 dB when the separation distance is twice the dipole length, and that the electric field in closer than that approaches a fixed level proportional to the charge separation divided by the dipole length. When the observation point separation is one-tenth the dipole length, the Hertzian expression is 60 dB too high.

Since 1993, MIL-STD-461 has included in the CE102 limit rationale the information that, in the rod antenna range, the relationship of the measured radiated field to the voltage on a 2.5-meter-long wire is such that the wire potential is 40 dB higher numerically than the radiated signal measured. Reference 32 provides analytical details.[32] If the wire potential is 40 dB above the signal measured a meter away, and the wire is suspended 5 cm above the ground plane (-26 dB above one meter), that makes the field intensity between the wire and ground plane 66 dB higher than at one meter. That is an upper bound on such scaling.

A shorthand model for this is shown in Figure 4 in Reference 24. One end of the dipole is now a wire suspended 5 cm above the tabletop ground plane and its image below the ground plane is the other end, for a net dipole separation of 10 cm. Looking at the circled point on Figure 4 of Reference 24, the field falls off beyond 20 cm from the wire as the cube of the distance ratio. So, from 20 cm to 1 meter away, the field falls off by a ratio of 5^3, or 42 dB. From 20 cm away from the wire to the wire, the field intensity increases by about 20 dB. The ratio of the field intensity between the wire and the ground plane beneath it to the field intensity found at a point a meter away is 62 dB. That calculation is for a pair of separated charges. The answer is within a few dB of the exact calculation for a cable of significant extent, measured not at a point but using a 41" rod antenna. Not bad, and it serves to dispel the mistaken superstition that Hertz says things should blow up.

It should be noted that this is not about radiated energy at all. This is the fringing field from a source of charge separation. In this model, the only current that could contribute to actual radiation is the displacement current between the wire and the ground plane, and using a value such as 10 pF/m yields next to no current over most of the rod antenna frequency range. The fringing field dominates, and it dominates even more so at 12" than at a one-meter separation. Citing NADC-EL-5515:

> *"In general, the ratio of the electric to the magnetic components surrounding an unshielded lead will vary directly as the impedance of the load terminating the lead, and the apparent impedance presented to the various pick-up antennas will vary in the same manner. This statement applies to radial and tangential field components as contrasted with the more usual concept of wave impedance encountered in shielding theory, which applies only to the components tangential to the line of propagation."*

One-Meter Measurements Are Not Scalable Outwards, Either

Similar to the conflation misconception just described, people attempt scaling the one-meter results to a larger distance. Figure 13 portrays this type of an error. Some people advocate changing the one-meter measurements to three meters or more, based on the assumed accuracy superiority of far-field measurements. Some advocate for including the option of three-meter measurements in lieu of a one-meter measurement. The erroneous assumption is that one can adequately replace the other. As explained earlier, there are two errors here: 1) the radiation source is not

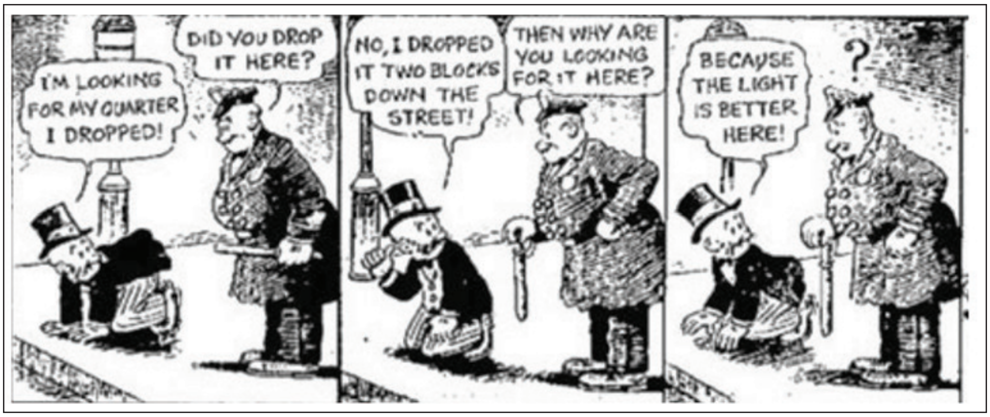

Figure 13: Controlling emissions at three meters or more for an interaction occurring at a one-meter separation

a point source at either one- or three-meter distance; and 2) the one-meter measurement is not the field at some point in space but the average over the physical dimensions of the EMI test antenna. So not a scalable value in any way, shape, or form.

Misapplying Antenna Factors

SAE ARP-958E (2021) now provides for separate horizontal and vertical polarization antenna factors for dipole-like antennas (dipoles, biconicals, log-periodic arrays). Under the right conditions this might make sense (given the *a priori* use of field intensity limits in the extreme near field) but it is indefensible given how they measure antenna factors.

The 1968 release SAE ARP-958 was for the newly mandated log spirals of MIL-STD-461.[33] SAE ARP-958 did not specify the height of the antennas above the floor, nor even if the floor would be reflective or not. But SAE ARP-958A (1992) specified a reflective floor and a three-meter height above the floor.[34] The purpose was to control ground plane effects and make them negligible relative to the direct coupling between transmit and receive antennas. All subsequent revisions maintained the three-meter height and the reflective ground plane.

Note that, while all one-meter separation radiated emission requirements (CISPR 25, RTCA/DO-160, and all revisions of MIL-STD-461/-462) place the antennas approximately one meter above the ground plane, SAE ARP-958E measures the separate polarization-based antenna factors three meters above the ground plane. Ground plane effects measured at three meter height are not even remotely applicable when antennas are one meter above the ground plane. Consider that over fifty years ago, just a few years after the biconical antenna was introduced in MIL-STD-461 (1967), a handbook warned that placing the lower tip of a vertically oriented biconical within two feet (61 cm) of the floor would capacitively load it sufficiently to change the antenna factor.[35]

The point is this: if you want the biconical placed with the lower tip one foot above the floor (CISPR 25), then fine, make it so. And make everyone do it the same way. But then don't apply a correction factor measured at three meters above the ground to correct for that. Don't correct for it at all. Just mandate the

Figure 14: A very small sampling of electromagnetics texts from Hertz onwards, in chronological order, with representation from every decade to one hundred years after Hertz (from the Museum of EMC Antiquities collection).

proper antenna, and its separation and orientation, and then record antenna output, adjusted for balun and cable losses.

Misapplying Far-Field Gain in Computing Power Density

The EMC departments of two aerospace vehicle manufacturers refused to perform system-level EMC verifications that required the use of RF absorber panel emplacements around their respective platforms. They based their decisions on the belief that the computed RF power density from a platform high-gain microwave dish exceeded the absorber power rating. This was based on computing the power density using the far-field gain (only achieved beyond 50 meters distance) at a distance of two meters from the dish.

In reality, the actual power density based on Figure 12 (in Part 3) was orders of magnitude less and much less than the absorber panel rating. Further, an elementary calculation of the area over which the far-field gain would concentrate the beam at a two-meter distance would have been a few centimeters on a side, which should have been a tip-off. Another tip-off would have been a Friis equation calculation showing more received power than transmitted using the far-field gain close in.

Basing RE Limits on the Far-Field Gain of a High-Gain Dish

A non-US space agency levied a millimeter wave radiated emission limit based on the far-field gain of a high-gain dish. The resulting limit was such that it could not possibly be instrumented. The Fresnel-zone gain of such a dish at a one-meter distance is again orders of magnitude less than in the far field, plus the potential noise sources are in the back lobes of the antenna or, in a worst-case scenario, a 90-degree side lobe, but certainly not in the main beam.

Antennas Are Not Interchangeable in the Near Field

Both RTCA/DO-160, section 21, and CISPR 25 recommend but do not require the use of standardized antennas for radiated emission measurements. This is a direct consequence of using field intensity limits, and the assumption that the use of antenna factors is enough to yield the proper result no matter what antenna is chosen. The 1995 release of CISPR 25 went so far as to claim:

> *6.5.1 Antenna systems*
>
> *"The limits … are listed in dB(uV/m), and thus theoretically any antenna can be used, provided that … the antenna correction factor is applied..."*

This type of error was identified in 1967 when MIL-STD-461 popularized the change from antenna-induced to field intensity limits.[36] The 2016 edition removes the egregious statement but only *recommends* standard antennas. In this regard, all versions of MIL-STD-461/-462 RE02/RE102 since 1967 are superior to RTCA/DO-160, section 21, and CISPR 25 in recognizing and accommodating the near-field nature of the measurement at a one-meter distance. The 41" rod antenna and 137 cm tip-to-tip length biconical have been required since 1967. From 1967 – 1993, log spirals were required from 200 MHz to 10 GHz. After 1993, the log spirals were replaced by double-ridge guide horns of specified aperture dimensions. Since 1993 the following rationale appendix wording explains the use of standardized antennas for requirement RE102:

> *"Specific antennas are required by this test procedure for standardization reasons. The intent is to obtain consistent results between different test facilities.*
>
> *"In order for adequate signal levels to be available to drive the measurement receivers, physically large antennas are necessary. Due to shielded room measurements, the antennas are required to be relatively close to the EUT, and the radiated field is not uniform across the antenna aperture. For electric field measurements below several hundred megahertz, the antennas do not measure the true electric field."*

The first clause of the very last sentence is unnecessary since even if the calculated far field of the test antenna is no greater than one meter, the far field of the two-meter-long test set-up is clearly well beyond one meter. It is not enough for the transmitting source to be in the far field of the receive antenna; the receive antenna must also be in the far field of the source transmitter. Now it could certainly be the case that the transmitting source at microwave frequencies happened to be a small slot or aperture in the test sample enclosure, and if that were the sole radiating structure, it could be a far-field measurement. But the point is, one cannot know that *a priori*.

CONCLUSION

Converting near-field radiated emission control from field intensity to antenna-induced limits brings the following advantages:

- Clear delineation between near-field vehicle and home/office/industrial plant far-field radiated emission controls;
- Better correlation between equipment-level radiated emission limits and system-level EMC goals (direct correlation with spectrum analyzer noise floor surveys of platform antenna-connected receivers);
- Diminution of wrong-headed EMC "engineering" comparing RE and RS controls as complementary functions; and
- As a corollary, it would raise awareness of the real issues involved in RE control and improve the quality of EMC engineering, reducing episodes where bad science is used to justify programmatic decisions.

Even if a majority of the EMC discipline found these arguments persuasive, it would be wildly unrealistic to expect that over a half-century of tradition would be overturned. Given that reality, but with the understanding that antenna-induced is the ideal for one-meter radiated emission control, significant benefits could still result. The major such benefit would be dropping SAE ARP-958 altogether and using polarization-independent far-field antenna factors. Another possible advantage would be the adoption of EMI test antennas that better modeled those connected to platform-installed receivers that are the motivation for the levying of radiated emission controls.

And whether or not we return to antenna-induced near-field limits, the discipline would benefit immensely if EMC engineers rediscovered the lost science of near-field measurements. They could do worse than reading NADC-EL-5515. It also might not hurt to read Hertz's original work on his dipole.

A WWII historian once remarked that other historians read books previous historians wrote, and then write a new book based on what they had read. In contrast, this historian always cited WWII-era sources. There is something to be said for original sources. The Museum of EMC Antiquities exists to preserve such knowledge and foster its study until such time that the present Dark Ages give way to an EMC Renaissance.

ENDNOTES

29. Pearlston, C.B. Jr., "The Systems Approach in Designing a Specification for the Control of Radio Interference in an Airborne Environment," Proceedings of the 5th Conference on Radio Interference Reduction and Electronic Compatibility. October 1959. In this work, Pearlston compares RE limits for protecting radio reception to susceptibility limits simulating rf transmitters, and while acknowledging the true purposes of each type of control, still manages to compare such limits and conclude that "100 dB" margins exist.
30. A complete derivation, leaving no "exercises for the reader," is presented in Adamczyk, Bogdan, *Foundations of Electromagnetic Compatibility with Practical Applications*, John Wiley & Sons, 2017.
31. Javor, K. "Journey To The Center of The Dipole," *In Compliance Magazine*, September 2023.
32. Javor, K., "On the Nature and Use of the 1.04 m Electric Field Probe," *ITEM 2011.*
33. MIL-STD-461, *Electromagnetic Interference Characteristics, Requirements for Equipment*, 31 July 1967.
34. SAE ARP-958A, *Electromagnetic Interference Measurement Antennas; Standard Calibration Method*, November 1992.
35. White, Donald R. J., "EMI Test Instrumentation and Systems," Volume 4, Section 3.3.4 of the Handbook Series on EMI & EMC, 1971.
36. Pearlston, C.B. Jr., Air Force Report No. SSD-TR-67-127, dated 1967. "Historical Analysis of Electromagnetic Interference Limits." Pearlston makes the exact same points back at the inception that were presented in this article; these observations are hardly new:

    "An academic argument could be made, and often has been, that "field intensity" is not a proper term to use in describing the phenomenon being measured and that "antenna-induced voltage" is much more descriptive of that phenomenon. Field intensity is generally defined as a measure of the intensity of the electric field; the term implies that the measured electric field gives a valid indication of the power density in the wave front, and permits an estimate to be made of the power coupled into a receiving antenna. Such an estimate is valid only in the far field where the plane wave phase relationships of electric and magnetic fields are fixed. Thus, the measurement does not give a valid indication of power coupling.

    "Field intensity is also defined as the voltage induced in a conductor one meter long when held so that it lies in the direction of the electric field and at right angles to the direction of propagation and to the direction of the magnetic field. It can be argued that the equipment near-field does not have a uniphase front, and so the straight rod or dipole antenna will not necessarily be in the direction of the electric field. These near-field effects become even more marked at the higher frequencies where horn and parabolic reflectors are used.

    "The term field intensity should refer to a phenomenon which is independent of the measuring instrument rather than, as in the present case, being so highly dependent upon the particular antenna used. The phenomenon measured is not the actual electric field of the wave front, but consists of indications of partial components of that wave front in the near-field of the test sample. A better name for the phenomenon would be "apparent field intensity", but, as long as there is no confusion as to what is being measured, the name given to the phenomenon is not of great importance."

    Except of course his prognostication that the name change from "field intensity" to "apparent field intensity" is not really important was proven wrong, and in this case at least, Shakespeare may be more accurately paraphrased by saying that "A rose by any other name would stink."

2024

Product Resource Guide

Contents

Dear Reader,

Finding the right products to meet your unique compliance requirements can be challenging. Multiple considerations play into your decision-making process.

In Compliance Magazine's 2024 Product Resource Guide highlights twelve product categories—and offers guidance on choosing and using the right products and services for your applications.

We aim to provide you with the impartial, practical guidance you need to confidently make your compliance products and services purchase decisions in the year ahead.

We hope you'll find the information compiled in the 2024 Product Resource Guide to be useful, reliable, real-world information you can use immediately.

As always, we're here to help.

Lorie Nichols
Editor/Publisher

Contributing Author
Don MacArthur
Guest Contributing Writer

ESD Flooring
article by
Dr. Jeremy Smallwood
for EOS/ESD Association, Inc.

RF Absorption Loss of Shielding Materials

By Don MacArthur, MacArthur Compliance Services, LLC

The two primary shielding mechanisms are reflection and absorption. The two combined result in the familiar expression SE(dB) = R(dB) + A(dB), where SE(dB) is shielding effectiveness in decibels, **R** represents Reflection Loss, and **A** represents Absorption Loss (both also expressed in decibels). Often, absorption loss (also called penetration loss) is the energy that is not first reflected by the shield that is absorbed by it – the topic of this article.

Note: A third term involved in the SE equation called the multiple reflection factor B is often ignored if A is greater than 9 dB or if the field is electric or plane wave.

To determine a shielding material's potential absorption loss capability, you must first know the frequency or frequencies of concern and, second, what shield materials you have available. The skin depth of copper will be different from that of aluminum, which is different from steel, depending on frequency.

Absorption Loss Dependences for EMI Shields

It does not matter if the field impinging upon a shield is electric, magnetic, or simply a plane wave, the distance from the shield, or its wave impedance; the absorption loss the shield achieves depends entirely on the barrier thickness and skin depth. Barrier thickness is self-explanatory; however, the concept of skin depth is a little more complicated.

The Concept of Skin Depth

If you're involved with compliance engineering, you should have a pretty good understanding of skin depth. It is a topic of great discussion that often arises around office cubicles and water coolers of most engineering spacings. And if you are a compliance or EMC engineer, you'll be expected to know it regarding absorption loss and other areas.

Skin depth (or skin effect as it is often called) is the distance required for the impinging wave to be attenuated to 1/*e* or 37% of its original value, where *e*, Euler's number (pronounced "Oiler"), equals approximately 2.71828.

The equation for skin depth in meters (m) is:

$$\delta = \sqrt{\frac{2}{\omega\mu\sigma}}$$

where:

δ = Skin depth

w = 2πf (f is frequency)

μ = permeability of the shielding material

σ = conductivity of the shielding material

Skin Depth and Absorption Loss

If it is not obvious, the above equation indicates that absorption loss is caused by a decrease in shield current through the material due to skin depth and that the losses are affected primarily by two material properties, namely permeability and conductivity.

Also, notice the square root of frequency term in the above equation. This means that as frequency increases, absorption becomes the dominant term exponentially.

A useful formula for determining absorption loss (A) in dB is 8.69 * (t/δ) where t is barrier thickness and δ is skin depth. This means that absorption loss in a shield one skin depth thick is approximately 9 dB, and doubling the thickness of the shield results in double the amount of absorption loss in dB. Note also that there is no "20 log" term because skin depths are exponential and the log of an exponential function is a linear function.

Skin Depths of Various Materials

To determine a shielding material's potential absorption loss capability, you must first know the frequency or frequencies of concern and, second, what shield materials you have available. The skin depth of copper will be different from that of aluminum, which is different from steel, depending on frequency. For instance, steel offers greater absorption capability than copper at lower frequencies with high relative permeability. But perhaps you do not care about shielding effectiveness at lower frequencies so you can use a more cost-effective material, such as aluminum. This will require some research and I suggest putting it all in a table for easy comparison. Still, steel is generally better than copper at providing absorption loss; however, at low frequencies (~ 1000 Hz), a thick sheet of steel must be used to provide adequate absorption loss.

Summary

Absorption loss in shielding materials is proportional to thickness and inversely proportional to skin depth due to a decrease in shield current through the material. Skin depth is determined further by the permeability and conductivity of the material. Steel is better than copper at providing absorption loss.

References and Further Reading

1. Williams, T., *EMC for Product Designers*, 5th Edition, Newnes, 2017.
2. Kimmel Gerke Associates, Ltd., *EDN Designer's Guide to Electromagnetic Compatibility*, 2005.
3. Ott, H.W., *Electromagnetic Compatibility Engineering*, Wiley, 2009.

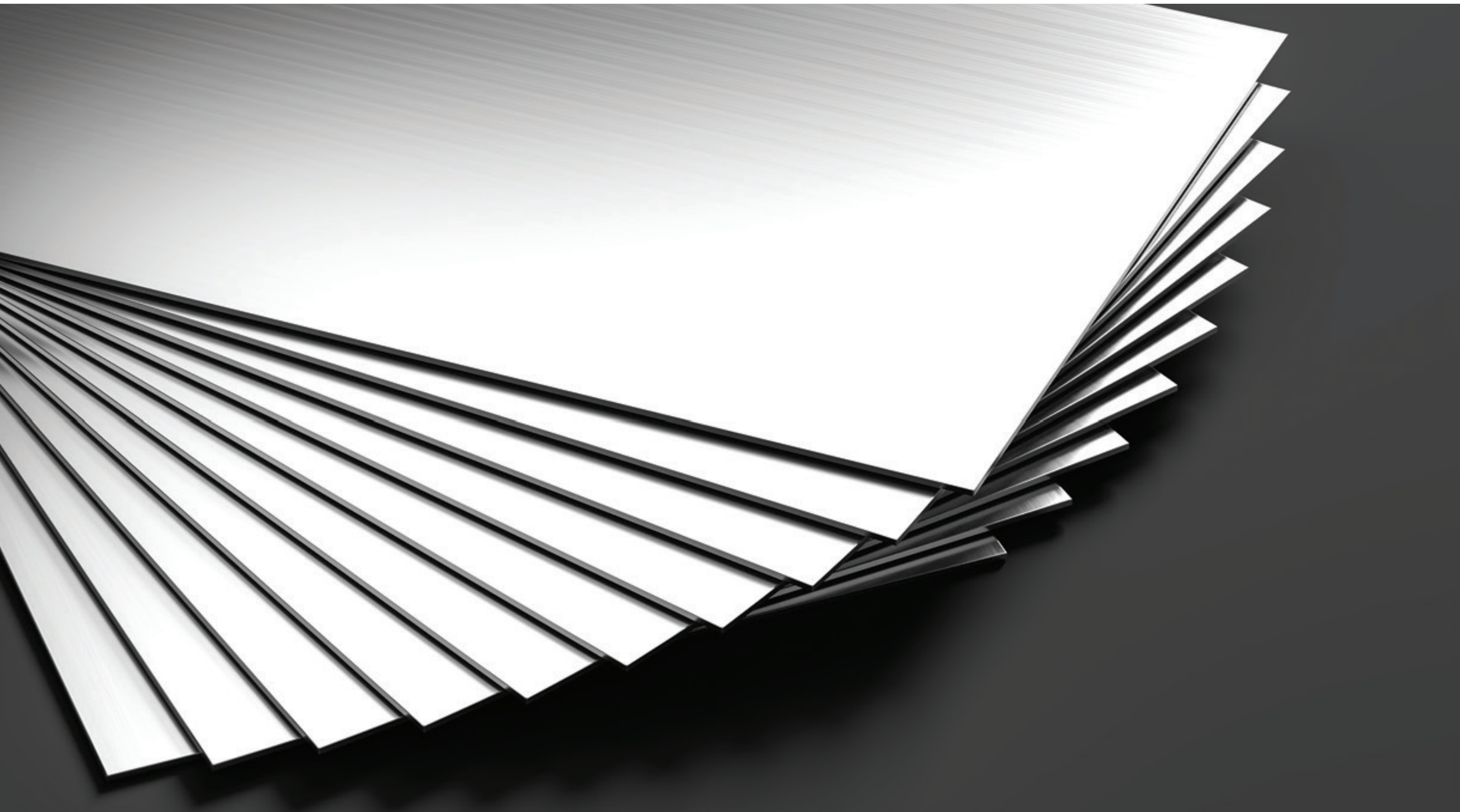

Quarter-Wavelength Impedance Matching Networks

By Don MacArthur, MacArthur Compliance Services, LLC

This article describes a loss-less impedance matching technique that does not require the use of discrete components but instead uses cables or printed circuit board (PCB) traces, i.e., distributed elements or transmission lines. It is a matching circuit built using a piece of transmission line whose length is equal to a quarter of the signal's wavelength, hence the name "quarter-wavelength impedance matching transformer" or "quarter-wavelength impedance matching network." But before jumping into specifics of the quarter-wavelength impedance transformers/networks, let us first discuss the use of discrete components (inductors, capacitors, etc.) and their limitations in matching networks.

What's wrong with using discrete components in matching networks?

Discrete components, or as used in this context, lumped elements, include non-useful traits (parasitics) that become dominant contributors of errors at higher frequencies. Capacitors act like inductors past their self-resonant frequency (SRF) due to parasitic series inductance of their leads. Inductors act like capacitors past their SRF due to parasitic parallel capacitance of the windings. Transformers have similar issues that crop up as the frequency of interest increases. As the frequency increases, it becomes nearly impossible to design matching networks using discrete components and their associated interconnections that contain parasitic effects. It is impossible to make parasitics effects negligible using these devices. When using discrete components, the parasitics dominate the circuit's behavior, so we must utilize other solutions. These other options utilize distributed (not lumped) elements; one such device is called the quarter-wavelength matching network or quarter-wavelength matching transformer.

What is a quarter-wavelength matching transformer?

The quarter-wavelength matching transformer or network works by transforming or inverting the impedance of the source and load it is connected to. It is a transmission line (distributed element) that has a specific characteristic impedance and allows matching source and load impedances of the line using the following equation:

$$Z_{Line} = \sqrt{Z_{Source*}Z_{Load}}$$

Note that this equation is only valid at the frequency where the transmission line length is equal to a quarter of the signal's wavelength (or odd multiples of a quarter-wavelength, which we will discuss later).

Theory of Operation

Recall that a wave traveling through a transmission line with a different impedance than the connecting element will partially reflect at both ends. Suppose the line has a quarter of the wavelength. In that case, the first reflection will occur after a quarter-wavelength, so the wave will return to the start of the transmission line after another quarter-wavelength, for a total of half a wavelength – one quarter-wavelength down the line and one quarter-wavelength back. This condition means that the wave arriving at the beginning of the line will be inverted or 180 degrees phase shifted in reference to the incident wave. Based on this phase inversion and the reflection coefficients at the ends of the line, the final impedance equation is determined. Impedance transformation with transmission lines will occur with any line length and with any type of impedance, but the simple formula only works with quarter-wavelengths and real impedances.

Example

Imagine you have a 100 MHz source of 100 Ω driving a load of 25 Ω and want to construct a quarter-wavelength matching network that minimizes reflections and losses.

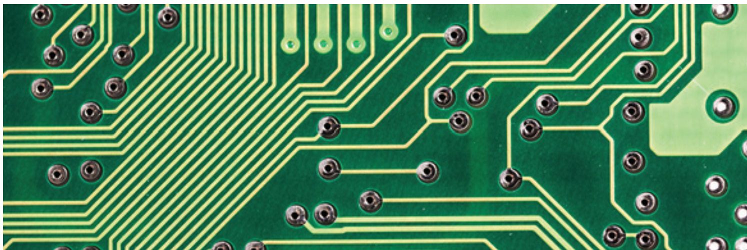

$$Z_{Line} = \sqrt{Z_{Source*}Z_{Load}} = \sqrt{100 * 25} = 50\,\Omega$$

Using the equation provided, you determine the line impedance should be 50 Ω.

To find the correct line length, you first determine the wavelength (l) using the following equation:

$$\lambda = \frac{C}{F} = \frac{3\,x\,10^8\,m/s}{100\,MHz} = 3\,m$$

The correct line length that will provide quarter-wavelength (l/4) impedance matching for this example is 3 m divided by 4 or 0.75 m.

This matching network will provide correct matching at 100 MHz and some other frequencies, i.e., 300 MHz, 500 MHz, 700 MHz, and so on, which are all odd multiples of the fundamental 100 MHz frequency. Proper matching also occurs at multiple odd quarter-wavelengths because the line needs to invert the signal that is passing through it, for a quarter-wavelength line. But if the line is a half-wavelength (2 times l/4), then the reflected signal ends up being phase shifted by 360 degrees and is in phase with the incident signal at the beginning of the line resulting in no inversion. The inversion process occurs again for a line that is three-quarters of a wavelength long (3 λ/4). Continuing with this thought process, we can put together multiple combinations of inverting (l/4) and non-inverting (l/2) segments that result in impedance matching if they are odd-multiples of a quarter-wavelength (3l/4, 5l/4, 7l/4, 9l/4, etc.). Together they form a line that generates a phase inversion. For any given length of transmission line, you can determine the multiple frequencies where the phase inversion occurs and see that these are odd multiples of a quarter-wavelength.

Summary

This brief article described the limitations of discrete components in matching networks. It provided a solution through the use of quarter-wavelength impedance matching networks that work at a frequency that corresponds to a quarter-wavelength and at multiple odd quarter-wavelengths.

References

1. "Quarter-wavelength impedance matching (1/2)," FesZ Electronics. https://www.youtube.com/watch?v=ie0eBuPohHs

TIPS FOR SELECTING *Amplifiers*

1. Determine the frequency range of operation needed, sometimes more than one amplifier is required.
2. Determine if you need a Pulse or CW type of amplifier. Example: HIRF EMC applications require high power pulse amplifiers..
3. Determine the minimum acceptable linear or saturated power needed from the amplifier. Harmonics should be considered based on the frequency range. Example: As you go up in frequency antenna gain improves so a lower power amplifier may be acceptable but the higher gain of the antenna may affect the Harmonic Level.
4. Assess the system losses between the amplifier and the antenna/DUT. Example: If the test setup has 6dB of losses then the Amplifier power needs to be 6dBm higher.
5. Some modulations if required for the test application, would require a higher power amplifier. Example: When performing an 80% AM modulation test the amplifier needs to have 5.1dBm of margin to accommodate the peak.
6. Antennas, cables, DUTs, and rooms have cumulative VSWR, it is best to allocate for some power margin. Example: working into a 2:1 requires 12% more forward power.
7. Consider the application, is this a single test or will it be used repetitively?
8. Consider your desired RF connection types and locations to be optimal for your application.
9. Consider if automation will be used so the appropriate remote capability is included.

These tips are presented by

EXODUS ADVANCED COMMUNICATIONS

IEEE Recommended Practice for Antenna Measurements

By Don MacArthur, MacArthur Compliance Services, LLC

Those involved in compliance engineering are often required to read many standards and comprehend them so they can guide others. Although informative, many of these same standards are not very exciting to read, are often confusing, and seem like they contain conflicting requirements. Most are not meant to be read like a novel but are better suited to reading small sub-sections at a time. There are exceptions to the rule, and the following briefly describes an exceptionally well-written standard that breaks the typical mold.

Introduction

On September 23rd, 2021, the IEEE Standards Antennas and Propagation Society approved and released a new 207-page version of IEEE Recommended Practice for Antenna Measurements. This 2021 version of the standard is identified as IEEE Std 149Ô and was developed by the Antennas and Propagation Standards Committee, Working Group APS/SC/149_WG. The previous version of the standard was dated as far back as 1977 but was reaffirmed in 2008. It has been over 40 years since the original version of the standard was published and much of the technology available at that time is now obsolete. Therefore, this new updated major revision and expansion of the original standard is a welcomed addition to the compliance test and engineering community.

Due to advances in technology over the past 40 or so years, it was not possible to maintain the intent of the original standard as a standardized test procedure for antennas. Therefore, the committee reclassified IEEE Std 149-1977 as a recommended practice, intending to have it function instead as a guideline for obtaining the highest quality measurements without prescribing an exact method. The new recommended practice, however, does preserve many familiar areas covering antenna measurements and range evaluations but depicts them using the latest state-of-the-art industry best-practice methods and contemporary tools.

Participants

When the 2021 version of the IEEE Recommended Practice for Antenna Measurements was completed, the working group responsible for its construction had a Chair, Vice Chair, Secretary, and over 60 members. The number of balloters (those who may have voted for approval, disapproval, or abstention) was 36.

When the IEEE SA Standards Board approved this recommended practice, its membership was comprised of a Chair, Vice Chair, Past Chair, Secretary, and 22 individual members, one of which was listed as Member Emeritus.

What's included in the new recommended practice?

The standard's abstract indicates the new recommended practice includes fundamentals related to measurements of antenna transmitting and receiving properties. The standard assumes that any antenna to be measured can be treated as a passive, linear, and reciprocal device where radiation properties can be measured in either the transmitting or the receiving mode. It includes the important note that a fundamental property of any antenna is its radiation pattern. Therefore, the measurement of radiation patterns in an antenna test facility is

examined. Furthermore, the design of antenna test facilities is explained along with instrumentation requirements for the proper operation of the antenna facility, directions for evaluating an (existing) range, and the operation of ranges is included. An additional benefit of the standard is that references that clarify measurement techniques and where additional details may be found are provided.

Scope

The scope of the standard is chock full of useful information on all things related to measurements of antennas.

For example, the standard includes measurement of radiation patterns in an antenna test facility, design of antenna test facilities, instrumentation requirements, and directions for evaluating and operating antenna ranges.

A parameter that frequently limits the useful bandwidth of the antenna is the input impedance to the antenna (this important parameter controls power transfer from generator to antenna); therefore, measurement procedures and network descriptions for antenna impedance are included.

Measurement of the radiation pattern includes errors. A method of measurement uncertainty analysis is provided for its applicability to the various test facilities portrayed. This is a valuable resource for anyone running an accredited test facility who must provide a measurement uncertainty budget as part of the accreditation process.

Purpose

This recommended practice provides a guideline for the conventional approaches and techniques used to describe the functioning of conventional antennas.

Specific Contents

Specific notable contents in the order they are presented in the standard include the following:

- Normative References
- Definitions, Acronyms, Abbreviations
- Antenna Range Design
- Antenna Range Instrumentation
- Antenna Range Evaluation
- Measurement of Radiation Patterns
- Measurement of Gain and Directivity
- Measurement of Polarization
- Measurement of Radiation Efficiency
- Measurement of Impedance
- Special Measurement Techniques
- Uncertainty Evaluation
- Antenna Range Operation
- Electromagnetic Radiation Hazards
- Antenna Testing Under Environmental Conditions
- Informative Annexes
  - Annex A – Bibliography
  - Annex B – Field Regions
  - Annex C – Reciprocity
  - Annex D – Over-the-air (OTA) Measurement of Integrated Devices
  - Annex E – Electrical to Reference Boresighting
  - Annex F – Impedance Mismatch Correction Deviations

Conclusion

The working group responsible for updating this standard should be proud of their accomplishment. In approximately 200 pages, they have managed to succinctly communicate all that needs to be known about performing antenna measurements correctly and with engineering rigor. Even if you are not involved in the practice of the measurement of antennas but have a passing interest and would like to learn more, this is the standard to read. Doing so will quickly get you up to speed, saving you many hours of unnecessary research and much confusion.

Further Reading

1. IEEE Std 149™-2021, of IEEE Recommended Practice for Antenna Measurements.

Low Frequency Magnetic Field Shielding

By Don MacArthur, MacArthur Compliance Services, LLC

As compliance engineers and technicians involved in new product development, much of our time spent developing shielding (or consulting with others who do) is mostly devoted to developing shielding that is suitable for high frequency (HF) signals (those signals that have frequencies greater than 100 kHz). In case you need a refresher on how this type of shielding is accomplished, reference 1 covers this topic at a high level.

Occasionally, we are asked to help develop shielding that is effective for near-field low frequency (LF) magnetic fields. Perhaps in a situation where some regulatory agency has imposed limits on LF magnetic field emissions of our product and we are forced to comply? In this situation, we find ourselves caught a bit off guard and may not know what to do since the shielding design techniques we know well (those used for shielding HF signals) will not work for LF magnetic fields. If you find yourself in this situation and are unsure what it takes to develop shielding that is effective for LF magnetic fields, please read on.

Reflection and Absorption at HF vs. LF

When working with HF fields, we can utilize the reflection and absorption properties of the shielding material (for instance, aluminum, copper, or steel) in our design to provide a reasonable amount of shielding effectiveness without too much difficulty. Our largest items of concern then become how to deal with penetrations in the shield (seams, slots, holes, etc.) necessary for most products that must do something with input and output signals. For HF shielding, it is the penetrations, not reflection and absorption properties of the shielding material, and how we deal with the penetrations, that contribute most to how effective (or non-effective) the shielding is.

For LF magnetic field shielding, the amount of attenuation provided by the reflection and absorption properties of the shielding material is essentially nil. Therefore, we cannot rely on reflection and absorption to save the day, like it sometimes does when dealing with HF signals. Something else must be done. This "something else" has only two options:

1. *Use high-permeability shielding materials to divert the magnetic flux.*
2. *Utilize the "shorted-turn" method.*

Divert the Magnetic Flux

To divert the magnetic flux around an item that requires shielding, use a high-permeability, ferromagnetic material that provides a low-reluctance path that the magnetic flux can take. This path diverts the magnetic flux away from the shielded item in a controllable manner. Note that Mumetal is a material that has a high relative permeability (>10,000 from DC to ~ 1 kHz).

Caution: High permeability materials are more prone to saturation than low permeability materials – more on this later.

Use the "Shorted-turn" Method

I call this the "fight fire with fire" method. Here we utilize Faraday's law to create a magnetic flux via a conductor loop placed such that the incident magnetic field (the one we intend to suppress) penetrates the loop, and this creates a magnetic field that is counter to the original magnetic field, thereby reducing the incident magnetic fields total net effect. You may have seen the shorted-turn concept in practice, where you noticed a band of copper (belly-band) placed around a transformer of a switch-mode power supply. This band utilizes the shorted-turn method to reduce the radiated magnetic fields of the leakage flux of the transformer.

Degradation of LF Magnetic Field Shielding Effectiveness Using Diversion Technique

Nothing in engineering is perfect, and just as we experience degradation of shielding effectiveness in HF shielding via penetrations in the shielding, we also experience degradation of shielding effectiveness in LF magnetic field shielding when we use the diversion technique. Except in LF magnetic field shielding, we do not have to concern ourselves too much with penetrations but must now to two other factors that degrade shielding effectiveness. These two factors are:

1. *With increasing frequency, permeability decreases.*
2. *With increasing magnetic field strength, permeability decreases, and saturation is likely.*

Knowing about item 1, beware of the permeability specifications given for Mumetal at low frequencies, such as 1 kHz. The material does not have the same level of permeability at higher frequencies, such as 20 kHz, where cold-rolled steel is just as good as Mumetal but is less costly.

In the case of item 2, two layers of magnetic field shielding are required. The first layer is often a low permeability material with high saturation capability used to reduce the field strength of the initial magnetic field. The next layer with high permeability and low saturation capability then takes over and effectively diverts the magnetic flux as previously described using the diversion method.

Summary

Shielding for LF magnetic fields is not the same as shielding for HF fields, and what works well for the latter does not work well for the former and vice versa. Knowing the rudimentary concepts of LF and HF shielding is important in the compliance engineering profession. This article focused on LF magnetic field shielding using the divert magnetic flux and shorted-turn methods.

References and Further Reading

1. "What Every Electronics Engineer Needs to Know About Shielding," *In Compliance Magazine,* August 2018.
2. Keller, R.B., *Design for Electromagnetic Compatibility – In a Nutshell*, Springer, 2023.
3. Williams, T., *EMC for Product Designers*, 5th Edition, Newnes, 2017.
4. Paul, C.R., Scully, R.C., Steffka, M.A., *Introduction to Electromagnetic Compatibility*, Third Edition, John Wiley, and Sons, 2023.
5. Mediano, A., "Shielding Low Frequency Magnetic Fields," Omicron 12th Power Analysis & Design Symposium, March 15th, 2023. https://youtu.be/woiVZ155I4E

Shielding for LF magnetic fields is not the same as shielding for HF fields, and what works well for the latter does not work well for the former and vice versa. Knowing the rudimentary concepts of LF and HF shielding is important in the compliance engineering profession.

System Components Used to Reduce Electromagnetic Interference

By Don MacArthur, MacArthur Compliance Services, LLC

A few basic system components are frequently used to mitigate or suppress electromagnetic interference (EMI) in devices. As engineers and technicians involved in compliance engineering, it is important to know what these components are, what they do, how they're most effective, and when they're ineffective. You will often be involved in reducing EMI or Electrostatic Discharge (ESD) to pass compliance tests or simply need to make your product more robust to EMI/ESD. So, it would be wise to know a little about systems components used to reduce EMI. In alphabetical order, some of these components are:

- *Capacitors*
- *Common Mode Chokes*
- *Diodes*
- *EMI Filters*
- *Ferrites*
- *Inductors*
- *Resistors*

The following will briefly describe the characteristics of each one and how they are used to reduce EMI/ESD.

Capacitors

Capacitors are comprised of a dielectric material sandwiched between conductive top and bottom plates.

Capacitance (measured in Farads: pF, nF, mF, etc.) is the charge needed to create a certain potential between the plates. Larger capacitors can store more charge than smaller ones, and the dielectric quality is a determining factor for capacitance.

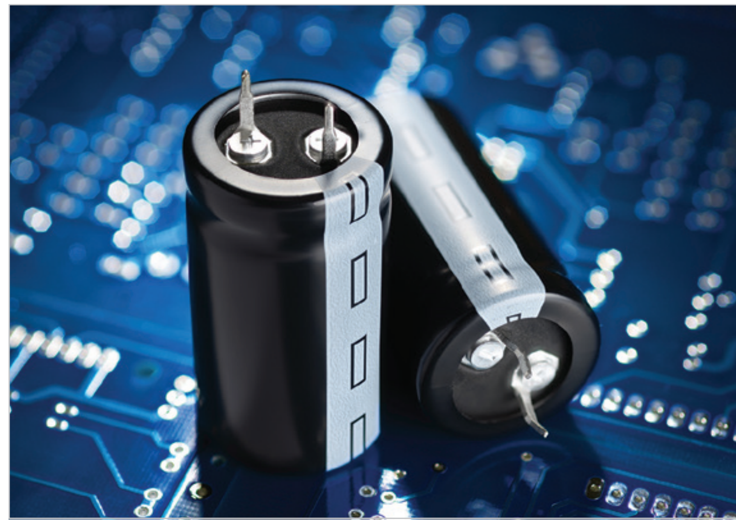

The material used for the dielectric can be air, paper, fiber, glass, PP, PET, Mica, Aluminum Oxide, Tantalum Oxide, Titanium Oxide, and Barium Titanate, all producing various dielectric constants (ε).

Capacitors that filter out system noise are called bypass or decoupling capacitors.

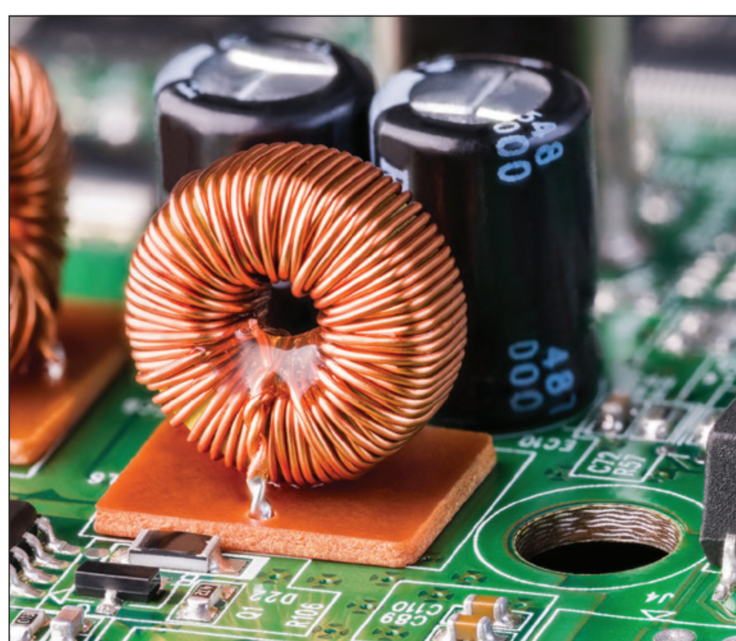

Bypass capacitors create a shunt path to ground to remove system noise and prevent it from getting to susceptible areas. Decoupling capacitors are installed near digital devices to provide a localized DC power source. Ceramic capacitors are usually selected for decoupling.

Each type of capacitor (with its varying dielectric types) comes with pros and cons, the length of which is too vast to cover here. We cover more on this in "Capacitor Technologies Used in Filtering" on page 67.

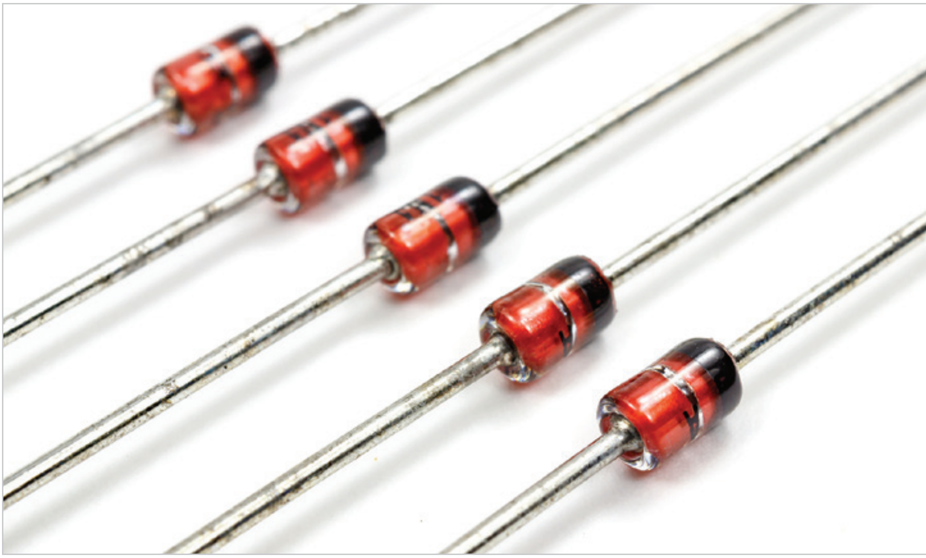

Common Mode Chokes

Common mode chokes are special inductors used to attenuate unwanted common mode signals.

Often seen at the front end of switch-mode power supplies, these devices come in various types that offer varying degrees of attenuation of various lines that require noise suppression.

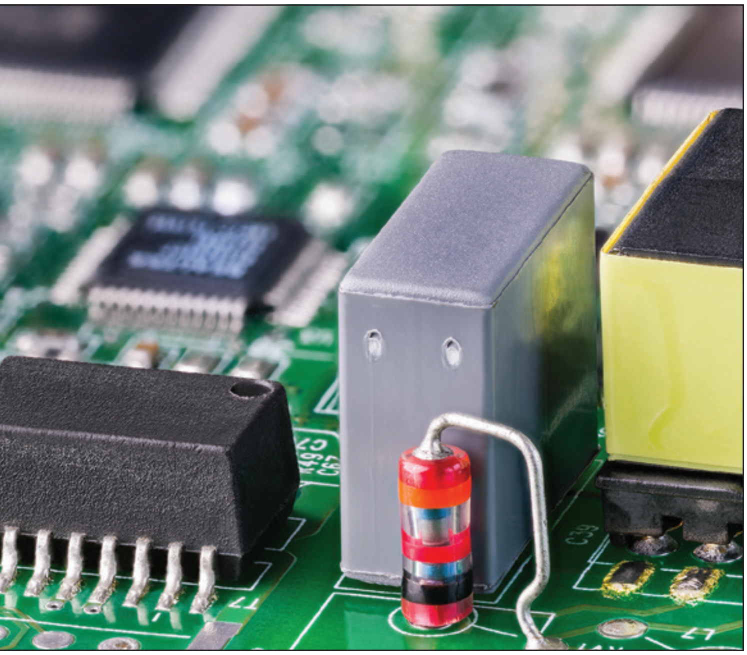

Diodes

Diodes are analogous to one-way check valves, frequently used in plumbing.

As such, in switching applications involving large inductive loads, diodes are often placed across plus/minus control terminals and as close to the transient noise source as possible to act as a transient voltage suppressor/clamp.

There are several different types of diodes used in EMI suppression. These include:

- Rectifier
- Schottky
- Transient voltage suppressor (TVS)
- Varistor
  - Metal Oxide Varistor (MOV)
  - Voltage-dependent resistor (VDR)
- Zener

Each type of diode listed above has various characteristics that work best to reduce specific types of EMI. This is a vast topic not covered here.

EMI Filters

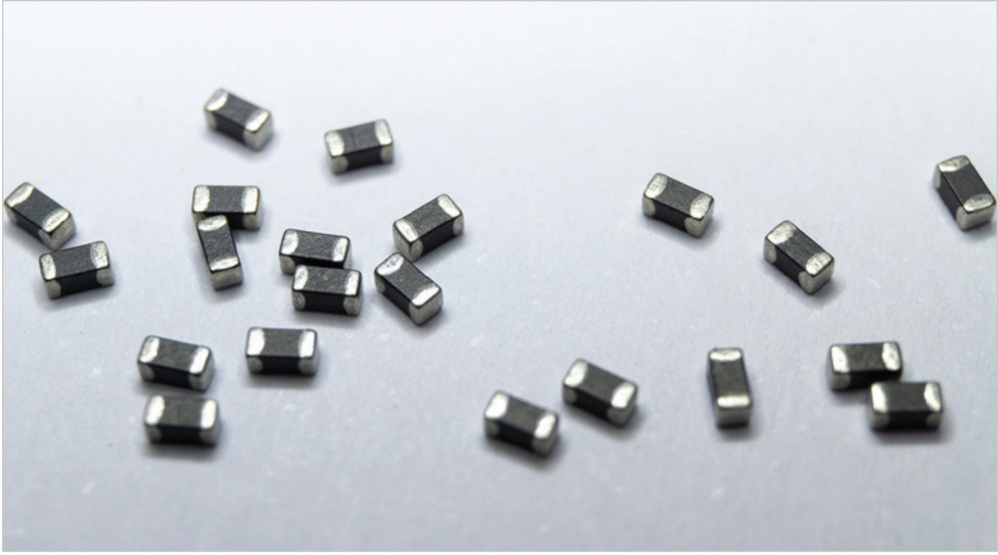

EMI filters are low-pass filters used in a wide variety of situations.

They are dual purpose in that they not only stop noise from entering a system but also stop noise in the system from leaving it.

There are various types of EMI filter configurations. The so-called feed-through capacitor is the simplest, consisting of only one component. Another simple form is called the L-circuit filter. More complex forms, comprised of both L & C components, is the PI-circuit or T-circuit filter. The latter two types are determined by the impedance (Z) of the circuit node that requires filtering. A high-Z noisy node needs a low-Z path (capacitor) to provide a diversion path for the noise current to flow. This situation requires a PI-circuit filter (capacitor-inductor-capacitor). A low-Z noisy node needs a high-Z filter element (inductor) to suppress the noise. This situation requires a T-circuit filter (inductor-capacitor-inductor).

See Reference 2, “What Every Electronics Engineer Needs to Know About: Filters” for more information about EMI Filters.

Ferrites

Components, like ferrite beads and inductors that are made from ferromagnetic materials, are widely used for EMI noise suppression.

They have three important properties to consider when applying them to various EMC applications. These properties are saturation, frequency response, and the ability to concentrate magnetic flux. In addition, these materials have large relative permeabilities (μr) that decrease when the current passing through it increases (saturation). Inductance also decreases with increased current. The high permeability of these materials creates the ability to concentrate the magnetic flux created in them. Nickel-Zinc (NiZn) material tends to have lower relative permeabilities than that of Manganese-Zinc (MnZn) materials (about half) but at the benefit of a flatter frequency response.

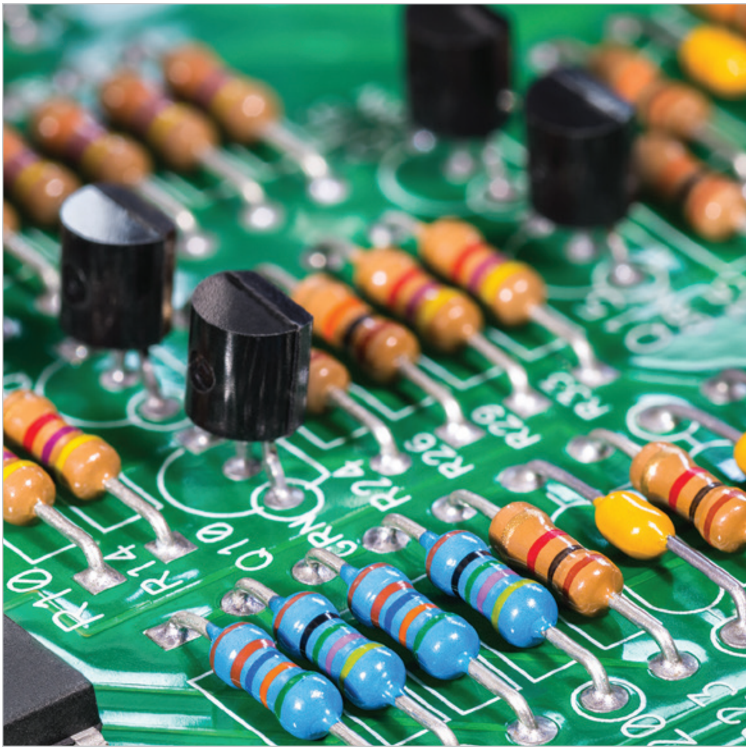

The authors of Reference 3 provide the most practical explanation of how a ferrite works I have ever read. They state, "Ferrites are your friends for ESD. They're like penicillin for ESD problems. The materials are very lossy in the 100- to 500-Mhz range, so they act like resistors against ESD. (Small beads look like 50 to 100Ω at 100 MHz)."

Inductors

Inductors are electrical elements used to introduce a desired amount of inductance into a circuit.

Inductors are typically used in conjunction with capacitors to form low-pass filters.

Resistors

Resistors are typically used for Z-matching in signal integrity applications, current limiting, and in conjunction with capacitors to form RC low-pass filters

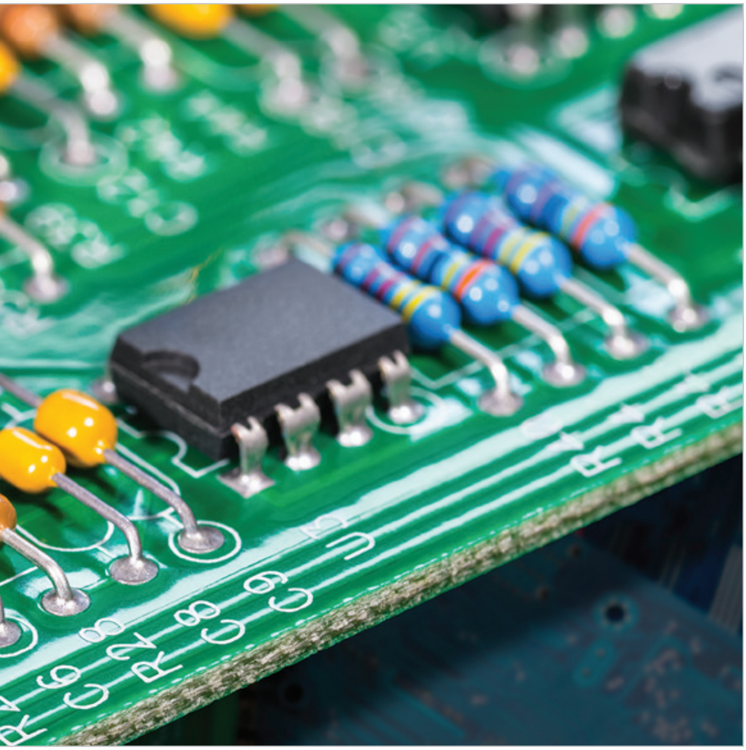

where sometimes the resistor used by itself will help suppress undesired EMI.

The carbon film type is the most widely used resistor type. Other popular types include carbon composition, metal film, metal oxide, foil and wire-wound. Due to undesired inductive effects, wire-wound versions should be avoided for EMI critical applications.

Parasitic Behavior

When using any of the described components to reduce EMI, it's important to consider their non-ideal, parasitic behavior.

You may experience this effect when first trying to use a component to suppress an unwanted signal, only to find out it doesn't work. This could be because of the component's non-ideal, parasitic behavior. This is where capacitors no longer act like capacitors above their self-resonant frequency and act more like inductors! Similarly, inductors may act like capacitors above their self-resonant frequency. In your study of system components used for EMI, it is important to understand how each behaves above their self-resonant frequencies and no longer acts like a real capacitor, inductor, resistor, etc.

References and Further Reading

1. Hu, R., *PCB Design and Fundamentals for EMC, RANDSpace* Technology LLC, 2019.
2. "What Every Electronics Engineer Needs to Know About: Filters," *In Compliance Magazine*, November 2018. https://incompliancemag.com/article/filters
3. Paul, C.R., Scully, R.C., Steffka, M.A, *Introduction to Electromagnetic Compatibility*, 3rd Edition, John Wiley & Sons, 2023.
4. Kimmel Gerke Associates, Ltd., *EDN Designer's Guide to Electromagnetic Compatibility*, 2005.

Cavity Resonances of Shielding Boxes and Cans

By Don MacArthur, MacArthur Compliance Services, LLC

Many years ago, the author experimented on a metal enclosure of one of his company's main products. The experiment involved placing an electric field probe inside the empty metal enclosure (no electronics inside) and applying 10 V/m using the IEC 61000-4-3 radiated RF immunity test system. The E-field levels measured by the probe were recorded over the frequency range of 80 to 1000 MHz. The probe was placed in several locations within the box. The results were supersizing, to say the least. One would expect the 10V/m signal to be highly attenuated by shielding effectiveness of the metal box of 40 dB or so; however, over certain frequencies, the signal was amplified! I recall seeing levels as high as 60 V/m or more inside this empty metal box. The most likely culprit of this unexpected result was probably due to cavity resonance.

Cavity Resonance

The metal box tested formed a resonant cavity, where standing waves in the field were formed between opposite sides when the dimension between the sides of the box was a multiple of half-wavelengths. The electric field was enhanced in the middle of the cavity, as the experiment showed when the probe was placed in the middle of the box. Although the cavity resonance and higher than normal E-fields levels present inside the box, as witnessed by performing this experiment, would most likely change once the box was filled with circuit boards, wires, filters and other components, this cavity resonance effect can still have implications when performing real susceptibility and emissions tests on fully operational products.

Resonances degrade shielding effectiveness; therefore, the peaks in the profile could mean the internal electronics placed in the metal box are subjected to higher immunity severity levels at certain frequencies than the standard requires. Also, the emissions emanating from the electronics inside the box could be enhanced, resulting in emissions above the Class A or B limits. The resonant effect could also cause slots or seams in the enclosure to receive or emit RF noise more than possible had the resonance not existed in the first place. Tracking down these types of issues can be difficult.

Determining the Frequency of Resonance

There is a well-known formula for determining the frequency of resonance in MHz of an empty metal box. This formula is:

$$F = 150\sqrt{\left[\left(\frac{q}{h}\right)^2 + \left(\frac{r}{d}\right)^2 + \left(\frac{s}{w}\right)^2\right]}\,MHz$$

Where "*h*", "*d*" and "*w*" are the metal box dimensions in meters (h = height, d = depth, w = width) and "q", "r", and "s" are positive integers (0, 1, 2, 3…), but no more than one at a time can be zero.

Note: A slightly modified version of the above formula can be used to determine the cavity resonances of a printed circuit board shielding can except where the shielding-can's dimensions ("*h*", "*d*" and "*w*") are in millimeters, and the calculated frequency is in GHz.

If the three dimensions of the empty metal box are equal, then the frequency of resonance in MHz can be determined using this simplified formula:

$$F = \frac{212}{h} = \frac{212}{d} = \frac{212}{w}\,MHz$$

How is knowing the resonant frequency helpful?

Knowing the resonant frequency of the empty metal box is helpful in situations where you might have an emission or immunity problem at that specific frequency (frequency of concern). Recall that cavity resonance can only exist if the largest dimension is greater or equal to one-half the wavelength and that below the cutoff frequency, cavity resonance cannot exist. If “h” is less than “d” which in turn is less than “w” then the transverse electromagnetic (TE) mode with zero waves in the “h” direction and one mode each in the “d” and “w” directions is dominant. This “TE_{011}” mode occurs at the lowest frequency at which cavity resonance can occur.

In this situation, you may be able to add an internal shield or other metal structure inside the shielding-box or shielding-can, which shifts the resonant frequency of the box or can away from the problem frequency, thereby allowing the product to pass the compliance test. If this attempted solution does not work, the resonance frequency was not shifted far enough away from the problem frequency, or the resonance effect may not be the root cause of the problem, and further troubleshooting is required.

Summary

Given the above short background, it is evident that it is best to use shielding boxes or shielding-cans with dimensions (length and width) much smaller than a half-wavelength at the highest frequency of concern. This will help prevent cavity resonances from occurring in the first place. Knowing the frequency of concern in your product and using some simple formulas, you can quickly determine if cavity resonance is occurring.

References and Further Reading

1. Williams, T., *EMC for Product Designers*, 5th Edition, Newnes, 2017.
2. André, P. G., Wyatt, K., *EMI Troubleshooting Cookbook for Product Designers*, SciTech Publishing, 2014.
3. Armstrong, K., E*MC Design Techniques for Electron Engineers*, Armstrong/Nutwood UK, 2010.

Understanding Footwear and Flooring in ESD Control

By Dr. Jeremy Smallwood for EOS/ESD Association, Inc.

I have a floor that complies with IEC 61340-5-1 and ANSI/ESD S20.20, and buy footwear that also complies, so that's sorted then?

Well, not really. It's a good starting point, but you need to know that the flooring and footwear work together. Unfortunately, I've seen cases where they don't. If that happens, you're fooling yourself if you think you've got human body ESD risk under control. I've seen a person wearing footwear that measures about 10 MΩ, standing on a floor that measures about 10 MΩ, but their resistance from body to ground was over 1 GΩ, and a body voltage test while walking showed well over 100 V.

Hang on – how can that be? If the footwear and flooring were both about 10 MΩ, surely the resistance from body to ground should have been about 20 MΩ?

In an ideal world, you might think so – but there's another factor – contact resistance between the footwear and the floor.

So how does a footwear and flooring system work, and why does it sometimes not work?

Footwear and flooring work together as a system to ground the person wearing the footwear. For grounding to work, you need a continuous connection between the body and ground. The ESD control footwear, say a shoe, makes the connection between the person's body and the sole of the shoe. The ESD control floor makes a connection between the floor surface and ground. When the shoe is in contact with the floor, we have contact from body through footwear and flooring to ground. At least, that's the plan.

But many types of floors rely on small amounts of conductive material to form the connection through a sea of high resistance material. So, another question is, how well does the conductive material in the footwear contact with the conductive material in the floor? If both footwear and floor materials rely on relatively small amounts of conductive materials, or

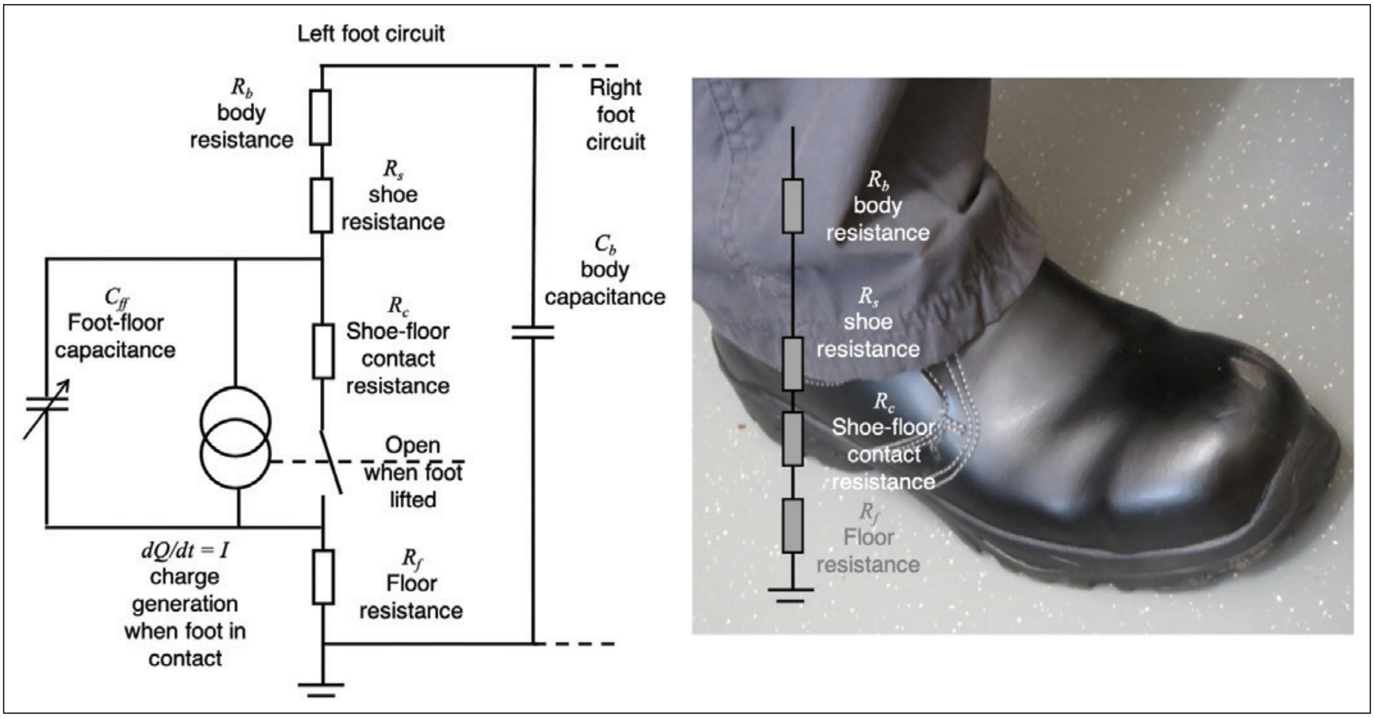

Figure 1: Flooring – footwear circuit model and illustration

there's another reason they don't easily make contact, maybe the answer is "not so well!"

But surely as long as the resistances are within the ANSI/ESD S20.20 and IEC 61340-5-1 limits, we're ok?

Life's not so simple, and that's why both standards insist we must qualify each type of footwear we use in combination with each type of floor we will use it with. A circuit model, as shown in Figure 1, can help us understand why this might be. It might look complicated, but it's actually much too simple, and only the left foot circuit is shown - the right foot circuit is similar.

Let's imagine that the body is like a capacitor C_b. While walking, this capacitance gets charged and discharged via the body resistance R_b and the shoe R_s, because charge is generated by shoe-floor contact. While the shoe is in contact with the floor there is a contact resistance R_c and lifting the foot acts as a switch breaking contact. With the foot in contact with the floor, discharge is through the contact resistance R_c and the floor R_f.

Charge is generated by shoe-floor contact. Let's assume this actually charges a foot-floor capacitance C_{ff} while there is contact. C_{ff} is a highly variable capacitance, which varies from a high value when there is shoe-floor contact, to a low value when lifted. Assuming that at the moment of lifting there is some charge Q on C_{ff}, a voltage is produced which increases as C_{ff} reduces ($V_{ff} = Q/ C_{ff}$). It's this voltage that charges C_b via R_s and R_b and produces the peaks seen in a body voltage walking test.

Assuming the person is walking, C_b discharges at the same time through the other foot circuit via R_b, R_s, R_c, and R_f. The rate of discharge depends on the total of these resistances. The higher this total, the greater the voltage produced by a given current flow. To stop the body voltage from increasing, the current flow through the discharging part of the circuit must be greater than the charging current from the reducing capacitance of the opposite foot lifting.

So, this model tells us some useful things. It tells us that there are many factors other than shoe and floor resistance that contribute to the body voltage waveform in a walking test. This can include things like shoe size and the way we walk, as this affects C_{ff} and the way it changes as the foot is lifted.

The charge on C_{ff} is affected by the way the footwear and floor materials charge against each other – high charging material combinations would be expected to give a higher charge on C_{ff} on lifting the foot. So, two sets of footwear and flooring with otherwise identical resistance characteristics (including contact resistance) can give different charge generation and therefore different body voltages.

Importantly, the footwear-floor contact resistance can differ for footwear-floor combinations that have otherwise similar footwear and floor resistance characteristics. If this contact resistance is greater than the footwear and flooring resistance, it can dominate the total resistance and charge dissipation characteristics and give a much higher body voltage for the same charge generation.

So, if you really want to know whether your footwear and flooring are working together, measure the resistance from the wearer via footwear and flooring to earth (ground). Then, do a walk test to show what body voltage is produced. And, yes, do this for every combination of footwear and flooring you plan to use.

And, by the way, be careful how you clean your floors – surface contaminants like cleaning materials and polishes can change both the contact resistance and charge generation characteristics of the footwear-flooring combination.

In manual component handling, all of this gets more important as the components you handle get more sensitive (lower withstand voltage), especially below 100 V HBM.

Human Body Model ESD Testing

By Don MacArthur, MacArthur Compliance Services, LLC

The most common system-level method for electrostatic discharge (ESD) testing is what is sometimes referred to as the Hand Metal Model (HMM). This ESD testing method is performed per familiar standards such as IEC 61000-4-2, DO-160, MIL-STD-461 CS118, etc. We've previously covered other important points about the HMM method of ESD testing under the Product Insight's category of *In Compliance Magazine* (See References 1 through 4 for details).

To provide further in-depth coverage of ESD testing methods, in this article, we look at another type of ESD testing based on the "Human Body Model" (HBM) method of ESD testing.

The HBM method exists because ESD is a common cause of micro-electronic circuit failures where HMM testing is lacking (HBM is performed at the micro-level whereas HMM is performed at the system-level).

It is well-known that many micro-electronic devices can be damaged or destroyed by an ESD event as low as 20 V or lower. However, what might not be so well-known is that over the past several years, sensitivity to ESD has become more evident through the use, testing, and failure analysis of these same semi-conductor/micro-devices. Additionally, the trend in technology is towards greater complexity and increased package density, which means thinner dielectrics between active elements, resulting in newer, state-of-the-art micro-electronic devices becoming even more sensitive to ESD events. For these reasons, their customers require many integrated circuit component producers to test their device's ESD susceptibility per the HBM test method.

Common HBM ESD Test Standards

At the time of this writing, the most common HBM ESD test standards are MIL-STD-883 and JEDEC JS-001 (formerly JESD22A-114 and ANSI/ESD STM5.1-2007). The formal version of the standard is titled "ANSI/ESDA/JEDEC JS-001 Human Body Model Testing of Integrated Circuits."

The joint ESDA/JEDEC HBM Standard JS-001-2010 merged the JEDEC HBM Standard, JESD22-A114F, and the ESDA HBM Standard, ANSI/ESD STM5.1-2007, into a single document.

ESDA/JEDEC Joint Technical Report JTR001-01-12 explains how to use the merged document to apply HBM tests to IC components.

HBM VS HMM ESD Waveform Characteristics

Item	HBM	HMM
Resistance (Ω)	1500	330
Capacitance (pF)	100	150
Nominal Peak Current at 2 kV (A)	1.34	7.5
Rise-time (ns)	2 to 10	0.6 to 1
Decay time (ns)	130 to 170	60

HBM ESD Simulators

Caution is the order of the day when selecting an ESD Simulator for properly conducting HBM ESD testing. Just because the simulator is known to be adequate for the typical HMM testing while using the 330 Ω/150 pF high-voltage (HV) coupling network does not mean it will also be suitable for use performing HBM testing just by fitting it with the HBM 1500 Ω/100 pF HV coupling network. The waveform obtained by the latter ESD simulator may not be compliant with JS-001, i.e., it does not output the correct HBM waveform characteristics (peak current and rise time) when verified. Additionally, adjustment of the coupling network is likely impossible with these ESD simulators. If the incorrect HBM simulator is chosen, over-testing the IC component is likely to occur.

The author believes only a couple ESD simulator solutions are available that fully meet JS-001 waveform characteristics. If looking to purchase an HBM ESD simulator, the best thing to do is thoroughly research potential suppliers, ensuring they can provide waveform captures showing compliance with JS-001. These suppliers would be able to make assurances that the ESD simulator they manufacture is suitable for HBM testing. In addition, sending an ESD simulator out to an accredited, third-party test facility, with the capability to check the tester's output waveform before purchasing, is a viable option.

Caution is the order of the day when selecting an ESD Simulator for properly conducting HBM ESD testing.

References and Further Reading

1. "What Every Electronics Engineer Needs to Know About: ESD Simulators," *In Compliance Magazine*, February 2018. https://incompliancemag.com/article/esd-simulators
2. "Let's Talk About Design for ESD Immunity," *In Compliance Magazine*, February 2019. https://incompliancemag.com/article/lets-talk-about-design-for-esd-immunity
3. "The Importance of Checking the Calibration of ESD Simulators," *In Compliance Magazine*, February 2020. https://incompliancemag.com/article/the-importance-of-checking-the-calibration-of-esd-simulators
4. "A Non-Typical Use for An ESD Simulator," *In Compliance Magazine*, February 2021. https://incompliancemag.com/article/a-non-typical-use-for-an-esd-simulator/
5. "Overview of Equipment for Human Body Model ESD Testing," ESD Guns. https://www.youtube.com/watch?v=1fmvTMZYOfE

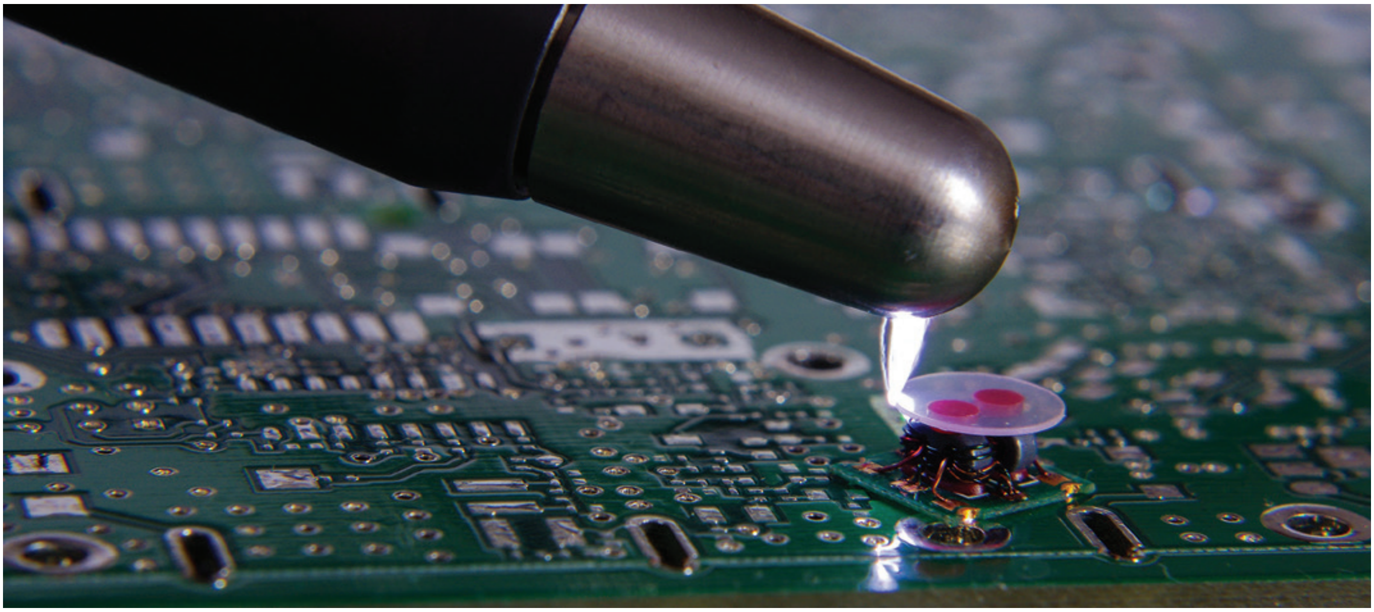

Capacitor Technologies Used in Filtering

By Don MacArthur, MacArthur Compliance Services, LLC

Capacitors are used to filter out system noise to obtain the best EMC performance of a product, usually in bypass or decoupling scenarios. Many common capacitor technologies are used in these filtering applications, each exhibiting unique behaviors. Although understanding each capacitor type and behavior is daunting and difficult to memorize, it is prudent that every aspiring engineer and technician involved in design for EMC at least have a rudimentary understanding of what capacitor technologies are available. This short article intends to provide a primer for you to obtain additional knowledge as required by your unique circumstance and filtering requirements.

Capacitor Technologies

Some of the most common capacitor technologies available for filtering applications today are:

- *Aluminum electrolytic*
- *Aluminum polymer*
- *Aluminum hybrid polymer*
- *Ceramic*
- *Plastic Film*
- *Mica*
- *MLCC*
- *Tantalum*

Only a small handful of the above capacitor technologies are addressed in this article.

Characteristics of Capacitors

When considering the various capacitor technologies for filtering applications, categorizing capacitors by their differing characteristics is helpful. To keep things straight, it is helpful to construct a table that summarizes information according to the following:

- Range of capacitance (or maximum capacitance)
- Equivalent series resistance (ESR)
- Leakage
- Voltage rating (or maximum voltage)
- Current rating (or maximum current)
- Temperature range (or maximum temperature range)
- Sensitivity to temperature and humidity
- Safety ratings (if applicable)
- Application examples

Constructing this table and having it readily available helps one quickly determine if a certain capacitor technology is suitable or not for any specific filtering need.

Multilayer Ceramic Capacitors (MLCCs)

MLCCs are comprised of two classes, uniquely identified as Class 1 and Class 2.

Class 1

Class 1 NP0/C0G ceramic capacitors have relatively small values of permittivity; therefore, small values of capacitance are possible. This characteristic makes them suitable for high-frequency filtering applications. Additionally, their capacitance value is linear over temperature and they do not age much. Class 1 MLCCs have a very small DC-bias voltage dependency.

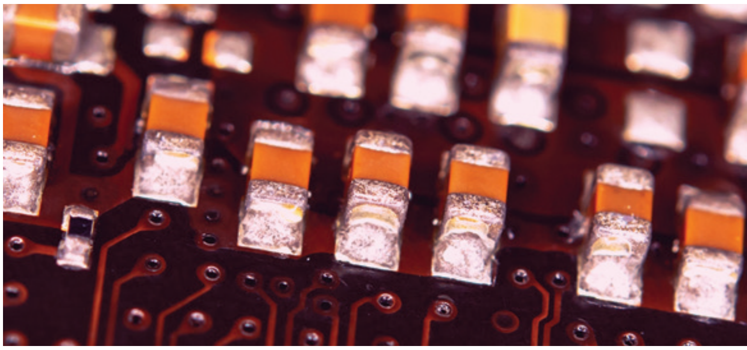

Class 2

In contrast to Class 1 MLCCs, the characteristics of Class 2 X7R, X5R, Y5V, etc., capacitors are at the other end of the extreme. They have relatively high values of permittivity (high values of capacitance are possible), a non-linear temperature dependency, do not age well, and have a high DC-bias voltage dependency.

Film Capacitors

Film capacitors have a special structure for the electrodes, consisting of two different types: metal film and metallization on dielectric. The type of dielectric for each of these two different structures is paper and plastic film. The four types of dielectrics are Polyester (PETP), Polycarbonate (PC), Polypropylene (PP), and Polystyrene (PS).

Safety Ratings of Film Capacitors

One of the most important concepts to compliance engineering professionals regarding film capacitors is their safety ratings. In short, X-capacitors are used to filter out differential-mode noise in line-to-line situations. Y-capacitors are used to filter out common-mode noise line-to-ground. Due to leakage current limitations imposed by most product safety standards (the harshest of which are found in medical device regulations), the capacitance value of Y-caps is very low.

There are two different categories of X and Y-caps. X1 caps have an impulse rating of 4kV X2 caps are rated for 2.5 kV. Y1 caps have an impulse rating of 8 kV, whereas Y2 caps are rated 5 kV.

For more information covering the safety classes of capacitors, see IEC 60384-14 / UL 60384-14.

Pro Tip: Document each capacitor type's sensitivity to humidity and temperature

When conducting your own research for each of the available capacitor technologies, take note of each one's sensitivity to humidity and temperature. Based on your product's Life Cycle Environmental Profile (LCEP), you will likely encounter certain types of unsuitable capacitors, and you can cross them off your list as potential candidates in your design.

Aluminum Electrolytic Capacitors

Aluminum electrolytic capacitors have been around forever and are made from well-proven technology. They support the highest voltages and have the largest range of capacitance values available due to their larger size. These capacitors' expected lifetime is doubled for approximately every 10°C drop in temperature they see, which is below their maximum specified temperature rating.

Aluminum Polymer Capacitors

Aluminum polymer capacitors are a new technology type of capacitor. They look a lot like aluminum electrolytic capacitors, except the top has no vent. Other benefits of aluminum polymer capacitors over their electrolytic cousins are that they have a lower equivalent series resistance (ESR) value, they cannot dry out (they are made of solid polymers), and they have higher expected lifetimes. Their expected lifetime increases by a factor of 10 for approximately every 20°C drop in temperature they see, which is below their maximum specified temperature rating. The downsides of aluminum polymer capacitors are increased leakage current and susceptibility to vibrations.

Summary

This article briefly covered the latest capacitor technologies used in filtering. See the references and further reading suggestions below for a more in-depth review.

References and Further Reading

1. "Introduction to the capacitor technologies and how to use them," Würth Elektronik Group. https://youtu.be/0cfxaztb5Pc
2. Hu, R., *PCB Design and Fundamentals for EMC*, RANDSpace Technology LLC, 2019.
3. Keller, R.B., *Design for Electromagnetic Compatibility – In a Nutshell*, Springer, 2023.

The Importance of High Frequency Measurements

By Don MacArthur, MacArthur Compliance Services, LLC

Anyone involved in the development of high-tech products should understand the consequences brought about by such items as component die-shrinks, lower voltage levels, faster rise/fall times, higher switching speeds, etc. These elements often mean more diligence and thoughtful attention to detail is required in laying out circuits today, more so than they ever have been in the past. These extra precautions are required to ensure proper circuit functionality and to meet timing, signal integrity and electromagnetic compatibility (EMC) requirements, to name a few.

Have you ever done everything you could to ensure that your design met all the necessary requirements before building an actual prototype, only to discover issues once you had the functioning hardware in hand? These issues could be related to functionality, signal integrity, EMC, or something else, and they could prevent your design from being released to production on time. If you don't have a way to quickly troubleshoot these high-speed or high frequency issues within your design, you will be left with guessing what could be wrong. You may make changes based on engineering judgment and intuition, but you will likely have to repeat the process until a solution is found.

It's easy to see that the trial-and-error approach of guessing what is wrong with your design is flawed and consumes a lot of time and resources. Furthermore, upper management may not be pleased if a solution isn't found quickly enough. To escape this seemingly endless and frustrating cycle, you must be resourceful and use high frequency probing and measurement techniques to gather actual measured data. You'll need certain knowledge and tools to develop this skill, which will be discussed shortly. But first, let me clarify what I mean when I say "be scrappy."

A Quick Note on What it Means to "Be Scrappy"

As engineers and technicians working in compliance engineering, we must always deal with constraints. For instance, we don't always have the ultimate budget that affords us the luxury to buy the best, most expensive new probe or other fancy test equipment. Or we may not have exactly the right hardware to get initial "engineering scan" EMC testing completed on our new widget that's operating under a tight schedule. Or we might not have enough time to allow us to test everything we want to validate a design. We must "be scrappy" in such situations and determine the best path forward. High-frequency probing is an area where we can "be scrappy" and shine. We don't always need to buy an expensive probe. When making high frequency measurements, we can build our own that accomplish exactly what we need them to do and when we need them to do it! This is what I mean when I say "be scrappy."

Basics of High Frequency Measurement Techniques

Before diving too deep into the nitty gritty of high frequency probing techniques, it's imperative to understand a few basics, as described in the remaining portion of this article. The basics include probe calibration and null measurements and a description of the various types of voltage probes available, including their strengths and weaknesses.

Probe Calibration and Null Measurements

Just like you wouldn't attempt to drive your car without first ensuring the tires are properly inflated and it had enough fuel or electric charge (if electric) to get you where you want to go, you shouldn't attempt to take a measurement on a high frequency circuit without first ensuring the voltage or current probes you're using are measuring adequately. This is a key first step to performing high frequency measurements properly and not doing it is a mistake that I often see even the most seasoned professionals make. Don't be like the others!

Be wise and diligently perform probe calibrations and null measurements for every high frequency measurement you intend to make.

Calibration

Calibration is typically where you use the 1 kHz square wave output provided on the oscilloscope to "square up" the signal shown on the display by making an adjustment located on the end of the probe. If you move the scope probe to another channel, it is best to re-calibrate it for that specific channel. Don't assume the calibration won't change when you move the probe to another channel. If you don't perform this simple step, you may see overshoot and ringing in your measurement data that really isn't present in the circuit you're measuring! These anomalies could thwart your efforts to understand the problem you're trying to solve.

Don't say I didn't warn you about the importance of proper probe calibration.

Null Measurements

For a voltage probe, a null measurement is a method for determining how much the common mode noise present in the measurement setup is affecting the measurement result. It sounds counter-intuitive, but for a typical scope probe, the null experiment is performed by first tying the ground lead of the probe to the probe tip and then touching the tip to the circuit under test while the rest of the circuit and any auxiliary equipment is operated normally. The amount of voltage picked up is the margin of error in the actual measurements you will perform when using this probe to collect data.

For a current probe, a null measurement has the same purpose as a voltage probe, except it is conducted a little differently. To conduct a null measurement on a current probe, loop the wire to be measured so that it bends back on itself. Where the wire bends, it should sit flush from the opposite side of the probe body and not go all the way through it. As with the voltage probe, the amount of voltage picked up is the margin of error in the actual measurements you will perform when using this probe to collect data.

Voltage Probes

There are three general types of oscilloscope probes. These include the high impedance (Z) passive, high Z active, and low Z probes.

High Z Passive Probes

High Z passive probes, like the typical 10x probes found in most test laboratories, are the most popular oscilloscope probes available. These probes are characterized by their capacitive input Z and must be compensated to the input Z of the scope used. To fully meet its specification, this type of probe must have a bandwidth that matches that of the scope. High Z passive probes are sensitive to high Z electric field coupling that could ultimately affect the measurement circuit.

High Z Active Probes

High Z active probes are characterized by their low capacitive input (~ couple of 2 pF) and high input resistance (< 1 MΩ); therefore, they are useful where circuit loading must be minimized. Like the high Z passive probes, these types of probes are also sensitive to coupling from high Z electric fields, except to much higher frequencies than is typically seen with high Z passive probes. Other downsides to high Z active probes include lower bandwidth capability for balanced designs (over what is available in passive probes), increased cost, and inability to take the normal handling abuse as typically seen in a normal laboratory environment. Experience has shown that the typical engineer and technician are not too kind to their equipment, especially in the heat of battle (product development or testing), when things get hectic and they are in a crunch for time.

Low Z Passive Probes

Characterized by a resistive input resistance over a wide range of frequencies, low Z passive probes are useful in many measurement situations. If you want to "be scrappy" these types of probes are easy to construct and provide accurate measurements up to 500 MHz. At low frequencies, low-impedance passive probes are not very sensitive to electric field coupling at very low frequencies. It's interesting to note that > 50 MHz, the input Z of this type of probe usually exceeds that of high Z passive probes!

Summary

There are many other elements and depths to high frequency probing not discussed here but are definitely worth further study. These include probe ground lead effects (resonance and induction), high Z passive probe compensation, differential measurements, magnetic loop and other noncontact measurements, current probes (theory and uses) and measurements of pulsed EMI effects on electronic circuits. Please consult reference 1 for more details on these additional topics. Although written 30 years ago, reference 1 still contains valuable information that is even more applicable today.

References and Further Reading

1. Smith, D.C., *High Frequency Measurements and Noise in Electronic Circuits*, 3rd Edition, Springer, 1993.

No Spectrum Analyzer? No Problem – Use Python's SciPy Module Instead

By Don MacArthur, MacArthur Compliance Services, LLC

Spectrum analyzers are used to capture the amplitudes and frequencies of time-domain signals, plotting these signals horizontally across a display, with lower frequencies on the left and higher frequencies on the right. Spectrum analyzers operate on the principle of the Fast-Fourier Transform (FFT) algorithm and have many important uses in compliance engineering, including noise analysis of measurement systems.

A measurement system could be a circuit that measures voltage or current using an analog-to-digital converter (ADC) that outputs ADC counts that represent the time-domain signal captured by the system. In such systems, it is important to determine how much unwanted noise is in the system as this noise could negatively impact the accuracy of the measurement system because the unwanted noise could mask the wanted signal.

A spectrum analyzer is a useful tool for hunting down unwanted noise in a measurement system. But what if, for whatever reason, you didn't have a spectrum analyzer at your disposal? Not determining the noise characteristics of your system is not an option, so what else could you do to determine how much noise was in your measurement system? Well, if you had a way to capture the output of the ADC, for instance, then you could use the Python programming language, and its SciPy FFT module to analyze this data. Since it's a little tricky getting the SciPy FFT function to give you the correct output (you can't just plop your measurement data into the FFT module and expect it to work correctly), you'll want to have a rudimentary understanding of how to use Python as a pseudo-spectrum analyzer. If you're interested in learning how to do this, read on. The following is provided to get you started using the SciPy FFT function as a replacement for a spectrum analyzer.

Importing Python Modules

After you have installed the latest 3.x.x version of Python onto your machine, the first thing you will want to do is import the Python modules necessary for use later in the script. Imported Python modules are placed at the top of every Python script. The required modules for FFT analysis and how to import them are noted below:

```
import numpy as np

import matplotlib.pyplot as plt

from scipy.fft import fft
```

If you don't already have these modules installed as part of your Python environment, you must install them using the PIP command first. See reference one for how to install Python modules using the PIP command.

Document the Steps of the Python Script

The next thing I like to do is document the purpose of the script and what the script is doing. In Python, anything following the # symbol is considered just text and is skipped by the Python interpreter. Therefore, documenting the purpose of the script and each of the steps may look something like this:

```
# Perform FFT using SciPy Module

################## Steps ##################

# 1: Construct Time Domain Signal

# 2: Perform FFT using SciPy 'fft' Function

# 3: Plot Frequency of Spectrum using matplotlib

###########################################
```

Note: As a personal preference I like over-documenting the code I write. I think that if I put the time into figuring out how to code something, then I don't want to spend a lot of time re-learning it six months down the road when I may have forgotten what I was originally doing. Some might consider my over-commenting as unprofessional. My boss and other users of the code I write most likely appreciate the speed at which I get my coding work done.

Step 1: Construct the Time Domain Signal

Here is what the Python script needs to set things up and construct a time-domain signal. This creates a 1 V peak signal at 60 Hz and a 0.5 V DC signal (designated as y), which, if the rest of the script works correctly, will show up in the plots that are generated.

Note: Once the script works correctly, you can play around with the signals you want to inject. Instead of just injecting a 1 V, 60 Hz and 0.5 V DC as the steps below show, try something like the following and see what the script outputs:

```
y = 1 * np.sin(2 * np.pi * f0 * t) # Create single time-domain signal, or
```

```
y = 1 * np.sin(2 * np.pi * f0 * t) + 4 * np.sin(2 * np.pi * 3 * f0 * t) # Time-domain signal plus a second signal, or
```

```
y = 1 * np.sin(2 * np.pi * f0 * t) + 4 * np.sin(2 * np.pi * 3 * f0 * t) + 2 # Time-domain signal plus a second signal plus DC signal (0 frequency) of amplitude equal to  2, etc.
```

The possibilities are endless!

Here's the code for Step 1:

```
# Step 1: Construct Time Domain Signal

Fs = 1000 # Sampling frequency (Hz). Can reconstruct signal to half of this frequency (Nyquist Sampling Theorem).

tstep = 1 / Fs # sample time interval

f0 = 60 # input signal frequency (Hz)

N = int(100 * Fs / f0) # number of samples. Ex.: Use int(10*Fs/F0) to increase number of samples (10 cycles of samples)

t = np.linspace(0, (N-1) * tstep, N) # Create time steps of time domain signal

fstep = Fs / N # freq interval for each frequency bin (sampling frequency divided by number of samples)

f = np.linspace(0, (N-1) * fstep, N) # Create freq steps --> x-axis for frequency spectrum

y = 1 * np.sin(2 * np.pi * f0 * t) + 0.5 # Create a 1 Vpk 60 Hz time domain signal and a 0.5 Vdc signal
```

Step 2: Perform FFT Using SciPy FFT Function

```
# Step 2: Perform FFT using SciPy 'fft' function

X = fft(y) # X is a series of complex numbers

X_mag = np.abs(X)/ N # Magnitude of fft output normalized to number of samples

f_plot = f[0:int(N /2 + 1)] # Only plotting half of sampling frequency (just positive frequencies)

X_mag_plot = 2 * X_mag[0:int(N/2+1)] # Get Magnitude

# Get correct DC Component (does not require multiplication by 2) and does not require taking log.

X_mag_plot[0] = X_mag_plot[0] / 2  # Compute DC
```

Step 3: Plot Frequency of Spectrum Using Python's matplotlib Library

The following shows how to plot both the time-domain signal we created in Step 1 and its frequency domain counterpart.

```
# Step 3: Plot Frequency of Spectrum using matplotlib

fig, [ax1, ax2] = plt.subplots(nrows=2, ncols=1)

fig.set_figheight(8)

fig.set_figwidth(8)

ax1.plot(t, y, '-', lw=0.4, c='black')

ax2.plot(f_plot, X_mag_plot, '-',  lw=0.4, c='black')

ax1.set_title('Sinusoidal Signal')

ax2.set_title('Magnitude of Spectrum')

ax1.set_xlabel('Time(s)')

ax1.set_ylabel('Count(s)')

ax1.minorticks_on()

ax2.set_xlabel('Frequency (Hz)')

ax2.set_ylabel('Amplitude (pk)')

ax1.grid()

ax2.grid()

ax1.set_xlim(0, t[-1])

ax2.set_xlim(0, f_plot[-1])

plt.tight_layout()

plt.show()
```

Plots

If you take the information from steps 1, 2, and 3 and create your own Python script and run it, then you should see something like Figure 1.

The plots in Figure 1 show the time-domain on the top and the frequency-domain on the bottom. Notice that the script seems to be working correctly, as it can pick out the 0.5 V DC signal at 0 Hz and the 1 V peak signal at 60 Hz that we injected.

Analyzing Real Data

The above Python script does not require any external ADC count data to work (recall that we created our signal to verify the script works correctly) but does provide enough information to create your script for analyzing real ADC count data. Replace the script-generated time-domain signal with your AC count data. This may come in the form of a Comma Separated Values (CSV) file or some other form.

Additionally, the frequency-domain plot above is shown using a linear scale. This is OK for demonstration purposes, but you will want to have the data presented logarithmically (because it's easier to analyze). It doesn't take too much head-scratching to figure out how to plot data in Log form with Python.

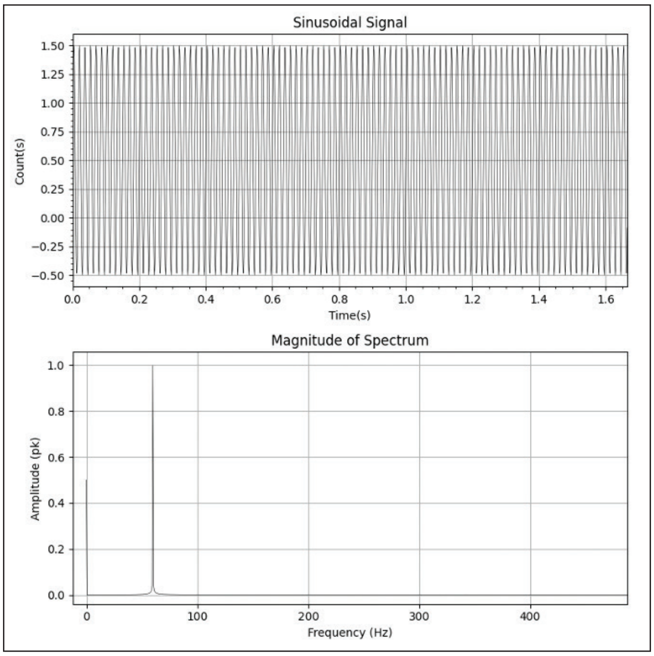

Figure 1

Figure 2 shows a taste of what you can do with Pythons SciPy FFT function. The measured signal is 120 V, 60 Hz, as shown in the top waveform. The middle plot shows the FFT amplitude in dB on the vertical axis, with a plot of linear frequency on the horizontal. The bottom plots show the FFT amplitude in dB on the vertical axis and log frequency (Hz) on the horizontal.

Histogram

Something else that is valuable to plot is a histogram of the count data. This also can easily be accomplished using Python, and since you already have the data, it's a smart thing to include in any analysis. Figure 3 shows what that might look like.

Summary

In this article, we described a method for analyzing data using the FFT algorithm found in Python's SciPy module. The reader should know that the SciPy module also includes methods for other FFT algorithms, such as the Inverse FFT and Discrete Sine and Cosine methods. See https://docs.scipy.org for more details.

Also note that there is one downside to using Python's SciPy module as a pseudo-spectrum analyzer that wasn't addressed above. A spectrum analyzer captures data in near real-time, whereas with Python, the data is analyzed on a one-shot basis after the fact. This could result in not capturing spurious noise intermittently, before or after the signal data was initially captured. Certainly not a showstopper, just something to be aware of.

In short, the above code should give you enough to develop your own Python FFT script. Have some fun and play around with it!

References and Further Reading

1. Sweigart, A., *Automate the Boring Stuff with Python – Practical Programming for Total Beginners*, 2nd Edition, No Starch Press, 2020.
2. Kong, Q., Siauw, T., Bayen, A.M., *Python Programming and Numerical Methods – A Guide for Engineers and Scientists*, Academic Press, 2021.

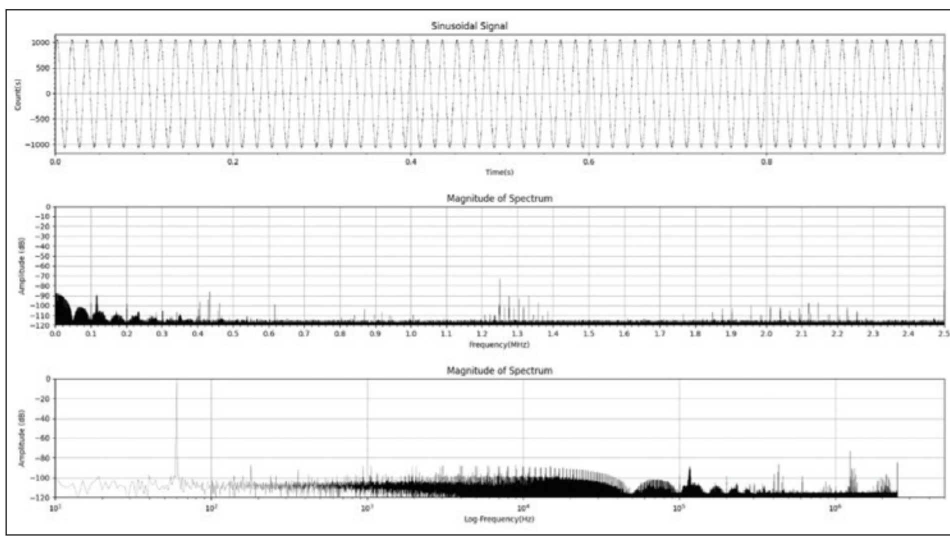

Figure 2

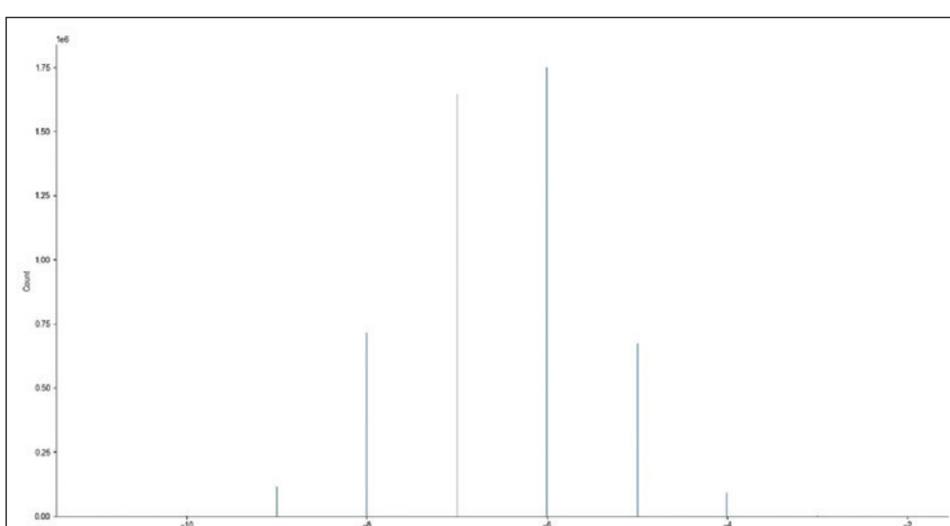

Figure 3

Why It Is Important To Control and Measure CDN Impedance Per IEC 61000-4-6

By Don MacArthur, MacArthur Compliance Services, LLC

IEC 61000-4-6 is titled "Electromagnetic compatibility (EMC) - Part 4-6: Testing and measurement techniques - Immunity to conducted disturbances induced by radio-frequency fields." This "conducted RF immunity" standard covers the conducted immunity requirements of electrical and electronic equipment to electromagnetic disturbances from intended radio-frequency (RF) transmitters in the frequency range 150 kHz up to 80 MHz.

Note: In Europe, IEC standards that become equivalent European Norm (EN) standards are designated with an 'EN' instead of an 'IEC' prefix. In most cases, there is no difference between IEC and EN standards.

Coupling/Decoupling Networks

A major component of conducted RF immunity testing per 61000-4-6 is the coupling/decoupling networks (CDNs). There are various types of CDNs used, the configuration of which depends on the circuit under test (signal, communications, input/outputs, Ethernet, etc.).

As one can imagine, the coupling (C) part of the CDN is used to couple energy into the equipment under test (EUT). In contrast, the decoupling (D) part of the CDN is used to prevent unwanted injected test signals from disrupting any auxiliary equipment used to provide functional signals to the EUT.

CDN Impedance

The impedance (Z) that the CDN contributes to the overall path that RF current flows as part of the leveling process is tightly controlled in the standard.

From 150 kHz – 26 MHz, the standard requires Z equal 150 Ω ± 20 Ω.

From 26 MHz - 80 MHz, the standard requires Z equal 150 Ω + 60 Ω, -45 Ω.

Why does the impedance of a CDN change value?

Test laboratories are busy environments where it is possible to easily damage a CDN in such a manner that its Z changes without anyone ever knowing. Failures could result from dropping, applying too much current, over-voltage conditions, spikes and transients, surges, or other similar events.

If CDN impedance changes, why is it not recognized?

The reason why changes to CDN-Z are not recognized by laboratory personnel is that the level-setting procedure results in the correct voltage regardless of CDN-Z. Laboratory personnel might be looking for 10 V, and no further analysis is conducted when the level-setting procedure obtains this result. If the level-setting procedure is only performed once

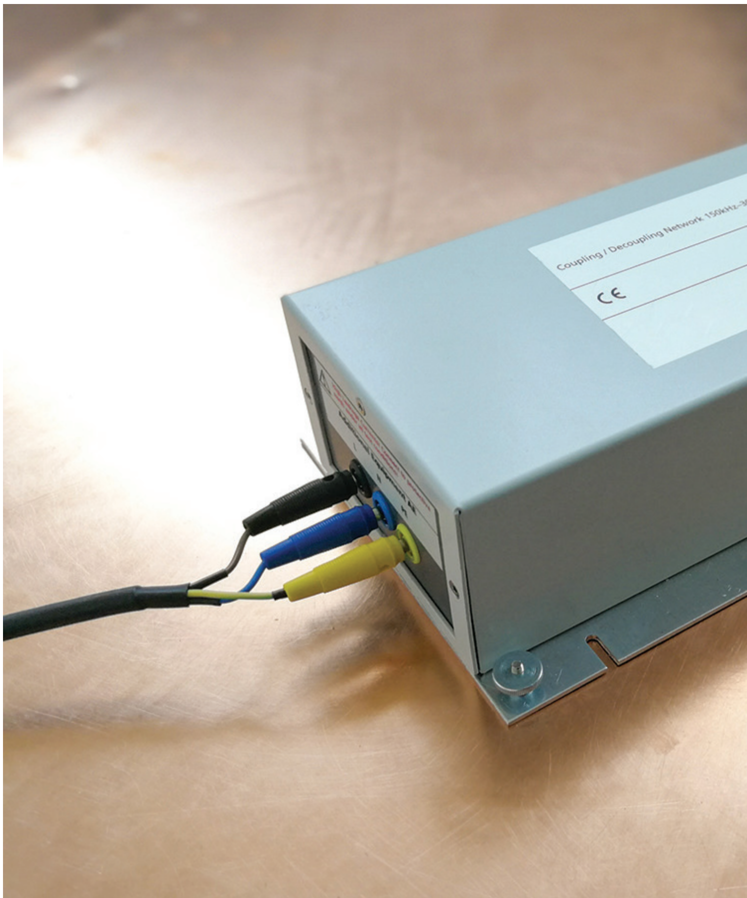

per year, any changes to CDN-Z occurring after the procedure will only be recognized the next time the level-setting procedure is attempted.

Why does CDN impedance manner?

CDN-Z matters because tight control of CDN-Z means fairness in testing. If CDN-Z is wrong, the test facility could either be over-testing (inadvertently applying too much signal) or under-testing (inadvertently not applying enough signal). Over-testing could result in failing a product that should have passed, and under-testing passing a product that should have failed. In addition, CDN-Z matters in situations where an EUT will be tested at several different laboratories. It is important the results are repeatable amongst these various laboratories.

Reference 1 contains two sets of example Spice simulations that show how a change in CDN-Z from 150 Ω to 300 Ω, using an identical EUT load of 1000 Ω while applying the same laboratory calibrated 10V test level, resulted in an increase in current applied to the load of 7.8 mA to 8.4 mA. This change resulted in 7.8 V and 8.4 V developed across the EUT load, respectively. This is a 7 % increase in current applied from what should have been the standard level and could make the difference between a pass or fail of the EUT.

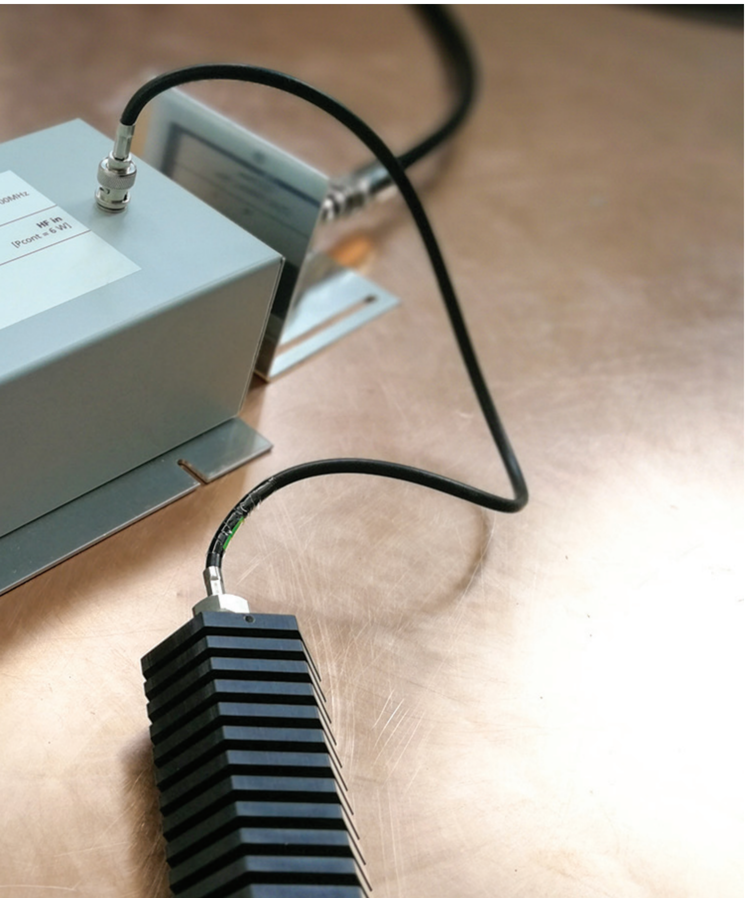

What can be done to ensure CDN impedance is correct?

The first step in maintaining correct CDN Impedance is the training of staff.

Ensure they know the importance of maintaining the correct CDN impedance and reporting any misuse or abuse they witness. Have any suspected damage to CDNs investigated immediately and before using again.

The second step in maintaining correct CDN impedance is to have the Z of all your CDNs periodically calibrated at an ISO17025 accreditation test facility (or alternatively, learn how to do it yourself).

You may end up saving you and your customer many hours in lost revenue, re-work time, and delays.

Conclusion

This article briefly described CDN impedance requirements of IEC 61000-4-6 for conducting RF immunity testing and why maintaining the correct CDN impedance is important. Additionally, it provided methods for ensuring the correct CDN impedance is maintained.

References and Further Reading

1. "Why is it important to control and measure CDN impedance for EN61000-4-6 testing?" *The Equipment Calibration Business.*
2. IEC 61000-4-6:2013. Electromagnetic compatibility (EMC) - Part 4-6: Testing and measurement techniques - Immunity to conducted disturbances, induced by radio-frequency fields. Available from https://webstore.iec.ch/publication/4224

PRODUCT MARKETPLACE

AK-40G Antenna Kit 20 Hz- 40 GHz

A.H. Systems' AK-40G Portable antenna kit offers the best frequency range and performance in one case. This is the antenna kit you need for everyday testing. Just grab it and go. Inside the case is all the reliable antennas, current probes, and cables needed to satisfy a wide array of customer requirements. The antenna kit also comes with a tripod with azimuth and elevation head for antenna positioning and a tripod carrying case. Excellent performance, compact size and a lightweight package make this kit a preferred choice for field-testing and can ship with next-day, on-time delivery. Other antenna kits available.

A Kilowatt On Your Desk

More compact power than ever thought possible. Generate 200 V/m and up to 1 GHz with a single-phase input voltage with the 800W1000. For more information, visit https://www.arworld.us or contact us at info@arworld.us or (215) 723-8181.

A Better Way to UL & CSA

Most companies struggle to obtain their UL, CSA, & CE Certifications. That is because they are not properly prepared. Take the test to see if you are ready:

- Do you know what standards are required?
- Do you own a copy of the standards?
- Do your design engineers know the standards and how to comply?

Answer "NO" to any of these questions? You need to contact CertifiGroup. We will help you all the way! That includes performing the entire certification process in our 25,000 sq. ft. test lab. On time, on budget! Contact us today at 800-422-1651.

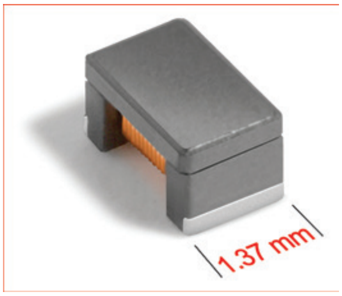

Wirewound Ferrite Beads – Free Evaluation Samples!

Coilcraft 0805PB Series wirewound ferrite beads offer exceptional impedance performance and extremely low DCR that is optimized for high-frequency noise suppression on high-current power supply lines, providing superior performance than traditional multilayer ferrite beads. They also feature a robust mechanical structure, and are AEC-Q200 Grade 1 qualified for use in automotive applications and other harsh environments. Request free samples!

IPX1 / IPX2 Drip Box System

Products intended for outdoor environments, or wet environments, often require Ingress Protection (IP) Code testing. ED&D's cutting-edge solution for the IPX1 and IPX2 tests is the DBX Series Drip Box Test Systems. ED&D also invented IP Code Turntables, including a mini-turntable (shown) that allows for meeting requirements of the IP Code. ED&D also offers the device mounted in a chamber or it can be offered in combination with the Spray Test Chamber (STC-DBX Series). Other products for the IP Code include Dust Chambers, Spray Test Chambers, Spray Nozzles, Jet Nozzles, Accessibility Probes, and Oscillating Spray Testers.

ETS-Lindgren: Your Wireless/OTA Service Partners

ETS-Lindgren has dedicated experts committed to our customers' success. We understand how downtime can affect our customers' development, production, and testing schedules. Let ETS-Lindgren assist you to ensure optimal utilization of your assets. Services include engineering and consulting, education and training, calibration and repair, product testing, and more! Contact your local ETS-Lindgren representative or visit https://www.ets-lindgren.com.

Exodus, Another Industry First!

Exodus Advanced Communications is a "Best-in-Class" SSPA manufacturer delivering products from 10kHz to >51GHz. Our extremely ruggedized product line consists of LDMOS, GaN (HEMT) & GaAs devices. We manufacture many of our own devices. We use clean rooms for manufacturing the latest technological advancements, designing, and fabricating low, medium, and high power amplifiers with chip and wire technology. We also have an extensive range of stand-alone modules, chassis configurations, and full turn-key systems to satisfy customers' demands.

All New EMC Partner Transient Generator

Conducted immunity testers according to IEC standards (IEC 61000-4-x) up to up to 8kV Surges and 8kV EFT/Burst pulses. Ready for Surge, EFT/Burst, Ringwave, 10/700, Common Mode testing, Differential Mode Testing, Dips, Variations, Interrupts and more. Wide range of accessories (3 Phase CDN's, Data Line CDN's, Magnetic Field, ANSI coupling, etc). Modular architecture enables customized configuration. Powerful TEMA3000 automation software. Contact HV TECHNOLOGIES for more information.

Email Newsletters Designed for Compliance Engineers

Our email newsletters are designed to provide you with the latest compliance engineering news, technical resources, industry products and services, and new developments within the community. Choose from **The World in Compliance**, a biweekly communication of global compliance news and updates, **Product Insights**, a monthly feature of products and product advice; or **TechConnect** our monthly share of technical industry resources. Join for free to start receiving your choice of helpful and informative resources stratight to your inbox.

PRODUCT
MARKETPLACE

New Bidirectional Power Supplies from Kikusui Electronics

Engineers are facing growing needs and complexity as our world becomes more electrified and moves towards new greener energies. Thankfully, Kikusui is unveiling their new lineup of bidirectional high-capacity DC power supplies. The new PXB series is able to seamlessly transition from sourcing DC power to acting as a high-power load. The PXB also has many built-in features to help emulate batteries, inverters, LEDs, and even PV solar cells. Engineer the electrified future with PXB.

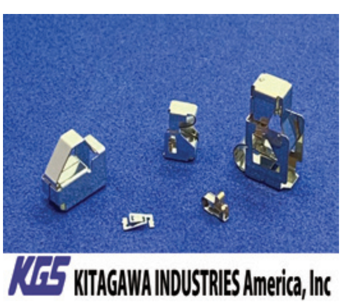

On-board EMC Grounding Contacts

KITAGAWA INDUSTRIES America's on-board contacts are all SMT (Surface Mount) type contacts, designed for PCB-level EMC grounding, shielding, and ESD.

- Effective for suppressing emission and immunity reduction
- All EMC mitigation can be done at the board-level
- Space-saving and robust design
- Easy to incorporate even where screws are included
- Tape-and-reel design allows for use with automated pick-and-place machine to increase efficiency and reduce manual labor

Discover the Future of Cooling Technology with Leader Tech's High Performance Thermal Interface Materials

Our Carbon Fiber, Graphene, and Indium series are engineered to redefine thermal management. Harness the power of Carbon Fiber for excellent heat conductivity and mechanical strength. Embrace efficiency with Graphene. Experience Indium's exceptional thermal interface properties. Trust Leader Tech for cutting-edge solutions that push the boundaries of heat dissipation. Keep your electronics cool, efficient, and high-performing with our advanced materials.

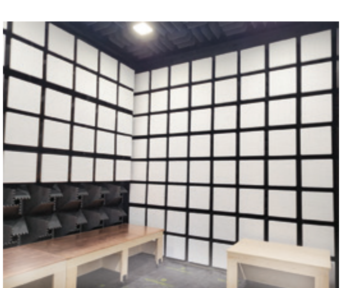

Raymond EMC: General Anechoic Chambers

Raymond's QuietChamberTM provides an interference-free and simulated free-space environment. A QuietChamberTM can be highly customized based on the clients' specifications and RF absorption required. Applications include 5G and antenna, among others. Raymond provides full turnkey solutions starting with design through to installation and RF Shielding Effectiveness certification. We also accommodate all electrical, HVAC, life safety and seismic requirements.

New Low Cost EMI Receiver Ideal for Conducted Measurements

The newly introduced R&S EPL1000 is a compact and fully compliant CISPR 16-1-1 test receiver designed for precise EMI measurements up to 30 MHz. Equipped with an additional spectrum analyzer and signal and tracking generator, the R&S EPL1000 offers unparalleled versatility for various laboratory applications. With its compact design and comprehensive features, the R&S EPL1000 serves as an ideal solution for engineers and technicians seeking quick and accurate EMI measurements.

Spira: A Leader in EMI Gaskets

Spira is at the forefront of EMI gasket innovation, design, and customer service. The unique spiral design offers extremely low compression set and long life. Providing superior EMI/RFI shielding, designed to be cost-effective & reliable for the life of a system. Environmental sealing also available. ISO 9001/AS9100 certified, expert technical support, and made in the USA. Choose Spira gaskets to pass your shielding tests the first time. Visit https://www.spira-emi.com to learn more.

ESD Seating: Part of a Comprehensive ESD System

According to a 2015 ASHRAE study, standing from a chair generates static charges in excess of 4000 V. StaticWorx Bolt ESD chairs, with carbon fibers in the upholstery and metal frame, facilitate the dissipation of ESD. All parts of the Bolt ESD chair are electrically bonded to the castors, which dissipate static through the ESD floor to ground. Combining Bolt ESD seating with StaticWorx ESD flooring can maintain human body charges below 20 volts.

Multifunction Compact Simulator CCS 800

The Multifunction Compact Simulator CCS 800 integrates EFT/burst, surge, ring wave, power frequency/impulse magnetic field, voltage dips/ interruptions/ variations tests according to IEC standard (IEC 61000-4-4/-5/-8/-9/-11/-12/-29) into a single equipment with test voltage up to 8kV for EFT/Burst, surge and ring wave test. It includes a CDN rated up to AC/DC 300 V, 20A, external 3-phase CDNs can be customized. The control software Corelab offers easy operation and test sequence functions. Visit: https://www.3c-test.com for more info!

The Key to Mobile Communications: Adrastea-I

Mobile communications is the preferred technology for IoT applications outside of local networks. The pre-certified high-performance multi-band LTE-M and NB-IoT module Adrastea-I from Würth Elektronik equips devices with “cell phone” capabilities. Due to its low power consumption and small size the module can be used for battery-powered portable applications. The integrated GNSS function allows applications to send location updates. Visit https://www.we-online.com/gocellular.

SUPPLIER INDEX

Absorbing Materials

AR RF/Microwave Instrumentation

160 School House Road
Souderton, PA
(215) 723-8181
https://www.arworld.us

ETS-Lindgren

1301 Arrow Point Drive
Cedar Park, TX
(512) 531-6400
https://www.ets-lindgren.com

Leader Tech Inc.

12420 Race Track Road
Tampa, FL
(813) 855-6921
https://www.leadertechinc.com

Raymond EMC

5185 Dolman Ridge Road
Ottawa, Ontario, Canada
(800) 362-1495
https://raymondemc.com

Amplifiers

A.H. Systems, Inc.

9710 Cozycraft Avenue
Chatsworth, CA
(818) 998-0223
https://www.ahsystems.com

AR RF/Microwave Instrumentation

160 School House Road
Souderton, PA
(215) 723-8181
https://www.arworld.us

Exodus Advanced Communications

3674 East Sunset Road
Las Vegas, NV
(702) 534-6564
https://www.exoduscomm.com

ETS-Lindgren

1301 Arrow Point Drive
Cedar Park, TX
(512) 531-6400
https://www.ets-lindgren.com

HV Technologies, Inc.

8526 Virginia Meadows Drive
Manassas, VA
(703) 365-2330
https://www.hvtechnologies.com

Rohde & Schwarz USA

6821 Benjamin Franklin Drive
Columbia, MD
(888) TEST-RSA (837-8772)
https://www.rohde-schwarz.com

Antennas

A.H. Systems, Inc.

9710 Cozycraft Avenue
Chatsworth, CA
(818) 998-0223
https://www.ahsystems.com

ETS-Lindgren

1301 Arrow Point Drive
Cedar Park, TX
(512) 531-6400
https://www.ets-lindgren.com

HV Technologies, Inc.

8526 Virginia Meadows Drive
Manassas, VA
(703) 365-2330
https://www.hvtechnologies.com

Thank you to this month's advertising partners for making the 2024 Product Resource Guide possible. We encourage you to learn more about their products and services.

Certification Services

Global Validity

8601 Six Forks Road, Suite 400
Raleigh, NC
(877) 464-6753
https://globalvalidity.com

Chambers

ETS-Lindgren

1301 Arrow Point Drive
Cedar Park, TX
(512) 531-6400
https://www.ets-lindgren.com

Raymond EMC

5185 Dolman Ridge Road
Ottawa, Ontario, Canada
(800) 362-1495
https://raymondemc.com

Components

Coilcraft

1102 Silver Lake Road
Cary, IL
(847) 639-6400
http://www.coilcraft.com

ETS-Lindgren

1301 Arrow Point Drive
Cedar Park, TX
(512) 531-6400
https://www.ets-lindgren.com

Kikusui America

3625 Del Amo Boulevard
Torrance CA
(310) 214-0000
https://www.kikusuiamerica.com

Kitagawa Industries America, Inc.

2860 Zanker Road
San Jose, CA
(408) 971-2055
https://kgs-ind.com

Leader Tech Inc.

12420 Race Track Road
Tampa, FL
(813) 855-6921
https://www.leadertechinc.com

Spira Manufacturing Corporation

650 Jessie Street
San Fernando, CA
(888) 98-SPIRA (77472)
https://www.spira-emi.com

Würth Elektronik

Max-Eyth-Strasse 1, Waldenburg
Baden-Württemberg, Germany
49 7942 945 - 0
https://www.we-online.com

EMI/RFI Shielding

AR RF/Microwave Instrumentation

160 School House Road
Souderton, PA
(215) 723-8181
https://www.arworld.us

Kitagawa Industries America, Inc.

2860 Zanker Road
San Jose, CA
(408) 971-2055
https://kgs-ind.com

Leader Tech Inc.

12420 Race Track Road
Tampa, FL
(813) 855-6921
https://www.leadertechinc.com

Spira Manufacturing Corporation

650 Jessie Street
San Fernando, CA
(888) 98-SPIRA (77472)
https://www.spira-emi.com

Würth Elektronik

Max-Eyth-Strasse 1, Waldenburg
Baden-Württemberg, Germany
49 7942 945 - 0
https://www.we-online.com

SUPPLIER INDEX

ESD Flooring

SelecTech

33 Wales Avenue, Suite F
Avon, MA
(877) 738-4537
https://www.staticstop.com

staticWorx, Inc.

372 Hurricane Lane
Williston, VT
(617) 923-2000
https://staticworx.com

ESD Simulators

HV Technologies, Inc.

8526 Virginia Meadows Drive
Manassas, VA
(703) 365-2330
https://www.hvtechnologies.com

Kikusui America

3625 Del Amo Boulevard
Torrance CA
(310) 214-0000
https://www.kikusuiamerica.com

Suzhou 3ctest Electronic Co, Ltd.

Anda Technology Park Jinshan Road, Suzhou, China
86-512-6807 7192
https://www.3c-test.com

Filters

Coilcraft

1102 Silver Lake Road
Cary, IL
(847) 639-6400
http://www.coilcraft.com

Kitagawa Industries America, Inc.

2860 Zanker Road
San Jose, CA
(408) 971-2055
https://kgs-ind.com

Leader Tech Inc.

12420 Race Track Road
Tampa, FL
(813) 855-6921
https://www.leadertechinc.com

Spira Manufacturing Corporation

650 Jessie Street
San Fernando, CA
(888) 98-SPIRA (77472)
https://www.spira-emi.com

Würth Elektronik

Max-Eyth-Strasse 1, Waldenburg
Baden-Württemberg, Germany
49 7942 945 - 0
https://www.we-online.com

Oscilloscopes

Rohde & Schwarz USA

6821 Benjamin Franklin Drive
Columbia, MD
(888) TEST-RSA (837-8772)
https://www.rohde-schwarz.com

Spectrum Analyzers

Rohde & Schwarz USA

6821 Benjamin Franklin Drive
Columbia, MD
(888) TEST-RSA (837-8772)
https://www.rohde-schwarz.com

Safety Test Equipment

Absolute EMC Llc.

14126 Wood Rock Way
Centreville, VA 20121
(703) 774-7505
https://absolute-emc.com

E. D. & D., Inc.

901 Sheldon Drive
Cary, NC
(800) 806-6236
http://www.productsafet.com

Kikusui America

3625 Del Amo Boulevard
Torrance CA
(310) 214-0000
https://www.kikusuiamerica.com

Test Equipment

Absolute EMC Llc.

14126 Wood Rock Way
Centreville, VA 20121
(703) 774-7505
https://absolute-emc.com

Lightning EMC

300 Hylan Drive #170
Rochester, NY
tel: (585) 552-2080
https://www.lightningemc.com

Ross Engineering Corporation

540 Westchester Drive
Campbell, CA
(408) 377-4621
https://www.rossengineeringcorp.com

Test Equipment Rentals

Advanced Test Equipment Rentals

10401 Roselle Street
San Diego, CA
(800) 404-2832
https://www.atecorp.com

Test Laboratories

Certifigroup

901 Sheldon Drive, Cary, NC
(800) 422-1651
https://www.certifigroup.com

F2 Labs

26501 Ridge Rd.
Damascus, MD
(301) 253-4500
https://f2labs.com

CORRELATION BETWEEN INSERTION LOSS AND INPUT IMPEDANCE OF EMC FILTERS

Part 1: LC and CL Filters

By Bogdan Adamczyk and Jake Timmerman

This is the first article of a three-article series devoted to the correlation between the insertion loss and input impedance of passive EMC filters. In this article, we focus on LC and CL filters. Based on the analysis, simulation, and measurement results, it has been observed that the frequencies where the insertion losses of the filters are equal are also the frequencies where the input impedances are equal. These frequencies define the regions where one filter configuration outperforms the other (with respect to the insertion loss). To determine these regions analytically, we compare the input impedances of the two filters. Subsequent articles will focus on π and T filters and cascaded LC and CL configurations.

Dr. Bogdan Adamczyk is professor and director of the EMC Center at Grand Valley State University (http://www.gvsu.edu/emccenter) where he performs EMC educational research and regularly teaches EMC certificate courses for industry. He is an iNARTE certified EMC Master Design Engineer. He is the author of the textbook "Foundations of Electromagnetic Compatibility with Practical Applications" (Wiley, 2017) and the upcoming textbook "Principles of Electromagnetic Compatibility: Laboratory Exercises and Lectures" (Wiley, 2024). He has been writing this column since January 2017. He can be reached at adamczyb@gvsu.edu.

Jake Timmerman is an EMC Engineer at E3 Compliance, which specializes in EMC & SIPI design, simulation, pre-compliance testing, and diagnostics. He received his B.S.E in Electrical Engineering from Grand Valley State University. Jake participates in the industrial collaboration with GVSU at the EMC Center. He can be reached at jacob.timmerman@e3compliance.com.

1. INSERTION LOSS DEFINITION

Consider the circuit shown in Figure 1.

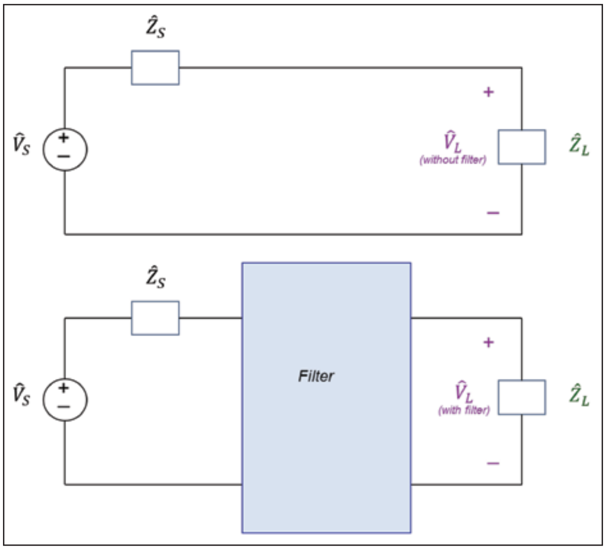

Figure 1: Illustration of the insertion loss of a filter

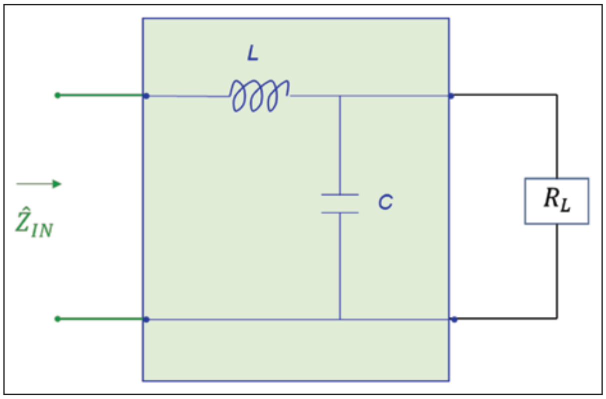

Figure 2: Input impedance to the *LC* filter

Insertion loss of a filter can be defined as

$$IL_{dB} = 20\,log_{10}\frac{V_{L,withoutfilter}}{V_{L,withfilter}} \tag{1a}$$

where V_L is the magnitude of the complex voltage $\hat{V}_L$. Since $V_{L,without\,filter} > V_{L,with\,filter}$ the insertion loss defined by Eq. (1a) is a positive number in dB. The insertion loss could alternatively be defined as [1],

$$IL_{dB} = 20\,log_{10}\frac{V_{L,with\ filter}}{V_{L,without\ filter}} \tag{1b}$$

In this case, the insertion loss in dB is the negative of the loss defined in Eq. (1b). We will use this definition when plotting the simulation results and comparing the simulation results to the VNA measurements.

2. INPUT IMPEDANCE TO THE LC FILTER

The input impedance, $\hat{Z}_{IN}$, to the *LC* filter is calculated from the circuit shown in Figure 2.

$$\hat{Z}_{IN}(s) = sL + \left(R_L \middle\| \frac{1}{sC}\right) = sL + \frac{R_L(1/sC)}{R_L + {}^{1}/_{sC}} \tag{2a}$$

or

$$\hat{Z}_{IN}(s) = \frac{s^2R_LLC + sL + R_L}{sR_LC + 1} \tag{2b}$$

or, in terms of the frequency

$$\hat{Z}_{IN}(j\omega) = \frac{(R_L - \omega^2R_LLC + j\omega L)}{1 + j\omega R_LC} \tag{3a}$$

The magnitude of the input impedance is

$$Z_{IN} = \frac{\sqrt{(R_L - \omega^2R_LLC)^2 + (\omega L)^2}}{\sqrt{1 + (\omega R_LC)^2}} \tag{3b}$$

3. INPUT IMPEDANCE TO THE CL FILTER

The input impedance, $\hat{Z}_{IN}$, to the *CL* filter is calculated from the circuit shown in Figure 3.

$$\hat{Z}_{IN}(s) = (sL + R_L) \left\| \frac{1}{sC}\right. \tag{4a}$$

or

$$\hat{Z}_{IN}(s) = \frac{sL + R_L}{s^2LC + sR_LC + 1} \tag{4b}$$

or, in terms of the frequency

$$\hat{Z}_{IN}(j\omega) = \frac{R_L + j\omega L}{1 - \omega^2LC + j\omega R_LC} \tag{5a}$$

The magnitude of the input impedance is

$$Z_{IN} = \frac{\sqrt{(R_L)^2 + (\omega L)^2}}{\sqrt{(1 - \omega^2LC)^2 + (\omega R_LC)^2}} \tag{5b}$$

4. LC FILTER VS. CL FILTER – INPUT IMPEDANCE – SIMULATIONS AND CALCULATIONS

Figure 4 shows the simulation circuit used for the comparison of input impedances.

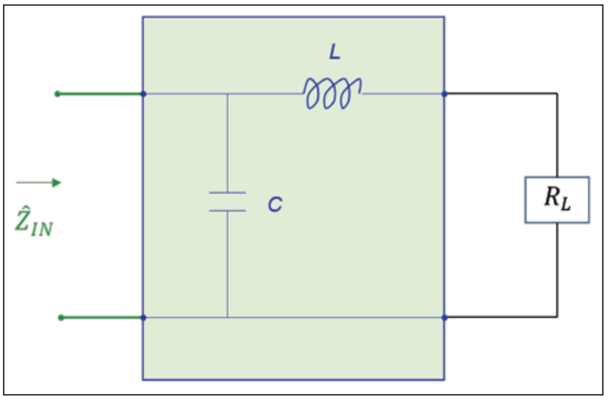

Figure 3: Input impedance to the *CL* filter

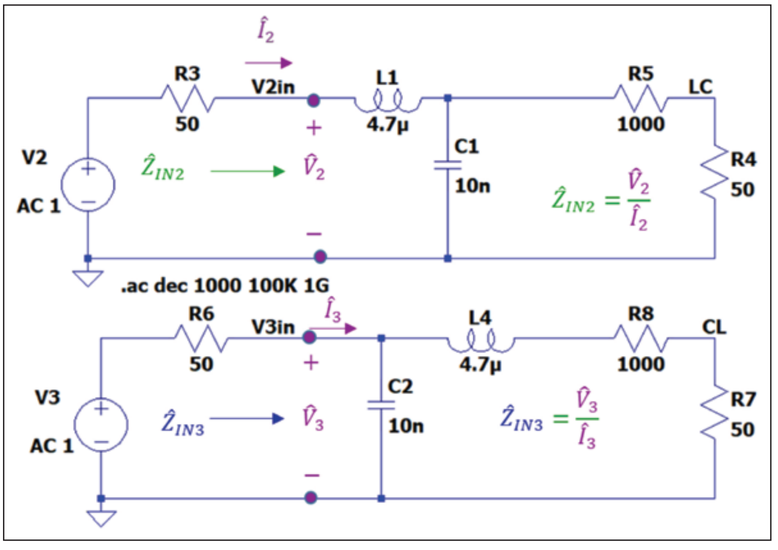

Figure 4: Simulation circuit for comparison of input impedances

The simulation results are shown in Figure 5.

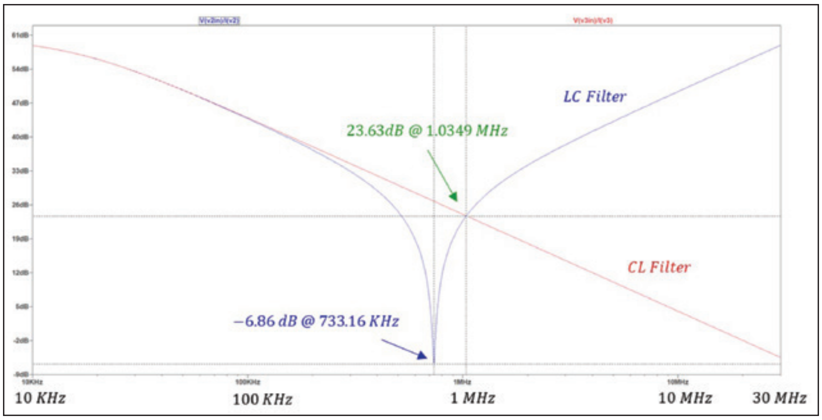

Figure 5: Simulation results: Input impedance – *LC* filter vs. *CL* filter

Note that the two input impedances are equal at the frequency of 1.0349 MHz. Figure 5 also shows the resonant frequency of the LC filter at 733.16 kHz. This result is confirmed by the calculations in Equation 6.

$$f_r = \frac{1}{2\pi\sqrt{LC}} = \frac{1}{2\pi\sqrt{10\times10^{-9}\times4.7\times10^{-6}}} = 734.127\ kHz \quad (6)$$

Next, let's calculate the frequency at which the input impedances of the two filters are equal. Equating the expressions in equations (3b) and (5b) produces

$$\frac{\sqrt{(R_L-\omega^2 R_L LC)^2+(\omega L)^2}}{\sqrt{1+(\omega R_L C)^2}} = \frac{\sqrt{(R_L)^2+(\omega L)^2}}{\sqrt{(1-\omega^2 LC)^2+(\omega R_L C)^2}} \quad (7)$$

This equation can be solved for ω, [2], resulting in

$$\omega = \sqrt{\frac{2}{LC}} \quad (8a)$$

or

$$f = \frac{1}{2\pi}\sqrt{\frac{2}{LC}} = \frac{\sqrt{2}}{2\pi\sqrt{4.7\times10^{-6}\times10\times10^{-9}}} = 1.038\ MHz \quad (8b)$$

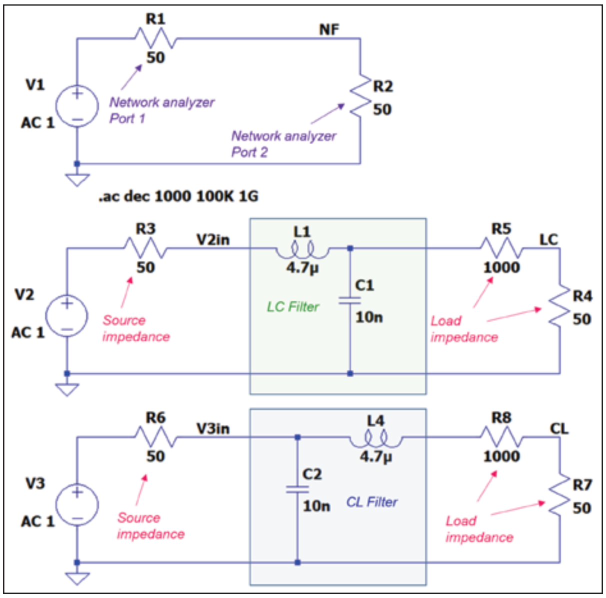

Figure 6: Simulation circuit for comparison of insertion losses

Which agrees with the simulation result shown in Figure 5.

5. LC FILTER VS. CL FILTER – INSERTION LOSS – SIMULATIONS AND MEASUREMENTS

Figure 6 shows the simulation circuit used for the comparison of insertion losses.

The simulation results are shown in Figure 7.

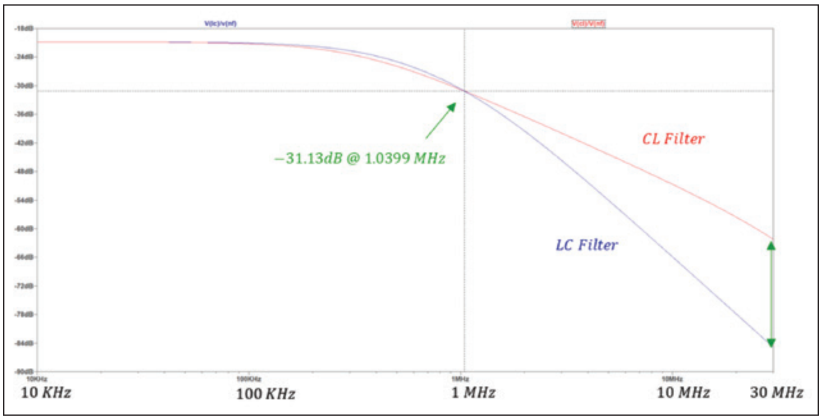

Figure 7: Simulation results: Insertion loss – *LC* filter vs. *CL* filter

The insertion losses of the two filters are equal at the frequency of 1.04 MHz. This is the same frequency at which the input impedances of the two filters were equal! Note that up to the frequency of 1.04 MHz the insertion loss of an *CL* filter is larger (in the absolute sense) than that of the *LC* filter. Beyond that frequency the insertion loss of the *LC* filter is larger. This means that the *LC* filter is more effective than the *CL* filter beyond the frequency of 1.04 MHz.

We have arrived at a very important observation: once the filter components values *L* and *C* are chosen, we can determine the frequency at which the insertion losses of *LC* and *CL* filters are equal. This is the frequency at which the input impedances are equal and given by Eq. (8b).

To verify the simulations results of the insertion loss the measurement setup shown in Figure 8 was used.

The measurement results are shown in Figure 9.

Note that the measurement results agree with the calculated and simulated results.

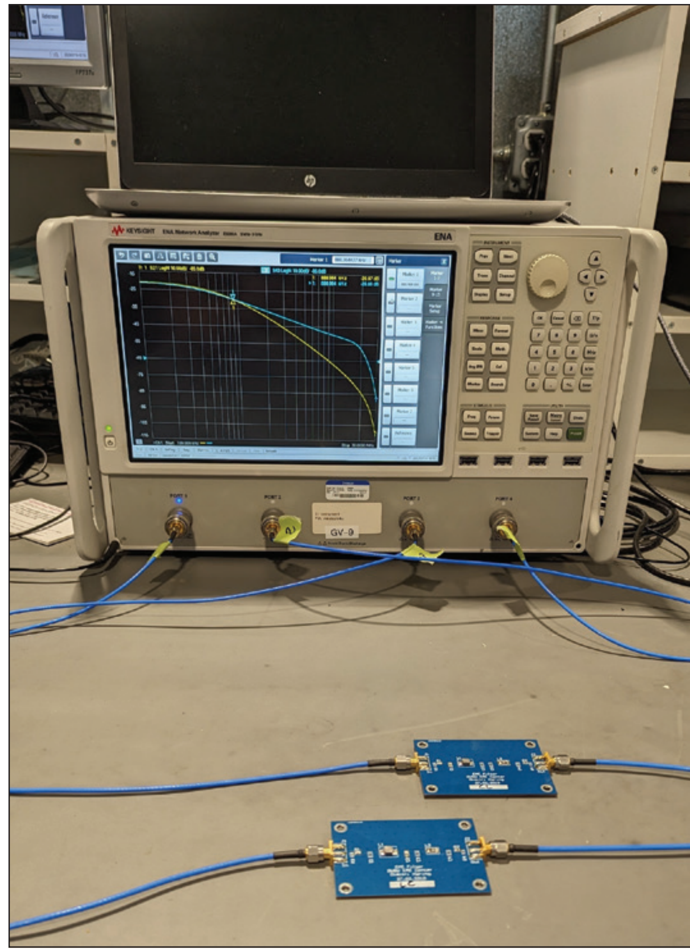

Figure 8: Measurement setup: Insertion loss – *LC* filter vs. *CL* filter

REFERENCES

1. Bogdan Adamczyk and Dimitri Haring, "EMC Filters Comparison Part I: CL and LC Filters," *In Compliance Magazine*, December 2019.
2. Bogdan Adamczyk, *Principles of Electromagnetic Compatibility: Laboratory Exercises with Lectures*, Wiley, 2024.

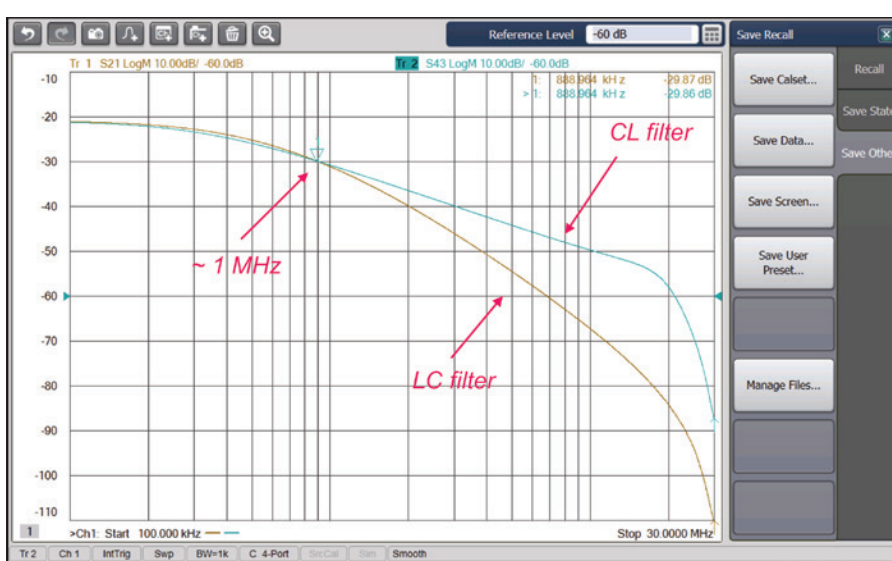

Figure 9: Measurement results: Insertion loss – *LC* filter vs. *CL* filter

CDE MODELING USING STAR-TREE IMPEDANCE NETWORKS FOR USB2 CABLE

By Peyman Ensaf and Timothy J. Maloney for EOS/ESD Association, Inc.

Peyman Ensaf is currently a Quality & Reliability Research and Development Engineer focused on ESD/RFI with Intel. While a student he completed summer internships at the Phillips Laboratory U.S. Air Force focusing on numerical electromagnetics, studying electromagnetic field behaviors within complex cavities of satellite sub-systems using numerical tools.

Timothy J. Maloney was a Senior Principal Engineer at Intel before retirement in June of 2016. He received the Intel Achievement Award for his patented ESD protection devices, which have achieved breakthrough ESD performance enhancements for a wide variety of Intel products. He is co-author of the book *Basic ESD and I/O Design* (Wiley, 1998) and is a Fellow of the IEEE.

Founded in 1982, EOS/ESD Association, Inc. is a not for profit, professional organization, dedicated to education and furthering the technology Electrostatic Discharge (ESD) control and prevention. EOS/ESD Association, Inc. sponsors educational programs, develops ESD control and measurement standards, holds international technical symposiums, workshops, tutorials, and foster the exchange of technical information among its members and others.

Previous studies of cable discharge events (CDE) have often used oversimplified models of the cable, such as a single 50Ω transmission line. This is not bad for an initial investigation, but the next level of detail is not difficult to capture for some familiar data cables. This work focuses on a star-tree impedance model for the 5-node USB2 cable and outlines a methodology for treating other cables, such as USB3 and HDMI.

The Cable Discharge Event (CDE) is an important ESD topic of continuing interest [1,2]. But to quantify CDE and observations, a simple and accurate electrical model of the cable itself is needed for future studies of on-silicon ESD protection optimizing for cost performance and improved reliability. Industry specifications leave much latitude at the expense of clarity. After considerable study and to promote understanding, we devised simple, lucid models for USB2, USB3, and HDMI cables based on star and tree networks [3]. These utilize measurements of capacitance and propagation velocity (and therefore inductance and impedance) that give models with reduced parameter count and agree well with the experiment. In this brief article, we model the five-node USB2 cable (Figure 1) and plan to cover similar models for USB3 and HDMI in the 2024 EOS/ESD Symposium.

METHODOLOGY & EXPERIMENTS

We began, using methods to be described below, by noting that a 5-parameter star network with a single center point [3] fits the 10 (i.e., C(5,2)) pairwise capacitance measurements for USB2 reasonably well. But then we found that adding an extra element from the center point to each pair's D+/D- and V_{BUS}/GND was substantially better, forming trees. One of those elements, from the center to the V_{BUS}/GND tree, turned out to be nearly zero impedance and thus is shorted in Figure 1. Finally, the elements of the two pairs D+/D- and V_{BUS}/GND are so similar that using a single impedance/capacitance for each pair and symmetrizing the associated measurements was done. The resulting star-tree network Figure 1 has just four Z (or C) parameters.

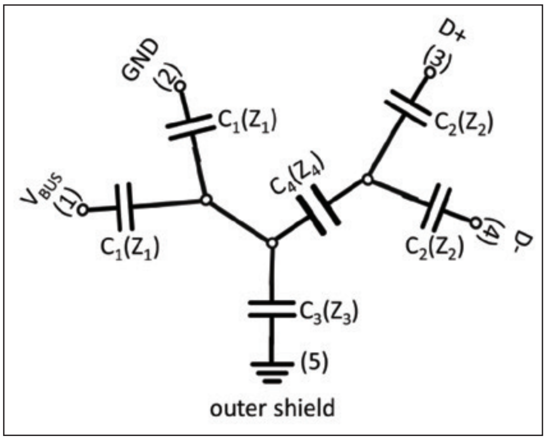

Figure 1: Star-tree capacitance (impedance) network for USB2 cable including V_{BUS}, GND, D+, and D- signal lines and the shield, plus nodal naming 1-5.

The final model will be transmission line impedance Z that captures both capacitance and velocity measurements, as Z=L/C and inductance L are derived from velocity v=1/LC, as discussed below. (C and L quantities are per unit length.) Let conductance G=1/C here, as it is the capacitive reactance with j/w normalized out as unity. Then, we can easily formulate a matrix describing the summed G elements corresponding to the ten pairwise (reciprocal) capacitance measurements between the numbered nodes in Figure 1. Linear regression using matrices, as below, solve for the four parametric values of (reciprocal) capacitance, whereupon we use measured velocity v to solve for each Z, Z_1-Z_4.

Let C_i be a column vector of parametric capacitances for the model in Figure 1.

$$[\boldsymbol{C_i}] = \begin{bmatrix} \boldsymbol{C_1} \\ \vdots \\ \boldsymbol{C_4} \end{bmatrix} \tag{1}$$

$$[\boldsymbol{G_i}] = \left[\frac{\boldsymbol{1}}{\boldsymbol{C_i}}\right] \tag{2}$$

$$\boldsymbol{A\ G = b} \tag{3}$$

In Eqns. 1-3, b is a 10x1 measured vector of $1/C_{ij}$, A is a 10x4 matrix of 1s and 0s (see Table 1a), considering the duplicates, Table 1a reduces to Table 1b, and G is a 4x1 vector (Eq. 2) of parametric reciprocal C values. Multiplying both sides of Eq. 3 by the transpose of the A matrix A^T (4 x 10) results in

$$\boldsymbol{(A^T A)\ G = \ A^T\ b} \tag{4}$$

Solving for G, where [C] = [1/G],

$$\boldsymbol{G = (A^T\ A)^{-1}\ A^T\ b} \tag{5}$$

Table 2 compares the various capacitances, as measured (by a capacitance meter) and as predicted by solving for **G** and applying **A**. The best solution comes from averaging the measured capacitances that should all be the same, as indicated by Figure 1 (Averaged cap column, Table 2). **G** comes from linear regression, using

A matrix, for AG=b	G_1	G_2	G_3	G_4
$b_1=1/C_{12}$	2	0	0	0
$b_2=1/C_{13}$	1	1	0	1
$b_3=1/C_{14}$	1	1	0	1
$b_4=1/C_{15}$	1	0	1	0
$b_5=1/C_{23}$	1	1	0	1
$b_6=1/C_{24}$	1	1	0	1
$b_7=1/C_{25}$	1	0	1	0
$b_8=1/C_{34}$	0	2	0	0
$b_9=1/C_{35}$	0	1	1	1
$b_{10}=1/C_{45}$	0	1	1	1

Table 1a: 10x4 A-matrix for all combinations

Reduced A matrix	G_1	G_2	G_3	G_4
$b_1=1/C_{12}$	2	0	0	0
$b_2=1/avg(C_{13}, C_{14}, C_{23}, C_{24})$	1	1	0	1
$b_3=1/avg(C_{15}, C_{25})$	1	0	1	0
$b_4=1/C_{34}$	0	2	0	0
$b_5=1/avg(C_{35}, C_{45})$	0	1	1	1

Table 1b: 5x4 reduced matrix based on Table 1a A-matrix.

Capacitances	measured caps	Averaged cap	Linear Regression	% Diff (Averaged Cap)
C_{12}	124.89	124.89	124.71	0.1635
C_{13}	77.95	78.58	78.66	0.1028
C_{14}	76.55			
C_{23}	79.75			
C_{24}	80.08			
C_{15}	212.33	212.19	212.73	0.2777
C_{25}	212.05			
C_{34}	63.02	63.02	63.02	0
C_{35}	106.57	106.57	106.44	0.1395
C_{45}	106.57			

Table 2: Measured capacitances/meter vs. and averaged values for the network in Figure 1. Right: 5x4 matrix solution for predicted measurement and percent error.

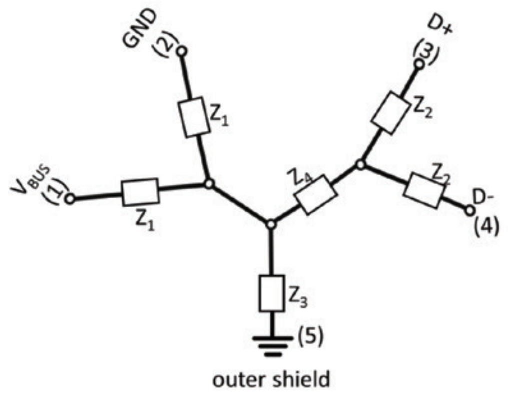

$Z_{i(1-4)}\ \Omega$	$C_{i(1-4)}$ pF/m	$G_{i(1-4)}$
19.67	249.38	0.013
38.92	126.04	0.026
3.38	1449.76	0.002
3.79	1294.44	0.003

Figure 2: USB2 star-tree impedances as derived from the capacitance solution of Figure 1.

linear algebra as in Eqs. 1-5 and employing the 5x4 **A** matrix of Table 1b and the 5x1 **b** vector of averaged (reciprocal) measured capacitances. As shown in Table 2, this gave agreement with the experiment to <0.3% worst case.

Table 2 shows the ten combinations of capacitance/length between the five nodes, beginning with measured values from the lab, with averaged and linear regression **AG** capacitance. Note the small difference between predicted and measured results. We achieved this with an averaged star-tree network of only four C (or Z) values, fitting five averaged values from 10 measurements as shown.

The four C values C_i, derived from the **G** solution, are converted to transmission line impedances (Z_i) once we have a propagation velocity V_p. Figure 2 shows $Z_1 Z_4$ values, found from $C_1 C_4$ using

$$V_p = \frac{1}{\sqrt{L_i C_i}}, Z_i = \frac{1}{C_i V_p}, L_i = \frac{Z_i}{V_p} \qquad (6)$$

Our best value of propagation velocity V_p for the transmission lines was measured by time-domain reflectometry on the cable to be 0.68c, c the speed of light. Values for different wire pairs were found to be very close, thereby simplifying the result. Figure 2, very similar to Figure 1, shows the star-tree impedances along with the calculated impedance values Z_i and capacitance values C_i from **G**.

The D+/D- twisted pair impedance $2Z_2$ = 77.84 ohms is within the USB2 spec limit of 90 ohms ±15%. For CDE problems, the capacitive DC limit, Figure 1, is used to describe initial charge storage, and the full impedance model of Figure 2 plus line terminations and switching can be used to determine the sequence and timing of CDE pulses. The Figure 2 network is comprehensive enough to describe line coupling in terms of even and odd mode impedances that can be written down by inspection, with Z_3 and Z_4 playing major roles. [4] Note that the twisted pair lines are more strongly coupled than the power lines, as desired. This comprehensive USB2 cable model is, of course, applicable beyond CDE and, for example could allow a quick grasp of USB2 signal integrity issues.

Simple star-tree networks, as shown here for USB2, should have wide applicability for cables carrying fast signals. The authors have extracted similar networks for USB3 and HDMI cables and plan to follow the present work by publishing solutions for those more complicated high-speed cables.

REFERENCES

1. S. Marathe, P. Wei, S. Ze, L. Guan, D. Pommerenke, "Scenarios of ESD Discharges to USB Connectors," 2017 EOS/ESD Proceedings, 3A.4.
2. M. Coenen, "Cable Discharge Event (CDE)," *Interference Technology*, July 31, 2019. https://interferencetechnology.com/cable-discharge-event-cde
3. https://en.wikipedia.org/wiki/Star-mesh_transform
4. See Maloney and Poon, 2004, https://bit.ly/3z7BTVe, and references therein.

ANSI Z535.3 – SAFETY SYMBOLS IN FOCUS

By Erin Earley

In our "On Your Mark" columns, we often discuss the importance of American National Standards Institute (ANSI) Z535. This family of U.S. standards was created to enhance safety communication and promote consistent hazard recognition and understanding – making it critical for manufacturers and workplaces across the country. The six (soon to be seven) Z535 standards create a guide for the design, application, and use of signs, colors, and symbols intended to identify and warn against hazards and for other accident prevention purposes. Our theme of exploring one of these standards in depth continues, this month focusing on *ANSI Z535.3 – Criteria for Safety Symbols*.

Erin Earley, head of communications at Clarion Safety Systems, shares her company's passion for safer products and workplaces. She's written extensively about best practices for product safety labels and facility safety signs. Clarion is a member of the ANSI Z535 Committee for Safety Signs and Colors, the U.S. ANSI TAG to ISO/TC 145, and the U.S. ANSI TAG to ISO 45001. Erin can be reached at eearley@clarionsafety.com.

WHAT IS ANSI Z535.3 – AND WHY DO SYMBOLS MATTER IN WARNINGS AND INSTRUCTIONS?

The ANSI Z535.3 standard focuses solely on guidelines for the design and use of safety symbols. It establishes criteria for creating symbols that effectively convey safety information across different languages and cultures. The goal: to promote the adoption of effective safety symbols for safety communication and to supply a procedure to do just that.

ANSI defines safety symbols as a configuration made up of an image, with or without a surround shape, that conveys a message without the use of words; the symbol may represent a hazard, a hazardous situation, a precaution to avoid a hazard, a result of not avoiding a hazard – or a combination of these.

According to the introduction of ANSI Z535.3, "Effective safety symbols have demonstrated their ability to provide critical information for accident prevention and personal protection. Signs with safety symbols can promote greater and more rapid communication of the safety message, and therefore greater safety for the general public."

Labels and signs that use safety symbols, instead of words alone, can help to achieve more rapid communication of the safety message and, ultimately, greater safety for those using, cleaning, or maintaining machinery. Also key in that is consistency. Effective symbols are consistent in their design, providing the ability to quickly glean important safety information across different languages, reading comprehension levels, and learning backgrounds. A consistent design allows for familiarity with images, making it easier to notice differences during potentially hazardous situations.

THE STANDARDS ORIGIN – AND LATEST UPDATES

What would a world without safety standards and consistent visuals look like? History prior to standardization, when there was a lack of visual communication, offers a glimpse. According to ANSI.org, in the early 1900s in the U.S., one of out of every four immigrant steel worker was killed or injured on the job and the accidents rates for immigrants were double that of English-speaking workers. When industrial safety conditions saw more exposure and reform take place, safety symbols began to be implemented.

In 1914, the Worker's Compensation Bureau published a booklet on best safety practices that included safety signs. While it advocated for safety signs – including those in the languages of workers – it didn't provide guidelines or formats for symbols. In 1941, the first U.S. standard for safety signs, ASA Z351.1 was published, outlining specifications for safety sign design and standard formats.

ANSI Z535.3 was published for the first time in 1991, offering extensive details about designing, evaluating, and using symbols. It was revised in 1998, when more substance was added to it, including providing well-tested procedures for evaluating symbols. Following that, revisions were made periodically, according to ANSI's cycle, including a 2011 update to delete a separate annex (C) with safety symbol examples, moving relevant parts to Annex A – essentially showcasing these not as examples (since they may be out of date or out of synch with updates to ISO 7010) but to illustrate principles and guidelines for graphic designs.

The latest revision to the standard was in 2022 and three changes were made: 1) an outdated method of symbol comprehension testing (multiple choice testing) was eliminated 2) several symbols in Annex A were updated and 3) a caveat was added to C1 Scope regarding variants in informative references.

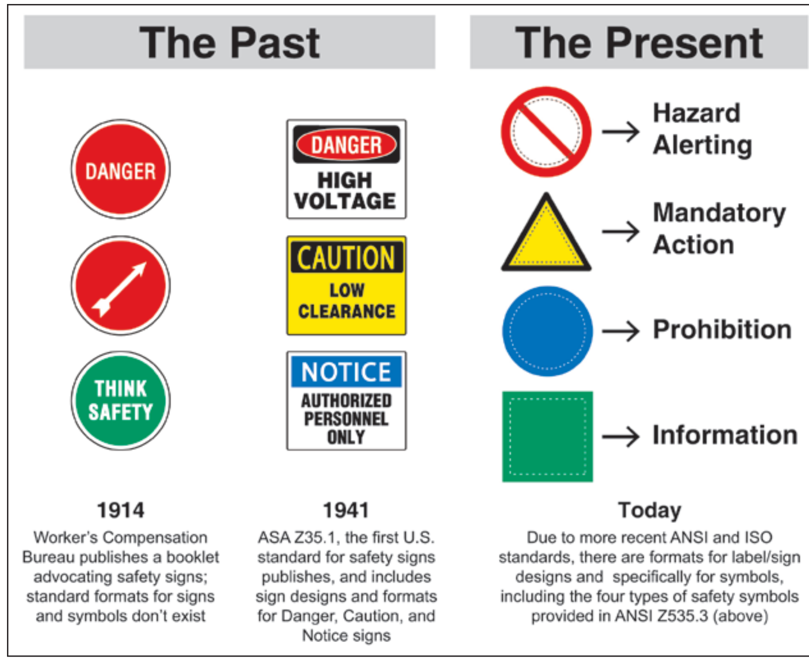

An abbreviated look at how visual safety communication and standardization of symbols have changed over time, with no standard symbols in the past and four distinct, standardized formats in the present.]

USING THE STANDARDS AND BEST PRACTICES IN YOUR SYMBOLS, LABELS, AND SIGNS

There are certain elements and sections of ANSI Z535.3 that are finite and concrete.

For example, helpful, specific areas from the standard that create important foundational elements for developing and using safety symbols include:

- *"Individual safety symbols should be designed, wherever possible, as elements of a consistent visual system."*
- *"There are four types of safety symbols that communicate different messages: hazard alerting, mandatory action, prohibition, and information."*
- *"Safety symbols used on safety signs should be placed within the normal field of view, and near the hazard or area for which action is required…they should be legible at the intended viewing distance."*
- *"Attention should be paid to environmental factors such as dirt, degradation, light level, and light quality that can impair the effectiveness of a safety symbol."*
- *"A safety symbol should have demonstrated understandability as verified by acceptable selection procedures involving an appropriate test group…a symbol training/recognition procedure is recommended to familiarize intended users with symbols and their meanings."*

The standard, without a doubt, contains much more details on these areas – and more.

However, when it comes to the practical application of the standard, there are many nuances and gray areas. That's because the standards aren't prescriptive in nature; they're meant to be guidelines.

According to Angela Lambert, head of standards compliance at Clarion Safety Systems and ANSI Z535 committee member, particular areas with question marks for equipment manufacturers charged with product safety are often:

- Safety alert symbol variations
- Symbol comprehension testing
- Abstract vs. representational symbols
- Use of only symbols vs. symbols and text
- Standardized symbols vs. your own creation

"ANSI Z535.3 doesn't necessarily provide answers to these questions. But, the standards do provide options, considerations, and formats that represent today's best practices. It's then up to the product safety professional, with their understanding of the product at hand, to apply these best practices to their warnings and instructions."

Banana Skins

433 Voltage disturbance problems with paper mill

The paper machine process requires precise control of the paper sheet tension as it progresses through the machine. On Caledonian Paper's paper machine this is achieved by controlling 23 separate DC variable speed drives, which are inherently vulnerable to voltage disturbances because of problems with the control of thyristor firing.

Firing angle control has difficulty following the voltage change, with possible consequential damage to thyristors. To prevent this damage, it is common for drives to be equipped with protection that trips the drive, using settings dependent on the drive's sensitivity to voltage disturbances, The manufacturers designed Caledonian Paper's drives at 90%, so that disturbances below this level for more than a few cycles caused a trip.

It was confirmed that the paper machine could be affected by voltage disturbances of only 10% variation from normal (90% retained) and as for as little as 100ms. Some events, which have affected production, only just come into the classification of a voltage dip, as described in the European Standard EN 51060, and the severity of events which cause disruption is not severe when compared with all possible disturbance events under equipment testing specifications, as described in IEC standard 1000-4-11 (now IEC 61000-4-11 – Editor). However, as a result of the voltage disturbance and associated DC drive trip, the paper machine suddenly stops in an uncontrolled manner with the potential for extensive damage particularly, in the wire and press sections.

The possibilities of damage and extensive downtime are greatest within the paper machine but disturbances can also affect the rest of the mill with activities downstream from the paper machine, such as the coater, supercalandars, and ancillary equipment suffering to varying but lesser degrees. The situation can also be exacerbated by having multiple incidents in a relatively short timeframe, e.g. a number of events over one day, especially when followed by a succession of disturbances over a period of several days.

(Extracted from "Special Feature: Electrical energy storage," IEE Power Engineering Journal, June 1999, pages 154 and 155.)

434 Wendy's restaurant interferes with satellite system

The FCC's Kansas City office received a complaint that the Search and Research Satellite Aided Tracking (SARSAT) system was experiencing interference from an unknown source. SARSAT is used by search-and-rescue teams to locate the radio beacon transmitters of crashed aircraft and distressed ships. Using mobile direction-finding gear, the FCC tracked the interference to a (presumably malfunctioning!) video display unit at a Wendy's restaurant.

(From "FCC's CIB Fight Interference," Newswatch…EMC, Compliance Engineering European Edition, September/October 1995, page 8.)

435 Cellphone interferes with ECG

Trigano et al, in [5] report an electrocardiogram recorded during 1800 MHz cellular phone ringing with high amplitude and high-frequency artefacts that appears 3 seconds before the first ringing tone and that persisted until end of ringing. As consequence of these facts many hospitals have prohibited the use of cellular phones in some areas.

[5] Alexandre Trigano, Olivier Blandeau, Christian Dale, Man-Faï Wong and Joe Wiart "Risk of cellular phone interference with an implantable loop recorder," *International Journal of Cardiology*, In Press.

(Taken from "Medical Equipment Immunity Assessment by Time Domain Analysis," Mireya Fernández-Chimeno, Miguel Ángel García-González and Ferran Silva, 2007 IEEE International Symposium on Electromagnetic Compatibility, 8-13 July 2007, Honolulu, Hawaii, ISBN: 1-4244-1350-8, IEEE EMC Society.)

436 Safety while swimming in a sea of electromagnetic energy

In this issue of Mayo Clinic Proceedings, 3 articles bring the issue of exposure to electrical transmissions and patient safety to the forefront. Tri et al1 report on their investigation of possible cell telephone interference with medical equipment in a hospital setting. Gimbel and Cox2 provide a report of 2 patients with implantable cardioverter defibrillators (ICD) who had adverse interactions with electromagnetic scanning devices in their community. Finally, Austin et al3 report on a person whose consumer electronic device interfered with an electrocardiogram (ECG) and led to an initial misdiagnosis of atrial flutter.

The current investigation by Tri et al1 is a follow-up to their previous 2005 in vitro report. In their earlier research, the authors discovered that cell phones produced interference in 44% of the tested devices, although the incidence of clinically important interference was only 1.2%. Older analog cell telephones that emit a relatively high-energy signal produced the most interference. Cell telephones had to be placed fairly close to the tested device (ie, <33 in) to produce any interference. Cell telephones were less likely to cause interference in newer medical technology. The authors concluded in 2005 that technologic advances had improved the resistance of medical devices to interference from cell telephones, but that the type and number of electronic designs were anticipated to steadily change, necessitating ongoing testing.

Tri et al heeded their own advice and tested newer technology, using a study design more relevant to daily patient care. Specifically, in the current 2007 report, they investigated cell telephone and wireless handheld device (Blackberry, Research In Motion, Waterloo, Ontario) interference of medical equipment while the equipment was being used on hospitalized patients, including those in intensive care units. The tested medical equipment was both diagnostic and therapeutic (e.g. physiologic monitors, infusion pumps, mechanical ventilators). The authors performed 300 tests of cell telephone interference and 40 tests of wireless handheld device interference. They found no interference with any of the tested medical technology. The authors concluded that institutions should consider revising hospital policies that restrict cell telephones.

In contrast, Gimbel and Cox reported on 2 patients having ICD devices that were triggered by electronic article surveillance (EAS) systems (ie, electronic devices placed at store exits to detect stolen merchandise). In both cases, the patient had relatively close contact with an EAS device at a retail store exit. In one case, when the patient collapsed after being shocked, an employee propped the patient against the EAS pedestal, thereby triggering further shocks. In both cases, the patients had ICDs from the same manufacturer. Austin et al reported on a similar but less dramatic electrical interference event. A healthy volunteer had an ECG recorded as part of an extra-hospital drug study. The ECG was read as atrial flutter with an atrial rate of 333/min. It was discovered that the volunteer had a portable compact disk (CD) player (Walkman, Sony Corp, Tokyo, Japan) close to the right-arm lead of the ECG. When the CD player was turned off, the ECG recording returned to normal sinus rhythm (also see Banana Skin number 422 – Editor).

(Extracts from: "Safety while Swimming in a Sea of Energy," Editorial, Mayo Clinic Proceedings, March 2007, Volume 82, Number 3, pages 276-277.)

The regular "Banana Skins" column was published in the EMC Journal, starting in January 1998. Alan E. Hutley, a prominent member of the electronics community, distinguished publisher of the EMC Journal, founder of the EMCIA EMC Industry Association and the EMCUK Exhibition & Conference, has graciously given his permission for In Compliance to republish this reader-favorite column. The Banana Skin columns were compiled by Keith Armstrong, of Cherry Clough Consultants Ltd, from items he found in various publications, and anecdotes and links sent in by the many fans of the column. All of the EMC Journal columns are available at https://www.emcstandards.co.uk/emi-stories, indexed both by application and type of EM disturbance, and new ones have recently begun being added. Keith has also given his permission for these stories to be shared through In Compliance as a service to the worldwide EMC community. We are proud to carry on the tradition of sharing Banana Skins for the purpose of promoting education for EMI/EMC engineers.

PRODUCT Showcase

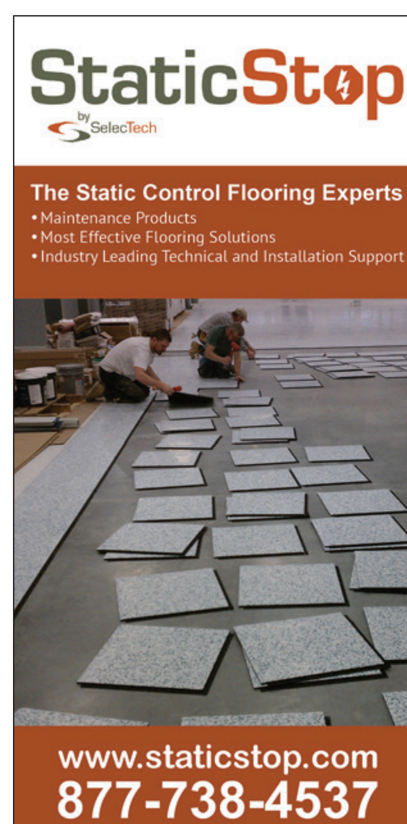

Advertiser Index

Upcoming Events

October 1-6
45th EOS/ESD Symposium and Exhibits

October 3
IEEE EMC Milwaukee Seminar: Printed Circuit Board Design for EMC Compliance

October 3-6 and 17-20
Applying Practical EMI Design & Troubleshooting Techniques

Advanced Printed Circuit Board Design for EMC + SI

Mechanical Design for EMC

October 4-6
The Battery Show India

October 8-13
45th Annual Meeting and Symposium of the Antenna Measurement Techniques Association (AMTA)

October 17
San Diego Test Equipment Symposium

October 19
EMC Mini Compliance Workshop and Exhibition

November 7-9
Fundamentals of Random Vibration and Shock Testing Training

December 4-7
Military Standard 810 (MIL-STD-810) Test Training

Always check the event website for current information.


EMC and Safety for Installations
VIEW CURRENT ISSUE
DOWNLOAD GUIDE
Visit Our Website